Copyright Warning & Restrictions

The copyright law of the United States (Title 17, United States Code) governs the making of photocopies or other reproductions of copyrighted material.

Under certain conditions specified in the law, libraries and archives are authorized to furnish a photocopy or other reproduction. One of these specified conditions is that the photocopy or reproduction is not to be "used for any purpose other than private study, scholarship, or research." If a, user makes a request for, or later uses, a photocopy or reproduction for purposes in excess of "fair use" that user may be liable for copyright infringement,

This institution reserves the right to refuse to accept a copying order if, in its judgment, fulfillment of the order would involve violation of copyright law.

Please Note: The author retains the copyright while the New Jersey Institute of Technology reserves the right to distribute this thesis or dissertation

Printing note: If you do not wish to print this page, then select "Pages from: first page # to: last page #" on the print dialog screen

ABSTRACT

BIODEGRADATION OF MIXED WASTES: BASIC KINETICS AND REACTION ENGINEERING FOR CYCLIC REACTOR OPERATION

by
Kung-Wei Wang

This study dealt with the determination of the detailed kinetics of the biodegradation of mixed substrates by pure cultures, and with reaction engineering studies of bioreactors employed in treatment of substitutable substrates under cyclic operation.

In the first part of the study the degradation of phenol and 4-chlorophenol (4-CP) by two strains of *Pseudomonas* species was investigated. Strain *P. putida O* was found to be capable of utilizing both phenol and 4-CP as sole carbon and energy sources. This suggests that this strain follows the *ortho*-cleavage pathway for the aromatic ring. Strain *P. putida N* could grow on phenol, and in its presence, could transform 4-CP to intermediates which are long-lived and do not serve as carbon and/or energy sources for the culture. These results suggest that *P. putida N* follows the *meta*-cleavage pathway for the aromatic ring.

The second part of the study dealt with the kinetics of glucose and phenol utilization by a pure culture of *P. putida OR*. It was found that the two substrates could serve as carbon and energy sources for the culture. The two substrates were used simultaneously, but were involved in a cross-inhibitory uncompetitive kinetic interaction. Inhibition from glucose on phenol removal was stronger. The kinetics were described by detailed mathematical expressions.

Based on the kinetic expressions obtained in the second part of the study, a detailed model describing biodegradation of phenol/glucose mixtures in a continuously operated cyclic reactor was derived. The dynamics of the system were studied numerically with computer codes based on the bifurcation theory for forced systems. The results, presented in the form of two-dimensional operating diagrams, show that there are regions in the parameter space where multistability occurs. The theoretical predictions were tested in experiments with a fully automated laboratory-scale unit. The experimental data validated the theoretical predictions. The quantitative agreement between theory and experiments was excellent.

The experimentally validated model can be used in design and process optimization studies.

BIODEGRADATION OF MIXED WASTES: BASIC KINETICS AND REACTION ENGINEERING FOR CYCLIC REACTOR OPERATION

by
Kung-Wei Wang

A Dissertation
Submitted to the Faculty of
New Jersey Institute of Technology
in Partial Fulfillment of the Requirements for the Degree of
Doctor of Philosophy

Department of Chemical Engineering,
Chemistry, and Environmental Science

May 1995

APPROVAL PAGE

BIODEGRADATION OF MIXED WASTES: BASIC KINETICS AND REACTION ENGINEERING FOR CYCLIC REACTOR OPERATION

Kung-Wei Wang

Dr. Basil C. Baltzis, Dissertation Advisor — Date
Professor of Chemical Engineering, NJIT

Dr. Gordon A. Lewandowski, Dissertation Co-Advisor — Date
Professor of Chemical Engineering and Chairman, NJIT

Dr. Ching-Rong Huang, Committee Member — Date
Professor of Chemical Engineering, NJIT

Dr. Piero M. Armenante, Committee Member — Date
Professor of Chemical Engineering, NJIT

Dr. Richard Bartha, Committee Member — Date
Professor of Microbiology, Rutgers University, New Brunswick, NJ

BIOGRAPHICAL SKETCH

Author: Kung-Wei Wang

Degree: Doctor of Philosophy in Chemical Engineering

Date: May 1995

Undergraduate and Graduate Education:

- Doctor of Philosophy in Chemical Engineering
  New Jersey Institute of Technology, New Jersey, 1995
- Master of Science in Chemical Engineering
  New Jersey Institute of Technology, New Jersey, 1991
- Bachelor of Science in Chemical Engineering
  Feng-Chia University, Taichiung, Taiwan, 1989

Major: Chemical Engineering

Publications:

K. -W. Wang, D. Tsangaris, B. C. Baltzis, and G. A. Lewandowski, "Biodegradation of Mixed Wastes in Continuously Operated Cyclic Reactors," *Applied Biochem. Biotechnol.* (submitted April 1995).

K. -W. Wang, B. C. Baltzis, and G. A. Lewandowski, "Treatment of Mixed Liquid Wastes in Cyclic Bioreactors," Submitted for publication in the proceeding of the 4th Conference on Environmental Science and Technology (Molyvos, Lesvos, Greece, September 4-7, 1995).

Presentations:
B. C. Baltzis, G. A. Lewandowski, K. -W. Wang, and D. Tsangaris, "Biodegradation of Mixed Wastes in Continuously Operated Cyclic Reactors," 17th Symposium on Biotechnology for Fuels and Chemicals, Vail, CO (May 7-11, 1995).

B. C. Baltzis, G. A. Lewandowski, and K. -W. Wang, "Biodegradation of Wastes in an Externally Forced Reactor: A Study with Mixed Substrates," AIChE Annual Meeting, St. Louis, MO (November 7-12, 1993).

B. C. Baltzis, G. A. Lewandowski, S. Dikshitulu, and K. -W. Wang, "The Effect of Population and Substrate Interactions on SBR Design Optimization," US EPA Symposium on "Bioremediation of Hazardous Wastes: Research Development, and Field Evaluation," Dallas, TX (May 4-6, 1993).

B. C. Baltzis, G. A. Lewandowski, S. Dikshitulu, and K. -W. Wang, "Aerobic Biodegradation of Phenolics in Optimally Designed Sequencing Batch Reactors," ACS 4th Chemical Congress of North America, New York, NY (August 25-30, 1991).

B. C. Baltzis, G. A. Lewandowski, S. Dikshitulu, Y. -S. Ko, and K. -W. Wang, "Biodegradation of Single and Multiple Hazardous Substances in a Sequencing Batch Reactor: Theory and Experimental Results," AIChE Annual Meeting, Chicago, IL (November 11-16, 1990).

This dissertation is dedicated to
my parents

ACKNOWLEDGMENT

The author would like to express his sincere gratitude to his dissertation advisor, Dr. Basil C. Baltzis, and co-advisor Dr. Gordon A. Lewandowski, for their moral encouragement and worthy guidance throughout this research. Especially, the author is highly grateful to Dr. Basil C. Baltzis who acted not only as supervisor of the research but also as a friend. Without his tremendous support, this work would not have been finished.

The author would like to express special thanks to Dr. D. Tsangaris for his help with the numerical analysis of the dynamics of cyclic reactors.

The author would also like to express his sincere thanks to Dr. Piero M. Armenante, Dr. Ching-Rong Huang, and Dr. Richard Bartha for serving as dissertation committee members.

The author appreciates the timely help and important suggestions from fellow students and friends including: Sitaram Dikshitulu, Zarook Shareefdeen, and Socrates Ioannidis.

Ms. Gwendolyn San Agustin and Mr. Clint Brockway provided timely and expert assistance with the analytical instruments used in the experiments.

Finally, the author would like to express his appreciation to Mei Liu for her endless patience and understanding, and to his parents for their full support and constant encouragement without which this work could not have been accomplished.

TABLE OF CONTENTS

Chapter	Page
1 INTRODUCTION	1
2 LITERATURE REVIEW	5
2.1 Kinetics and Biodegradation Pathways of Phenol and Chlorinated Phenolics	5
2.2 Kinetic Interactions Between Substrates	7
2.3 Studies with Classical SBRs	10
2.4 Biodegradation in Continuously Operated Cyclic Reactors	12
3 OBJECTIVES	15
4 MATERIALS AND METHODS	17
4.1 Microbial Cultures and Culture Media	17
4.2 Biomass and Chemical Assays	18
4.2.1 Biomass Assays	18
4.2.2 Phenol and 4CP Assays	19
4.2.3 Glucose Assays	19
4.2.4 Assay for 2H5CMA	22
4.2.5 Chloride Ions Assay	22
4.3 Experimental Reactor Unit	23
5 BIODEGRADATION STUDIES WITH PHENOL AND 4-CHLOROPHENOL	25
5.1 General Approach	25
5.2 Experimental Results and Discussion	25
5.3 Conclusions	30
6 KINETIC STUDIES ON THE UTILIZATION OF GLUCOSE AND MIXTURES OF PHENOL AND GLUCOSE BY CULTURE *P. putida OR*	33

TABLE OF CONTENTS
(Continued)

Chapter **Page**

6.1 Kinetics of Glucose Utilization 33

6.2 Kinetics of Simultaneous Utilization of Phenol and Glucose 39

7 REACTION ENGINEERING FOR A CYCLIC REACTOR EMPLOYED IN TREATMENT OF DISSIMILAR LIQUID WASTES 47

7.1 Theory 47

7.1.1 General Model Development 47

7.1.2 Mathematical Formulation for the Case of Phenol/Glucose Mixtures 50

7.2 Numerical Methodologies and Studies 56

7.3 Experimental Results and Validation of the Theory 63

8 CONCLUSIONS AND RECOMMENDATIONS 69

APPENDICES 73

A CALIBRATION CURVES AND SCHEMATIC OF THE EXPERIMENTAL APPARATUS 73

B DATA AND UV-SPECTRA FROM THE BIODEGRADATION EXPERIMENTS WITH PHENOL AND 4-CHLOROPHENOL 77

C1 DATA AND THEIR ANALYSIS FOR DETERMINING THE KINETICS OF GLUCOSE UTILIZATION BY *P. putida OR* 87

C2 DATA FROM BATCH EXPERIMENTS WITH MIXTURES OF PHENOL AND GLUCOSE UTILIZED BY *P. putida OR* 111

D CONDITIONS, GRAPHS, AND RAW DATA FOR EXPERIMENTS C-1 THROUGH C-5 129

E COMPUTER CODES 139

E-1 Computer code for predicting glucose and biomass concentration profiles in batch reactors (media without phenol). 140

TABLE OF CONTENTS
(Continued)

Chapter		Page
E-2	Computer code for predicting glucose, phenol, and biomass concentration profiles in batch reactors	142
E-3	Computer code for predicting glucose and biomass concentration profiles in continuously operated cyclic reactors	144
REFERENCES		149

LIST OF TABLES

Table		Page
6-1	Average specific rate of phenol removal (R_1) by *P. putida OR* in the presence of glucose. For all experiments the initial biomass concentration was about 13.7 g m^{-3}.	42
6-2	Average specific rate of glucose removal (R_2) by *P. putida OR* in the presence of phenol. For all experiments the initial biomass concentration was about 13.7 g m^{-3}.	43
B-1	Data from experiment K1-N. This experiment was performed with phenol only, and strain *P. putida N* under batch conditions.	78
B-2	Data from experiment K1-O. This experiment was performed with phenol only, using strain *P. putida O* under batch conditions.	78
B-3	Data from experiment K2-N. This experiment was performed with a mixture of phenol and 4CP, and strain *P. putida N* under batch conditions.	79
B-4	Data from experiment K2-O. This experiment was performed, under batch conditions, with a mixture of phenol and 4CP, and strain *P. putida O.*	79
B-5	Data from experiment K3-N. This experiment was performed, under batch conditions, with 4CP only and strain *P. putida N.*	80
B-6	Data from experiment K3-O. This experiment was performed, under batch conditions, with 4CP only and strain *P. putida O.*	80
B-7	Data from experiment K4-N. This experiment was performed, under batch conditions, with filtrate from experiment K2-N inoculated with suspension from the end of experiment K1-N.	81
B-8	Data from experiment K4-O. This experiment was performed, under batch conditions, with filtrate from experiment K2-N inoculated with suspension from the end of experiment K1-O.	81
B-9	Data from experiment K5-O. This experiment was performed, under batch conditions, by adding suspension from the end of experiment K1-O to the reactor contents at the end of experiment K3-N.	82
B-10	Data from experiment K6-O. This experiment was performed, under batch conditions, by adding suspension from the end of experiment K1-O to the reactor contents at the end of an experiment similar to K3-N.	82

LIST OF TABLES
(Continued)

Table		Page
C1-1	Summary of key information obtained from the kinetic experiments on glucose utilization by *P. putida OR*.	88
C1-2	Data for kinetic experiment G-1.	89
C1-3	Data for kinetic experiment G-2.	90
C1-4	Data for kinetic experiment G-3.	91
C1-5	Data for kinetic experiment G-4.	92
C1-6	Data for kinetic experiment G-5.	93
C1-7	Data for kinetic experiment G-6.	94
C1-8	Data for kinetic experiment G-7.	95
C1-9	Data for kinetic experiment G-8.	96
C2-1	Summary of conditions for the batch experiments with mixtures of phenol and glucose utilized by culture *P. putida OR*.	112
C2-2	Data from batch experiment PG-1.	113
C2-3	Data from batch experiment PG-2.	114
C2-4	Data from batch experiment PG-3.	115
C2-5	Data from batch experiment PG-4.	116
C2-6	Data from batch experiment PG-5.	117
C2-7	Data from batch experiment PG-6.	118
C2-8	Data from batch experiment PG-7.	119
C2-9	Data from batch experiment PG-8.	120
C2-10	Data from batch experiment PG-9.	121
C2-11	Data from batch experiment PG-10.	122
C2-12	Data from batch experiment PG-11.	123

LIST OF TABLES
(Continued)

Table		Page
C2-13	Data from batch experiment PG-12.	124
D-1	Operating and start-up conditions for experiments C-1 through C-5.	130
D-2	Data from experiment C-1. Operating conditions are given in Table D-1	131
D-3	Data from experiment C-2. Operating conditions are given in Table D-1	132
D-4	Data from experiment C-3. Operating conditions are given in Table D-1	133
D-5	Data from experiment C-4. Operating conditions are given in Table D-1	134
D-6	Data from experiment C-5. Operating conditions are given in Table D-1	135

LIST OF FIGURES

Figure **Page**

6.1 Determination of the specific growth rate (a) and yield coefficient (b) of *P. putida OR* on glucose from experiment G-6. 35

6.2 Data for the specific growth rate of *P. putida OR* on glucose. The data have been fitted to the Monod expression. 36

6.3 Comparison between experimentally obtained and model predicted concentration profiles for glucose (a) and biomass (b) for experiment G-7. 38

6.4 Experimentally obtained (symbols) and model-predicted (curves) concentration profiles for experiments PG-3 (a) and PG-7 (b). Information for these experiments is given in Table C2-1. 45

7.1 Schematic representation of the variation of the volume of the reactor contents during the cyclic operation. It is assumed that the flowrates during feeding and discharging are constant....48

7.2 Bifurcation diagrams of periodic states. These plots indicate the phenol concentration at the end of a limit cycle as a function of β when $\sigma_1 = \delta = 0.5$. The values of s_{1f} and s_{2f} (in g m^{-3}) are, respectively, 50 and 100 in (a) and 100 and 50 in (b)....57

7.3 Bifurcation diagrams of periodic states for the case where $\sigma_1 = \delta = 0.5$ and the medium contains phenol only at levels 50 g m^{-3} (a) and 100 g m^{-3} (b). These plots indicate the phenol concentration at the end of a limit cycle as a function of β....58

7.4 Operating diagrams on the $\beta - u_f$ plane when $\sigma_1 = \delta = 0.5$ and s_{2f} (in g m^{-3}) is 0 (a), 50 (b), or 100 (c). 61

7.5 Projection of operating diagrams on the $\beta - z_f$ plane when $\sigma_1 = \delta = 0.5$ and s_{1f} (in g m^{-3}) is 0 (a), 50 (b), or 100 (c). 62

7.6 Experimentally obtained and model-predicted concentration profiles for phenol (a), glucose (b), and biomass (c) for experiment C-2. Conditions for this experiment are given in Table D-1. The system reaches a survival periodic state.66

7.7 Experimentally obtained and model-predicted concentration profiles for phenol (a), glucose (b), and biomass (c) for experiment C-3. Conditions for this experiment are given in Table D-1. In this case the system reaches a washout state. 67

LIST OF FIGURES
(Continued)

Figure		Page
A-1	HPLC calibration curve for phenol concentration measurements.	74
A-2	HPLC calibration curve for 4-chlorophenol concentration measurements.	74
A-3	Calibration curve for chloride concentration measurement by the use of a special electrode	75
A-4	Schematic of the experimental cyclically operating reactor unit: (1) constant temperature water bath for feed tank; (2) feed tank, i.e., closed tank containing the untreated waste; (3) programmable sequence controller which is used for automating the cyclic operation; (4) peristaltic feed pump; (5) solenoid valve; (6) jacketed reactor; (7) circulating water bath; (8) thermometer; (9) dissolved oxygen probe; (10) air diffusion tube; (11) magnetic stirrer; (12) air pump; (13) peristaltic discharge pump; (14) discharge tank; (15) sampling port.	76
B-1	UV-visible spectra indicating absorbance at various wavelengths. Curves A and B are for samples taken 24 and 46 h, respectively, after initiation of experiment K1-N. Curves C and D are for samples taken 24 and 46 h, respectively, after initiation of experiment K1-O. Samples taken at 24 h were filtered before scanning, while those taken at 46 h were not.	83
B-2	UV-visible spectra indicating absorbance of samples at various wavelengths. Curves A and B are for samples from experiment K2-N taken 24 and 46 h, respectively, after the experiment started. Curves C and D are for samples from experiment K2-O taken 24 and 46 h, respectively, after initiation of the experiment. Samples taken at 24 h were filtered before scanning, while those taken at 46 h were not.	83
B-3	UV-visible spectra indicating absorbance of samples at various wavelengths. Curves A and B are for samples from experiment K3-N taken 24 and 46 h, respectively, after initiation of the experiment. Curves C and D are for samples from experiment K3-O taken 24 and 46 h, respectively, after the experiment started. Samples taken at 24 h were filtered before scanning, while those taken at 46 h were not.	84
B-4	UV-visible spectra of samples taken at the beginning of experiments K4-N (curve A) and K4-O (curve B). The samples were filtered before scanning.	85
B-5	UV-visible spectra of samples taken 50h after the initiation of experiments K4-N (curve A) and K4-O (curve B). The samples were filtered before scanning.	85

LIST OF FIGURES
(Continued)

Figure **Page**

B-6 UV-visible spectrum of a sample taken in the beginning of experiment K6-O. The sample was filtered before scanning. 86

B-7 UV-visible spectrum of a sample taken 25h after initiation of experiment K6-O. The sample was filtered before scanning. 86

C1-1 Determination of the specific growth rate (a) and yield coefficient (b) of *P. putida OR* on glucose from experiment G-1. 97

C1-2 Determination of the specific growth rate (a) and yield coefficient (b) of *P. putida OR* on glucose from experiment G-2. 98

C1-3 Determination of the specific growth rate (a) and yield coefficient (b) of *P. putida OR* on glucose from experiment G-3. 99

C1-4 Determination of the specific growth rate (a) and yield coefficient (b) of *P. putida OR* on glucose from experiment G-4. 100

C1-5 Determination of the specific growth rate (a) and yield coefficient (b) of *P. putida OR* on glucose from experiment G-5. 101

C1-6 Determination of the specific growth rate (a) and yield coefficient (b) of *P. putida OR* on glucose from experiment G-7. 102

C1-7 Determination of the specific growth rate (a) and yield coefficient (b) of *P. putida OR* on glucose from experiment G-8. 103

C1-8 Comparison between experimentally obtained and model predicted concentration profiles for glucose (a) and biomass (b) for experiment G-1. 104

C1-9 Comparison between experimentally obtained and model predicted concentration profiles for glucose (a) and biomass (b) for experiment G-2. 105

C1-10 Comparison between experimentally obtained and model predicted concentration profiles for glucose (a) and biomass (b) for experiment G-3. 106

C1-11 Comparison between experimentally obtained and model predicted concentration profiles for glucose (a) and biomass (b) for experiment G-4. 107

C1-12 Comparison between experimentally obtained and model predicted concentration profiles for glucose (a) and biomass (b) for experiment G-5. 108

LIST OF FIGURES
(Continued)

Figure **Page**

C1-13 Comparison between experimentally obtained and model predicted concentration profiles for glucose (a) and biomass (b) for experiment G-6. 109

C1-14 Comparison between experimentally obtained and model predicted concentration profiles for glucose (a) and biomass (b) for experiment G-8. 110

C2-1 Comparison between experimentally obtained and model-predicted concentration profiles for experiments PG-4 (a), PG-8 (b), and PG-12 (c). Information for these experiments is given in Table C2-1. 125

C2-2 Experimentally obtained (symbols) and fitted (curves) concentration profiles for experiments PG-1 (a) and PG-2 (b). Information for these experiments is given in Table C2-1. 126

C2-3 Experimentally obtained (symbols) and fitted (curves) concentration profiles for experiments PG-5 (a) and PG-6 (b). Information for these experiments is given in Table C2-1. 127

C2-4 Experimentally obtained (symbols) and model-predicted (curves) concentration profiles for experiments PG-9 (a), PG-10 (b), and PG-11 (c). Information for these experiments is given in Table C2-1. 128

D-1 Experimentally obtained and model-predicted concentration profiles for phenol (a), glucose (b), and biomass (c) for experiment C-1. Conditions for this experiment are given in Table D-1. The system reaches a survival periodic state. 136

D-2 Experimentally obtained and model-predicted concentration profiles for phenol (a), glucose (b), and biomass (c) for experiment C-4. Conditions for this experiment are given in Table D-1. The system reaches a survival periodic state. 137

D-3 Experimentally obtained and model-predicted concentration profiles for phenol (a), glucose (b), and biomass (c) for experiment C-5. Conditions for this experiment are given in Table D-1. The system reaches a survival periodic state. 138

NOMENCLATURE

b	biomass concentration in the reactor at time t ($g\ m^{-3}$).
b_o	biomass concentration in the reactor at the start-up conditions ($g\ m^{-3}$).
$f(u,z)$	dimensionless specific growth rate of a culture growing on two substitutable resources involved in uncompetitive cross-inhibition.
$g(z,u)$	dimensionless specific growth rate of a culture growing on two substitutable resources involved in uncompetitive cross-inhibition.
K_1	constant in the expression describing the specific growth rate of *P. putida OR* on phenol ($g\ m^{-3}$).
K_2	constant in the expression describing the specific growth rate of *P. putida OR* on glucose ($g\ m^{-3}$).
K_3	constant in the expression describing the specific growth rate of *P. putida OR* on phenol when glucose is also present in the medium ($m^3\ g^{-1}$). This constant describes the uncompetitive inhibition exerted by glucose on the degradation of phenol.
K_4	constant in the expression describing the specific growth rate of *P. putida OR* on glucose when phenol is also present in the medium ($m^3\ g^{-1}$). This constant describes the uncompetitive inhibition exerted by phenol on the degradation of glucose.
K_3'	constant in an expression which could describe the specific growth rate of *P. putida OR* on phenol in the presence of glucose, if glucose exerted competitive inhibition on the degradation of phenol ($g\ m^{-3}$).
K_4'	constant in an expression which could describe the specific growth rate of *P. putida OR* on glucose in the presence of phenol, if phenol exerted competitive inhibition on the degradation of glucose ($g\ m^{-3}$).
K_I	constant in the expression describing the specific growth rate of *P. putida OR* on phenol ($g\ m^{-3}$). This constant describes self-inhibition from phenol.
M	constant in the model describing cyclic reactor operation; M=1 during the first phase and M=0 during the second and third phase.
Q	flowrate of stream exiting from a cyclic reactor ($m^3\ h^{-1}$).
Q_f	flowrate at which medium (or untreated waste) is fed into a cyclic reactor ($m^3\ h^{-1}$).
Q'	dimensionless flowrate of stream exiting from a cyclic reactor.
Q_f'	dimensionless flowrate at which medium (or untreated waste) is fed into a cyclic reactor.
Q_f^*	reference flowrate related to cyclic reactor operation; it is defined as the feed flowrate during the first phase of the cycle ($m^3\ h^{-1}$).
s_1	concentration of phenol in the reactor at time t ($g\ m^{-3}$).

s_2	concentration of glucose in the reactor at time t (g m^{-3}).
$s_{1,o}$	initial concentration of phenol in a batch reactor (g m^{-3}).
$s_{2,o}$	initial concentration of glucose in a batch reactor (g m^{-3}).
s_{1f}	phenol concentration in the medium (or waste) fed into a cyclically operated reactor (g m^{-3}).
s_{2f}	glucose concentration in the medium (or waste) fed into a cyclically operated reactor (g m^{-3}).
$s_{1f,0}$	phenol concentration in a cyclically operated bioreactor at start-up conditions (g m^{-3}).
$s_{2f,0}$	glucose concentration in a cyclically operated bioreactor at start-up conditions (g m^{-3}).
t	time (h).
t_1	time indicating the end of the first phase of a cycle in cyclic reactor operation (h).
t_2	time indicating the beginning of the third phase of a cycle in cyclic reactor operation (h).
t_3	time indicating the end of a cycle in cyclic reactor operation (h).
u	dimensionless phenol concentration in a cyclically operated reactor at time θ.
u_f	dimensionless phenol concentration in the medium (or waste stream) fed into a cyclically operated reactor.
u_o	dimensionless phenol concentration in a cyclically operated reactor at time $\theta = 0$ (start-up conditions).
V	volume of contents of a cyclically operated reactor at time t (m^3).
V'	dimensionless volume of contents of a cyclically operated reactor at time θ.
V_m	maximum volume of contents of a cyclically operated reactor; value of V for $t_1 \leq t \leq t_2$; (m^3).
V_o	minimum volume of contents of a cyclically operated reactor; value of V at $t = 0$ and $t = t_3$; (m^3).
x	dimensionless biomass concentration in a cyclically operated reactor at time θ.
x_o	value of x at $\theta = 0$ (start-up conditions).
Y_1	yield coefficient of *P. putida OR* on phenol (kg-biomass / kg-phenol).
Y_2	yield coefficient of *P. putida OR* on glucose (kg-biomass / kg-glucose).
z	dimensionless glucose concentration in a cyclically operated reactor at time θ.
z_f	dimensionless glucose concentration in the medium (or waste stream) fed into a cyclically operated reactor.
z_o	dimensionless glucose concentration in a cyclically operated reactor at time $\theta = 0$ (start-up conditions).

GREEK SYMBOLS

β	dimensionless measure of the hydraulic residence time in a cyclically operated reactor; it is defined as $\beta = \hat{\mu}_1 V_m / Q_f^* \sigma_1$
γ	dimensionless constant, defined as $K_1 Y_1 / K_2 Y_2$.
δ	ratio of minimum to maximum volume of reactor contents during cyclic operation.
η	dimensionless constant, defined as $\mu_{m2} / \hat{\mu}_1$.
θ	dimensionless time.
θ_j	dimensionless time (j = 1, 2, 3) corresponding to t_j, j = 1, 2, 3.
λ_1	dimensionless cross-inhibition constant, defined as $K_2 K_3$.
λ_2	dimensionless cross-inhibition constant, defined as $K_1 K_4$.
$\mu_1(s_1)$	specific growth rate of *P. putida OR* on phenol, when phenol is the only carbon and energy source in the medium (h^{-1}).
$\mu_2(s_2)$	specific growth rate of *P. putida OR* on glucose, when glucose is the only carbon and energy source in the medium (h^{-1}).
$\mu_1(s_1,s_2)$	specific growth rate of *P. putida OR* on phenol, when glucose is also present in the medium (h^{-1}).
$\mu_2(s_2,s_1)$	specific growth rate of *P. putida OR* on glucose, when phenol is also present in the medium (h^{-1}).
μ_{m2}	constant in expression $\mu_2(s_2)$; it denotes the maximum specific growth rate of *P. putida OR* (h^{-1}).
$\hat{\mu}_1$	constant in expression $\mu_1(s_1)$.
σ_j	fraction of cycle time devoted to phase *j* (*j* = 1,...,3) of a cycle during cyclic reactor operation.
ω	dimensionless self-inhibition constant defined as K_1 / K_1.

CHAPTER 1

INTRODUCTION

Among the various technologies which are being used in the treatment of liquid waste streams of industrial and/or urban (municipal) origin, those which are based on biological treatment have a clear advantage. Biodegradation occurs usually at ambient temperatures, no expensive catalysts are required, and -if a system is properly selected and designed- the final products are innocuous. Biodegradation of wastes is widely applied, although many of its aspects are not well understood. The kinetics of the process are usually complex and oftentimes masked by the presence of severe mass transfer limitations [Wang et al. (1995b)]. In addition, the biomass (which is the catalyst of the process when looked at from an engineering perspective) is usually highly heterogeneous and, if at all, poorly characterized. Mixed cultures lead to very complex interactions and dynamics. Even a relatively simple system involving two microbial competitors used in biodegradation of phenol has been found to have extremely complex dynamics [Dikshitulu (1993); Dikshitulu et al. (1993)]. These complex dynamics translate to various regimes in the operating parameter space of a reactor. Some of these regimes imply instabilities or multistability. Knowledge of these dynamics may explain operational upsets and guide optimal reactor design.

There is no doubt that, despite the lack of complete knowledge of biodegradation, there is a number of very successful units which have been built and quasi-optimized based on entirely empirical or semi-empirical criteria. Up to a few years ago, propositions to perform fundamental studies on any aspect of biodegradation of wastes was viewed as of academic interest only. However, in the very recent years things have changed. There are now strong arguments for using well-defined cultures, understanding the microbiology of the process, addressing questions of biochemistry etc. [Finn (1983)].

Fundamental approaches to solving problems of treatment of volatile organics, as well as non-volatile recalcitrant compounds are now adopted by a number of companies (e.g., Envirogen). Fundamental approaches to reaction engineering and process optimization are also needed. Such approaches involve the basic principles of classical chemical engineering and are based on the knowledge of reaction rates and unit operations. For example, Lenas et al. (1994) have shown how process optimization can be done in a simple system involving a pure culture used in biodegradation of phenol.

Knowledge of the kinetics and dynamics of the biodegradation process can allow for process optimization, or increased efficiencies of existing units. This is of serious economical importance especially nowadays, since a constantly increasing public awareness regarding environmental issues has led regulatory agencies (both state and federal) to impose increasingly stricter limits on the amounts and levels of hazardous and/or toxic chemicals that can be released to the environment. For industry to meet these standards, large capital expenditures will be required unless either new technologies are developed or existing units are further optimized. Optimization based on trial-and-error, or just experimental approaches is a risky and expensive proposition. The complexity of the processes is such that trials in some regimes of the various parameters may last for a long time (cost) and may never be successful. The powerful tools which are now available for process simulation and analysis can reduce the cost of searching for optimal operating parameters by orders of magnitude, and can reveal some operating regimes which cannot be determined by intuition or common sense. However, in order to use these computer based methodologies one needs to have an accurate and realistic model for the process. Such a model cannot be derived unless the kinetics of biodegradation are known and the population interactions accounted for.

There are various ways of operating a particular reactor. As discussed in the next chapter, there is a special mode of operation of bioreactors employed in waste treatment and is known as SBR-technology. Sequencing batch reactors (SBRs) have been

extensively studied by various groups among which that of Irvine and co-workers [e.g., Irvine and Busch (1979)] has made pioneering contributions. SBR-technology is based on a semi-continuous cyclic operation. Each cycle is comprised of five phases: fill-, react-, settle-, draw-down-, and idle-phase. Among the various advantages of SBRs, which have been discussed by various authors [e.g., Arora et al. (1985); Chang (1987); Dikshitulu et al. (1993)] are flexibility in operation, ability to alternate between periods of anoxic and aerobic conditions, no need of a separate clarifier, and higher productivity (volumetric efficiency) when compared to equivalent continuous flow reactors (CSTRs).

The existence of usually long idle periods, makes classical SBR-operation discontinuous. Each cycle is essentially independent of the preceding one and thus, it has mostly features of batch or semi-continuous operation (considering the first two periods of each cycle).

When idle periods are eliminated, cyclic operation becomes continuous. Each cycle depends on the preceding one up to the point where a self-repeating cyclic pattern is reached. This approach has been followed by Baltzis, Lewandowski, and their associates in a series of studies which are viewed in the next chapter. In these studies biomass settling has been also eliminated in order to primarily study the consequences of the kinetics on the dynamics of the process. This approach to cyclic reactor operation has been shown to lead to even higher volumetric efficiencies than classical SBRs while it also allows for detailed process analysis utilizing the tools of the bifurcation theory for forced systems. Cyclic operation involving a filling-phase (input, no output), followed by a batch phase and then a draw-down-phase (output, no input) implies an operational protocol which has features of CSTR and batch systems. Batch operation implies temporal heterogeneities and is essentially the equivalent of tubular reactor operation where spatial heterogeneities apply. Usually, if the kinetics are simple, the reaction order determines whether a CSTR or tubular reactor should be used. What makes this cyclic

reactor operation better than a CSTR or a tubular reactor is that the kinetics of biodegradation are most often than not of shifting order.

This study is essentially a continuation of earlier ones [e.g. Chang (1987), Sanyal (1990), Dikshitulu (1993), Wang (1994)] and focuses, for the first time, on the aerobic biodegradation of mixed wastes in a continuously operated cyclic reactor. To reach the point of doing the reaction engineering analysis, a mixture had to be selected and its kinetics investigated first. Two systems were examined for their kinetics. One involved mixtures of phenol and 4-chlorophenol. This mixture was a model system of wastes similar in both molecular structure and origin (industrial operations). The second system involved mixtures of phenol and glucose. This mixture was selected as a model system for wastes which are dissimilar in both origin and molecular structure. It was the second system which was finally used in the reaction engineering studies. These studies involved mathematical modeling, analysis of system dynamics, and model validation via experiments with a fully automated laboratory-scale unit.

CHAPTER 2

LITERATURE REVIEW

There are a number of different topics which are pertinent to the work performed during the course of this dissertation. They involve kinetics and pathways of phenol and 4-chlorophenol biodegradation, kinetic interactions between substrates -especially when one of them is glucose-, classical SBR studies, and studies with continuously operated cyclic bioreactors. Due to the diversity of the various issues, the literature review has been organized in sections as follows.

2.1 Kinetics and Biodegradation Pathways of Phenol and Chlorinated Phenolics

The pathways of biodegradation of phenol, chlorophenol, and aromatic compounds in general have been investigated by a large number of researchers. These studies have utilized cells of different microbial species as well as extracts of cells for identification of the enzymes involved. Phenolics are first transformed to the corresponding catechols through the action of hydroxylases. Catechols are subsequently transformed through ring-cleavage which can occur either at the *meta* or the *ortho* position, through the action of 2,3-, or 1,2-dioxygenases, respectively. Eventually, intermediates are produced which enter the tricarboxylic acid cycle while in other cases intermediates which cannot be further transformed are produced. In Figure 2.1, the pathways which can lead to complete mineralization of phenolics are shown schematically.

Studies on the biodegradation of phenolics have been published by Bayly and Barbour (1984), Knackmuss (1981), Chaudhry and Chapalamadugu (1991), Knackmuss and Hellwig (1978), Rochkind et al. (1986), Haggblom et al. (1989), Buswell (1975), Gibson et al. (1967), Nishizuka et al. (1962), Dagley and Gibson (1965), Sala-Trepat et al. (1972), Bayly and Wigmore (1973), and many other researchers.

It appears that there is a general agreement among the various studies that catechol (or chlorocatechol) which is the first intermediate in the pathway of phenol (or chlorophenol) degradation is further transformed to final products through a mechanism of *meta*-cleavage of the ring structure. The alternate mechanism, involving *ortho*-cleavage of the ring structure seems to be less efficient, especially under conditions of no oxygen abundance [Knackmuss (1981)]. However, either through mutations or proper adaptation the *ortho*-cleavage enzyme systems can be induced and even become predominant in cases of various microorganisms [Bayly and Barbour (1984); Knackmuss and Hellwig (1978)]. The notion that phenol, especially with *Pseudomonas* sp., is degraded via the *meta*-cleavage pathway has been also discussed and adopted in the engineering literature [e.g., Yang and Humphrey (1975)]. However, there are also reports that the *ortho*-cleavage pathway may be predominant even for *Pseudomonas putida* [Kolenc et al. (1988)] after genetic manipulation.

For practical applications, it seems that for the case of phenol, it is not important to know whether a culture follows the *meta*- or *ortho*- cleavage pathway, as both are leading to an eventual complete mineralization of phenol. However, the mechanism involved in the degradation of chlorophenols appears to be of paramount importance. As discussed by Knackmuss (1981), haloaromatics in general are transformed to dead-end intermediates when the *meta*-cleavage pathway is involved. For the case of 4-chlorophenol (4CP), this intermediate is 5-chloro-2-hydroxymuconic semialdehyde (2H5CMA). In addition, the same author has reported that these dead-end metabolites exert irreversible inhibition on the *meta*-cleavage pathway enzymes (2,3-dioxygenases). Hence, in practical applications haloaromatics can cause severe problems. Clearly, unless complete mineralization of a pollutant is achieved, the treatment process is inadequate. Chlorinated compounds such as 4CP can be completely mineralized only via the *ortho*-cleavage pathway. In such cases, the chloride ion is released at the last step of the pathway before the final intermediate enters the TCA cycle and thus, monitoring of the

chloride ion concentration and recovery may be indicative of complete mineralization. However, there are reports [e.g., Rochkind et al. (1986)] suggesting that a high chloride recovery may be observed even when the *meta*-cleavage enzymes are employed. According to the aforementioned report, the pathway of chloride release has not been elucidated.

Phenol degradation kinetics is a topic which has been also very widely investigated. A comprehensive review of kinetic studies has been given recently by Dikshitulu et al. (1993). As discussed by the authors, there is a wide discrepancy among the published results due to the fact that in most cases the culture is not identified and the media used vary drastically in composition. Most existing studies with well defined media and cultures agree that phenol biodegradation follows inhibitory kinetics. The most commonly used expression for inhibitory kinetics is that of Andrews (1968).

Removal of 4-chlorophenol (4CP) has been reported to occur in the presence of phenol. In a report [Dapaah and Hill (1992)] which does not appear to be very conclusive, the authors report cometabolism of 4CP in the presence of phenol by *P. putida* (ATCC 17484), and present a first attempt to quantify and model 4CP removal.

2.2 Kinetic Interactions Between Substrates

Simultaneous biodegradation/utilization of chemical substances by heterotrophic bacterial populations may involve kinetic interactions between the substrates. This is an issue which has been examined by a number of investigators, although few are the studies which have dealt with the problem at a fundamental level and have led to the development of explicit expressions for describing such interactions.

Clearly, substrates may be substitutable or complementary resources for microbial cells. What is pertinent here concerns interactions between substitutable resources. Kinetic interference between substrates actually implies a degree of preference of a culture towards one of the substrates. Such interactions imply negative effects, or

inhibition, and -taken to the extreme and under batch conditions- lead to the diauxic growth known since the early studies of Monod (1942). In other cases, kinetic interference may involve a commensal/positive effect such as cometabolism of substrates. In the latter case, the resources are not really substitutable and for this reason, studies involving cometabolism are not reviewed here.

Early modeling of substrate interactions was performed by Yoon et al. (1977). These authors investigated -mainly through computer simulations- the possibility of coexistence of pure microbial competitors in a spatially and temporally homogeneous environment (such as a chemostat) when the two species compete for two substitutable resources. Their results have indicated that coexistence is possible even if both species show strong preference for one of the substrates.

Kinetic expressions similar to those of Yoon et al. (1977) have been recently used in describing kinetic interactions occurring during biodegradation of pollutants. For example, Oh et al. (1994) and Chang et al. (1993) have described the simultaneous removal of benzene and toluene by pure cultures or microbial consortia through kinetic expressions implying that the two pollutants (carbon/energy sources) are involved in a cross-inhibitory competitive interaction. The terminology for the interaction is taken by analogy from enzyme kinetics [Shuler and Kargi (1992)]. More recently, Wang (1994) and Wang et al. (1995b) have found that -under anoxic conditions- a pure culture of *Pseudomonas denitrificans* reduces nitrate and nitrite following kinetics which suggest that the two terminal electron acceptors (also serving as nitrogen sources for the culture) are involved in a non- or uncompetitive kinetic interaction. There are also reports suggesting that two pollutants may be degraded following independent kinetics (no interaction). For example, Hutchinson and Robinson (1988) have found that *P. putida* (ATCC 17484) could -under batch conditions- simultaneously utilize phenol and *p*-cersol, and that the data could be explained through a simple model implying no kinetic interaction between the two pollutants.

Since the present study investigated the kinetics of simultaneous utilization of glucose and phenol by a culture, it was of interest to find earlier reports dealing with kinetics, and possibly interactions, of substrates which are dissimilar in structure. Even more specifically, it was of interest to find studies dealing with mixtures involving pollutants (or hard to degrade substances) and readily degradable substrates such as glucose or more generally nutrient broths. Review of the literature regarding this issue has revealed that although there are studies, their conclusions are either conflicting or confusing. Confusion seems to stem from the fact that biodegradation rates are not specific (i.e. per unit amount of biomass), while interactions can be only judged from specific rates.

For example, Lackmann et al. (1980) have reported that 2,4-dichloro-phenoxyacetate (2,4-D) reduced the rate of glucose utilization while glucose had no effect on the rate of 2,4-D utilization. However, in a subsequent study from the same laboratory [Papanastasiou and Maier (1982)] when specific biodegradation (or growth) rates were used it was found that glucose and 2,4-D are involved in a cross-inhibitory interaction. This interaction has been described by unconventional expressions which depend on the initial concentration values for the two substrates. In another study, Kim and Maier (1986) found that nutrient broth addition to a 2,4-D-containing waste increased the rate of 2,4-D utilization but this increase was attributed to the presence of higher biomass quantities formed on the nutrient broth.

Orhon et al. (1989) have also studied the removal of 2,4-D in the presence of a nutrient broth. They have also examined mixtures of phenol and nutrient broth (BNB solution, Bacto). Their report is extremely confusing as they try to compare data from unacclimated and acclimated cultures. For example, they claim that 2,4-D is not degradable when introduced into a nutrient broth solution. However, later on they claim that 2,4-D (as well as phenol) severely reduced the utilization rate of the broth. They also claim that 2,4-D removal (in acclimated cultures) seems unaffected by the broth, although

their conclusion seems to point towards mutual inhibition as they refer to the work of Papanastasiou and Maier (1982) which was discussed earlier.

Rozich and Colvin (1986) have studied mixtures of phenol and glucose. Using overall rates (not specific growth rates), and regarding fully acclimated cultures, their conclusion was that glucose hinders the rate of phenol removal while phenol does not affect the rate of glucose utilization.

Schmidt et al. (1987) have studied the effect of glucose on the kinetics of *p*-nitrophenol mineralization by a pure culture of *Pseudomonas* sp. They found that the rate of *p*-nitrophenol removal increases in the presence of glucose. However, the increase is due to higher biomass presence (growth on glucose). This was proved through experiments with resting cells. These experiments suggested that glucose did not change the rate of *p*-nitrophenol removal. These results suggest that glucose does not interfere with the kinetics of *p*-nitrophenol degradation. No data were reported regarding the possible interference from *p*-nitrophenol with the kinetics of glucose utilization by the culture.

Hess et al. (1990, 1993) have studied the effect of glucose on the degradation of 2,4-dinitrophenol by a microbial consortium. Their experiments were performed with classical SBRs and show that glucose enhances the removal rate of 2,4-dinitrophenol, provided that glucose is not added to levels exceeding 1000 mg/L. If this level is exceeded, inhibition of the of 2,4-dinitrophenol rate is observed. The enhancement was attributed to higher levels of 2,4-dinitrophenol-degrading bacteria produced via growth on glucose and retained in the SBR. Inhibition was not explained, nor the effect of 2,4-dinitrophenol on the glucose utilization rate was discussed.

2.3 Studies with Classical SBRs

As has been discussed in the introduction (Chapter 1), classical SBRs involve a series of distinct cycles each one of which is comprised of five phases: fill-, react-, settle-, draw-

down-, and idle-phase. These reactors were originally investigated for treatment of municipal wastes [Chiesa and Irvine (1985); Irvine et al. (1983)]. Dennis and Irvine (1979) have studied to ratio of fill- to react-time in SBR cycles and its effect on optimal reactor performance.

A general overview of SBRs has been presented by Irvine and Busch (1979). Irvine and Richter (1978) compared the performance of SBRs to batch reactors. Ketchum et al. (1979) have presented a cost analysis of SBRs.

Sequencing batch reactors have been also studied for applications other than municipal wastewater treatment. For example, Hsu (1986) has studied the treatment of a petrochemical wastewater in SBRs. Ketchum and Liao (1979) have investigated the reduction of phosphorus in SBRs.

Studies with SBRs have also dealt with anaerobic (anoxic) operation for denitrification of wastes. In terms of denitrification, SBRs -which have features of semicontinuous operation- lead to better effluent quality [Hoepker and Schroeder (1979)]. Data on the performance of SBRs during denitrification, and population shifts occurring during the process have been studied by Abufayed and Schroeder (1986a, 1986b) and Wilderer et al. (1987), respectively.

The combination of nitrification/denitrification in SBRs (a process which involves alteration between aerobic and anoxic periods of operation) has been studied by Alleman and Irvine (1980), Silverstein and Schroeder (1983), Palis and Irvine (1985), and Jones et al. (1990a, 1990b).

As was already discussed in the previous section, Hess et al. (1990, 1993) have studied the removal of 2,4-dinitrophenol in SBRs under the presence of glucose.

Brenner et al. (1992) have studied degradation of mixtures containing phenol, and various isomers of cresol and dimethylphenol. SBR operation was alternated between aerobic and anoxic periods. Anoxic periods were primarily used in order to control the population of filamentous species. However, anoxic reactions resulted in accumulation of

extracellular intermediates which were not mineralized once aerobic conditions were restored. In this study, the discontinuous nature of SBRs is evident more than ever as diauxic phenomena were observed during cycles. Such phenomena cannot occur in continuous systems.

In the recent past, classical SBRs have been slightly modified in order to allow treatment of volatile compounds [Chozick and Irvine (1991)]. The modification involves the use of granular activated carbon as a temporary storage of volatiles such as toluene, and the use of membranes for oxygen supply in lieu of aeration which promotes volatilization. In this study, biofilms were formed on the submerged membranes but the results showed no problems from oxygen transfer to and through the biofilms.

The most recent trend in classical SBR research involves slurry systems [Irvine et al. (1993a, 1993b)] for treatment of contaminated soil. Experiments with soils contaminated with petroleum hydrocarbons, or bis-(2-ethylhexyl) phthalate (BEHP) have shown up to 96% treatment efficiencies, provided that the reactor was supplied with appropriate amounts of nitrogen and phosphorus.

2.4 Biodegradation in Continuously Operated Cyclic Reactors

As discussed in the introduction, a variation or extension of classical SBRs involves continuous cyclic operation of reactors. Studies with these reactors started in 1986 at the New Jersey Institute of Technology.

Chang (1987) and Baltzis et al. (1989) derived the first general equations for continuous cyclic operation of reactors employed in biodegradation of a single substrate by a pure culture under aerobic conditions. Calculations based on computer simulations showed that performance of this type of reactor operation can be always made superior to that of equivalent continuous flow reactors. Experiments were also performed with a pure culture of *P. putida* and phenol as the model compound. A subsequent study by Ko (1988) with the same model system was the first to show that the inhibitory kinetics of

phenol degradation lead to complex reactor dynamics. In fact, based on extensive simulations with the model and using time-consuming computer algorithms, this was the first study to demonstrate, experimentally as well as computationally, the existence of multiple outcomes (culture survival and washout) under identical operating conditions. Hence, it was the fist study to show multistability and start-up condition-dependent outcomes. Experimental data from the same study were used later by Lenas et al. (1994) in validating the analysis of the same system with advanced computational techniques which are based on the bifurcation theory for forced systems. Lenas et al. (1994) also performed the first study on optimizing cyclic operation and showed a methodology for selecting optimal values for various operating parameters.

Dikshitulu (1993) and Dikshitulu et al. (1993) studied cyclic operation and its importance in maintaining species diversity in the reactor. Using as model system two *Pseudomonas* sp. competing for phenol, these authors performed the first analysis of dynamics using principles of the bifurcation theory. They have also shown experimentally the existence of regimes in the operating parameter space where different outcomes occur (survival of one or the other of the species, coexistence of the competitors, culture wash-out). They have also shown multistability which seems to be a standard feature when substrate inhibition occurs.

Sanyal (1990), Baltzis et al. (1991), and Lewandowski and Baltzis (1992) examined denitrification in a continuously operated cyclic reactor. These studies involved calculations only. Based on kinetic data obtained from a pilot facility, removal of nitrate was described by Monod kinetics while nitrite removal was described by Andrews kinetics. These studies -based on simulations rather than systematic analysis of process dynamics- examined the effect of various parameters (minimum to maximum volume ratio, speed of filling the reactor, extent of cycle time) on the denitrification process. They have shown that under certain operating conditions nitrite remains practically untreated while nitrate can be completely removed. The results of these studies led to the

development of guidelines for reactor design which ensures complete removal of both nitrate and nitrite. These design criteria were used in the design of an actual facility which has been built for treating wastes from munitions manufacturing.

Detailed denitrification studies involving both experimental work as well as complete process analysis with modern computational techniques have been performed by Wang (1994) and Wang et al. (1995a, 1995b). These authors have performed detailed kinetic studies with a pure culture of *P. denitrificans* and shown that both nitrate and nitrite are removed following inhibitory kinetics. In addition, the authors found that the culture had very severe maintenance requirements which further complicated the dynamics of the system. Through a detailed analysis of the dynamics of the process when it occurs in a continuously operated cyclic reactor, these studies have shown that not only multistability occurs, but there are regimes in the operating parameter space where two survival states (implying two different degrees of denitrification) arise. The theoretical predictions have been fully validated through experiments with a 2-liter, fully automated unit.

Removal of mixtures of phenol and 4-chlorophenol in cyclically operated continuous reactors has been studied by Wang (1991). It was found that both substrates were degraded although 4-chlorophenol could not be removed in the absence of phenol. It was speculated at the time that 4-chlorophenol was cometabolized, however lack of detailed data such as chloride ion recovery do not allow for definite conclusion as to whether 4-chlorophenol was completely degraded or not. The results of the present study suggest that 4-chlorophenol was only converted to a stable intermediate.

Based on the foregoing discussion it becomes clear that there is a number of studies on the use of continuously operated cyclic reactors, and that these studies have used increasingly more elaborate experiments and computational methods. However there was no study involving the removal of two substitutable substrates under aerobic conditions, and this became the key objective of this dissertation.

CHAPTER 3

OBJECTIVES

The main objective of this study was to systematically investigate biological treatment of mixed substrates under aerobic conditions in a continuously operated cyclic reactor. This objective could not be met unless a model system was identified and detailed kinetic studies were performed with it. Thus, the first sub-objective was to select the model system.

Two approaches were followed in selecting the model system. The first was to use structurally similar compounds which could either both serve as carbon and energy sources for the culture, or one could serve as the carbon/energy source while the second substance could be cometabolized in the presence of the first. The second approach was to select structurally dissimilar compounds which could serve as substitutable carbon and energy sources for the culture.

In order to avoid complexities arising from population interactions, it was decided to use only pure cultures in the present study.

In view of the above, the objectives were set in the following sequence.

I. Kinetic studies with structurally similar compounds

This objective was met by studying the degradation of mixtures of phenol and 4-chlorophenol (4-CP). Two *Pseudomonas* cultures were used and were found to have the same behavior towards phenol but a drastically different behavior towards 4-CP. Spectroscopic studies were used in establishing the pathway for ring cleavage followed by each one of the cultures. The results of this study are presented in Chapter 5. Either of the two strains could have been used in meeting the main objective of the study, mentioned earlier. However, ultimately this was not possible as one of the cultures of

interest lost its activity at a certain point, while the other led to the formation of an unknown intermediate.

II. Kinetic studies with structurally dissimilar compounds

This objective was met by studying the kinetics of biodegradation of mixtures of phenol and glucose. Detailed studies, discussed in Chapter 6, have led to the determination of mathematical expressions describing the utilization rate of each substrate by the culture. Part of the work required for meeting this objective involved a series of experiments with media containing either glucose or phenol only as carbon and energy source for the culture.

III. Description of biodegradation of mixed substrates in a cyclic bioreactor and analysis of reactor dynamics

This objective was met by selecting the case of phenol/glucose mixtures as the model system. Utilizing the kinetic expressions determined in meeting objective II above, a general model was derived and then subjected to analysis of its dynamics by using computer codes based on the bifurcation theory for forced systems. The results from this study are presented in the first part of Chapter 7.

IV. Validation of the model and its predictions through experiments

A fully automated laboratory-scale unit operating in a continuous cyclic mode was used in meeting this objective. Experiments with media containing glucose and phenol at various concentration levels were performed. The design of the experiments from the point of view of selecting operating and start-up conditions was facilitated by calculations performed after objective III had been met. The theoretical predictions were validated, both at the qualitative and quantitative level, by the experiments. The results from this part of the study are presented in the second part of Chapter 7.

CHAPTER 4

MATERIALS AND METHODS

4.1 Microbial Cultures and Culture Media

In this work, experiments were performed with pure cultures of *Pseudomonas putida*. The culture came essentially from three sources. The first source, was inocula of *Pseudomonas putida* (ATCC 17514) purchased from the American Type Culture Collection (Rockville, MD). This culture was designated as *P. putida N*. The second source, was inocula from a culture which had been used in the laboratory for a period of over two years in experiments with phenol. Although the origin of this culture was again *P. putida* (ATCC 17514), it was found that it had a behavior towards 4-chlorophenol which was different from that of *P. putida N*. This culture was designated as *P. putida O*. After *P. putida O* had been used in a number of experiments, unfortunately, it lost its activity. However, it was revived through a new acclimation procedure and was designated as *P. putida OR*. All three strains (*O, N, OR*) could grow on glucose and phenol. Strains *N* and *OR* could not mineralize 4-chlorophenol, as opposed to strain *O*. Strains *N* and *O* were not used in experiments with glucose.

The media compositions, and the acclimatization procedures were the same as those described by Dikshitulu et al. (1993). These are as follows.

P. putida N was revived from freeze-dried samples by growing it in a nutrient broth of BBL product 11479 (Dickinson Microbiology Systems, Cockeysville, MD). The nutrient broth, after inoculation, was placed in an incubator at 30°C for about 24 h. Subsequently, a 2-mL sample from this culture was transferred to 100 mL of synthetic medium for acclimation on either phenol or 4-chlorophenol (4CP). The new suspension was placed in an incubator shaker (250 rpm, 28°C) until all phenol or 4CP had been depleted. At that point, a 2-mL sample was transferred to 100 mL of fresh synthetic

medium to form the secondary culture. The procedure was repeated once more, to get the tertiary culture. When the carbon source was depleted by the tertiary culture, the culture was declared "stock culture" and inocula from it were used in experiments.

Inocula of preexisting stock cultures of *P. putida OR* were acclimated to glucose by following the procedure described above with glucose (instead of phenol or 4CP) as the carbon source.

Stock cultures were maintained by spiking them periodically with the carbon source, and by occasionally transferring loops to fresh media when it was felt that chemicals other than the carbon source needed replenishment.

The synthetic media were prepared by adding phenol, glucose, and/or 4CP as required, from stock solutions carrying each substance at 2 kg m^{-3} to a 50 m*M* phosphate buffer (K_2HPO_4 and KH_2PO_4) solution of pH 7.2. This solution also contained (per liter of buffer), 0.5 g $(NH_4)_2SO_4$, 0.1g $MgSO_4$, 0.01g $MnSO_4$, 0.0005g $FeCl_3$, and 100 mL of tap water. Before any experiment, the synthetic waste (growth medium) was sterilized in an autoclave at 121°C for 20 min. The aforementioned chemicals as well as all others used in the experiments were A.C.S. certified and were purchased from Fisher Scientific (Fair Lawn, NJ).

4.2 Biomass and Chemical Assays

During various experiments the following quantities were determined: concentrations of biomass, phenol, 4CP, glucose; presence of 2-hydroxy-5-chloromuconic semialdehyde (2H5CMA); level of chloride ions.

4.2.1 Biomass Assay

The biomass concentration was determined by measuring the optical density of samples. The optical density was measured with a spectrophotometer (Varian DMS-200) at a wavelength of 540 nm, with deionized water as the reference sample. As discussed by

Dikshitulu et al. (1993), for optical densities up to 0.6, there was a linear relationship between optical density and biomass concentration, with a slope of 273.38 g m^{-3} per unit optical density. In rare cases, when the optical density of a sample exceeded 0.6, the sample was diluted with deionized water, and the measurement was repeated after thorough mixing.

4.2.2 Phenol and 4CP Assays

Phenol and 4CP concentrations were measured as follows. To a 5-mL sample taken from a shake-flask or the reactor, a drop of 6 N HCl solution was added to kill the microorganisms and ensure that the compounds of interest were in a non-ionized form. The sample was then filtered through a 0.2-μm filter paper (Gelman Sciences, Ann Arbor, MI) and the filtrate was immediately processed on a HPLC SP8800 (Spectra Physics Analytical, Piscataway, NJ). The mobile phase was a 55:45 volume ratio of methanol and deionized water. Each component of the mobile phase also contained acetic acid at 1% by volume. The flow rate of the mobile phase was 1 mL min^{-1}. The HPLC column was a Lichrosphere 60-RP-Select B (EM Separations, Gibbstown, NJ). The UV detector, a Spectra 200 (Spectra Physics Analytical, Piscataway, NJ), was set at a wavelength of 280 nm. The retention time was 2.4 min for phenol, and 4 min for 4CP. The data were processed on an IBM-compatible computer using a PE Nelson Model 2600 chromatography software Rev. 5.10. The data/computer interface was a PE Nelson 900 series interface (PE Nelson Systems Inc., Cupertino, CA). Calibration curves (which are shown in Figures A-1 and A-2) were originally prepared and then frequently tested with standard phenol and 4CP solutions to ensure the validity of the readings on actual samples.

4.2.3 Glucose Assays

Two different assays were used for glucose. They were both based on glucose diagnostic kits obtained from Sigma Chemical Co. (St. Louis, MO). Kit Sigma 510 was used in

cases where experiments were performed with glucose as sole carbon and energy source for the microbial culture. In experiments with both glucose and phenol as carbon and energy sources, kit Sigma 115 was used for monitoring the glucose concentration because the presence of phenol interfered with the glucose assay when kit Sigma 510 was used.

With kit Sigma 510, glucose concentration is determined via an enzymatic reaction involving glucose oxidase. The method involves use of a combined enzyme-color reagent solution which was prepared as follows. The contents of one capsule of PGO enzyme (Sigma 510-6) were added to 100 mL deionized water along with 1.6 mL of a color reagent solution. This color solution was prepared by reconstituting one vial of *o*-dianisidine dihydrochloride (Sigma 510-50) with 20 mL of water. The basis of the method is that when glucose is added to the combined enzyme-color reagent solution, it reacts with glucose oxidase to produce hydrogen peroxide. Hydrogen peroxide reacts with peroxidase and *o*-dianisidine dihydrochloride to form a brown colored solution of oxidized *o*-dianisidine. The final color intensity of the solution (obtained after completion of the reaction in 30 min at 37°C) is proportional to the glucose concentration.

The method was used as follows. A standard glucose solution of 50 g m^{-3} was originally prepared, as well as the combined enzyme-color reagent solution discussed above. Samples taken from the reactor at different instants of time were immediately filtered through a 0.2 μm pore size filter paper (Gelman Sciences, Ann Arbor, MI). In a test tube, labeled as "sample", 0.5 mL of the filtrate was transferred. In two other identical test tubes, labeled "standard" and "blank", 0.5 mL of the standard glucose solution and deionized water, respectively, was placed. Subsequently, 5 mL of combined enzyme-color reagent solution were added to each of the three tubes. After thorough mixing, the tubes were placed in an incubator at 37°C for 30 min. Then, the absorbance of the solutions in the "sample" and "standard" test tubes was measured (using the "blank" tube as a reference) at 450 nm by a Varian DMS-200 UV-Visible spectrophotometer. Since the absorbance is directly proportional to the glucose concentration, the readings for the

"standard" and "sample" test tubes yielded a direct measurement of the glucose concentration in the original sample. It should be added that the method is reliable for glucose concentrations up to 3 kg m^{-3}. If the glucose concentration in the original sample is higher than this upper limit, the sample needs to be diluted before the method is employed.

The glucose assay with the diagnostic kit Sigma 115 is based on an enzymatic reaction with hexokinase, which yields a colored final solution. For this method, the glucose assay reagent solution as well as a 0.1 N solution of HCl and a standard glucose solution (50 g m^{-3}) are needed.

The glucose assay reagent solution was prepared by reconstituting one vial of glucose enzyme reagent (Sigma 115-20) with 17 mL deionized water and then adding 4 mL of the color reagent solution (Sigma 115-5). The HCl solution was prepared by adding 8.6 mL of concentrated HCl to one liter of deionized water.

The measuring procedure was as follows. Samples from the reactor were first filtered through a 0.2 μm pore size filter paper (Gelman Sciences, Ann Arbor, MI). With a precisely adjustable digital microliter pipette (Pipetman, P-1000, Rainin Instrument Co. Inc., Woburn, MA) 0.02 mL of the filtrate, the standard glucose solution, and deionized water was placed in three identical test tubes. The tubes were labeled "sample", "standard", and "blank", respectively. To each of the three tubes, 1 mL of the glucose assay reagent solution was added. The contents of the tubes were mixed via gentle swirling, and allowed to stand at room temperature for 5 min. Subsequently, 10 mL of 0.1 N HCl were added to each tube. After thorough mixing, and using the "blank" tube as reference, the absorbance of the contents of the "standard" and "sample" tubes was measured at 520 nm with a Varian DMS-200 UV-Visible spectrophotometer. The whole test must be completed within 30 min after the addition of HCl in the tubes. The final color intensity is proportional to the glucose concentration. As in the case of kit Sigma 510 discussed earlier, the use of a standard glucose solution yields a direct measurement

of the glucose concentration in the original sample. The method is again reliable for glucose concentrations not exceeding 3 kg m^{-3}.

4.2.4 Assay for 2H5CMA

It has been reported (Molin and Nilsson, 1985) that when phenol is degraded via the *meta*-cleavage pathway the reaction medium (culture suspension) has a characteristic yellow color. The maximum absorbance of such media in the UV- Visible range occurs at 375 nm. This is indicative of the presence of 2-hydroxy-muconic semialdehyde (2-HMA).

When 4CP is transformed via the *meta*-cleavage pathway, another yellow intermediate is formed, 2-hydroxy-5-chloromuconic semialdehyde (2H5CMA) as reported by a number of researchers [e.g. Chaudhry and Chapalamadugu (1991); Knackmuss (1981); Knackmuss and Hellwig (1978); Rochkind et al. (1986)]

In the present study, in experiments involving 4CP and yielding a yellow color for the suspension, samples were scanned for their absorbance in the range from 300 to 550 nm with a Varian DMS-200 UV-Visible spectrophotometer. As discussed in Chapter 5 of this dissertation, the maximum absorbance occurred at 375 nm. As presence of 2-HMA was excluded, the absorbance was attributed to 2H5CMA.

4.2.5 Chloride Ions Assay

The concentration of chloride ions in experiments involving 4CP was monitored with an Orion Model 96-17B combination chloride electrode in conjunction with an Orion Model SA 720 pH / ISE (ion specific electrode) meter (Orion Research Inc., Boston, MA). Readings were taken in the millivolts range and converted to chloride ion concentrations through a calibration curve. Since the concentrations were typically below 10 g m^{-3}, the special procedure for low level concentration measurements, suggested by the manufacturer of the instrument, was followed with slight modifications. This procedure

requires allowance of adequate time for electrode stabilization. The calibration curve is shown in Figure A-3 and was prepared by following the instructions of the manufacturer as follows. An amount of 1 mL of low-level ISA (1.0 *M* $NaNO_3$, Ion Strength Adjuster; Orion Research Inc., Boston, MA) was added to 100 mL deionized water. To the resulting solution, amounts of a standard chloride ion solution were incrementally added in the following sequence: 0.1, 0.1, 0.2, 0.2, 0.4, 2, and 2 mL. The standard chloride ion solution was prepared by dissolving 1 g of NaCl in 1L of deionized water. The resulting chloride ion concentration in the standard was 607 g m^{-3}. After each addition of standard solution mentioned above, the low-level ISA solution was thoroughly mixed and the stable millivolt reading was recorded. After each addition, the millivolts corresponded to chloride ion concentrations of 0.6, 1.2, 2.4, 3.6, 6.0, 17.5, and 28.6 g m^{-3}. Based on these values, the curve shown in Figure A-3 was prepared.

During actual sample measurements, 0.05 mL of low-level ISA was added to a 5 mL sample. After mixing, the electrode was immersed into the vial and when the reading was stabilized on the display, it was recorded and subsequently converted to chloride ion concentration through the calibration curve.

4.3 Experimental Reactor Unit

A 7-L jacketed lucite reactor with an internal diameter of 16 cm was used in this study. For the runs under continuous cyclic operation, the maximum working volume was 4 L. The minimum working volume was always equal to one half of the maximum working volume (i.e., 2 L). The reactor was covered with a lid carrying ports. One port was used for sampling, while the others were used for fitting four air dispersion tubes, a dissolved oxygen probe (Series 900, New Brunswick Scientific Co., New Brunswick, NJ), a thermometer, as well as a feed and a discharge line. A magnetic stirrer was used for mixing the contents of the vessel. During the experiments, 28°C water was circulated through the jacket of the reactor.

Cyclic reactor operation was automated through the use of a programmable sequence controller (Omron, Model SCY-PO, Peabody, MA). The reactor was fed and discharged by using two flow pumps (Masterflex L/S Unified drives, Cole-Parmer Instrument Co., Niles, IL). The feed tank was kept in a water bath at 28°C. A schematic of the experimental unit is shown in Figure A-4.

During cyclic reactor operation, 5-mL samples were drawn at appropriate time intervals to measure concentrations of various components (biomass, phenol, glucose). The pH of the samples was also measured and found to be practically constant at values between 7.0 and 7.2.

To enhance oxygen transfer, diffuser stones were placed at the bottom of the reactor. The dissolved oxygen readings indicated that oxygen was present in the liquid at levels no less than 85 % of saturation.

Wall growth was never observed in the reactor. Occasionally though, biomass build-up was observed on the diffuser stones. In such cases, the experiments were stopped and the stones cleaned or replaced.

Before each experimental run, the reactor was washed with either a 75% methanol solution, or a dilute solution of hydrogen peroxide. Water was used for the second phase of cleaning.

The vessel discussed above was also employed in kinetic studies. The kinetics of utilization of glucose and phenol/glucose mixtures were investigated as discussed in Chapter 6 of this dissertation. For the kinetic studies, the controller was not activated and the reactor operated in the batch mode. The working volume of the reactor during the batch kinetic experiments was 0.5 L.

CHAPTER 5

BIODEGRADATION STUDIES WITH PHENOL AND 4-CHLOROPHENOL

5.1 General Approach

The first system examined in this dissertation involved phenol and 4-chlorophenol (4CP). These are structurally similar compounds and the objective was to determine if the two substances can be simultaneously used by pure cultures and eventually converted to biomass, carbon dioxide, and HCl (complete mineralization). Studies on the pathways of degradation of the two compounds by microorganisms have been discussed in Chapter 2.

The work presented here was performed in shake-flasks and employed two cultures, *P putida N* and *P. putida O*. In most cases, these cultures were first grown in a nutrient broth and then immediately used in the experiments discussed here without any prior lengthy acclimation to phenol and/or 4CP. Experiments were performed with three classes of media. The first contained only phenol as carbon source, the second involved mixtures of phenol and 4CP, while the third involved 4CP as the only chemical containing carbon. Another category of experiments involved the use of filtrate from the experiments mentioned above.

5.2 Experimental Results and Discussion

The experimental results are given in Tables B-1 through B-10 of Appendix B, and show optical density, phenol and 4CP concentration values, and readings from the chloride electrode. Conditions for each experiment are given in the heading of each table.

Tables B-1 and B-2 show results from experiments involving phenol only with strains *N* and *O*, respectively. As can be seen from these tables both cultures exhibited a similar behavior. Both grew on phenol as can be seen especially from the data after the second spike with phenol. The data from the initial spike indicate a relatively large

increase in the optical density (biomass formation). This is probably due to the existence of residual carbon source from the nutrient broth in which the cultures were originally grown. The same observation holds for the experiments reported in Tables B-3-B-6. Based on the data after the second spike with phenol one can see that the yield coefficients are essentially the same. More specifically, a value of 0.34 g-biomass/g-phenol can be calculated for strain *N* and a value of 0.39 for strain *O*. As expected, the readings from the combined chloride electrode are constant throughout the runs. These readings correspond to a chloride ion presence at levels of about 0.8 g m^{-3}, and are due to $FeCl_3$ present in the growth medium. The behavior of the two strains is the same even from the spectroscopic point of view, as can be seen from Figure B-1. These spectra indicate that there is no metabolite accumulating in the medium (reactor). At this point one should mention that when phenol is degraded via the *meta*-cleavage pathway, it produces 2-hydroxy-muconic-semialdehyde (2HMA) which has been reported to absorb at 375 nm [Molin and Nilsson (1985)]. Samples from neither culture exhibited a peak at 375 nm as can be seen from Figure B-1. However, this is not necessarily an indication that the two strains do not follow the *meta*-cleavage pathway. Since 2HMA is not a dead-end product, its life-span may be (and probably is) well below 24 h which was the time at which the first spectra were obtained.

The behavior of the two strains towards mixtures of phenol and 4CP was different, as can be seen from Tables B-3 and B-4. Although both phenol and 4CP disappeared from the flasks with either strain *N* or strain *O*, chloride recovery was complete only in the experiment with strain *O* (Table B-4). The percent chloride recovery at any time t was calculated as follows. The reading from the combined chloride electrode at time t was converted to g-Cl^- m^{-3} via the calibration curve shown in Figure A-3; thus, a value B was obtained. The same was done with the reading in the beginning of the experiment; thus a value A was obtained. The total amount of chloride contained in the 4CP added in the reactor from the beginning of the experiment to time t was calculated

using 4CP concentrations, 4CP and Cl^- molecular weights, and taking into account any effect from dilution with medium (if it occurred); thus a value C was obtained. The percent recovery (R) was calculated through the formula (A-B)/C.

Strains *N* and *O* in experiments K2-N and K2-O behaved differently from the spectroscopic point of view as well. This can be seen from the spectra shown in Figure B-2. The spectra from experiment K2-O show no sign of presence of any intermediate and are qualitatively similar to those shown in Figure B-1. On the contrary, the spectra from experiment K2-N show a pronounced peak at 375 nm. Since from experiments K1-N and K1-O it was determined that 2HMA is not detected 24 h into the experiment, this peak was attributed to 2H5CMA which is structurally very similar to 2HMA. Based on this evidence, it appears that strain *O* follows the *ortho*-cleavage pathway, while strain *N* follows the *meta*-cleavage pathway. However, more concrete conclusions can be reached after the next two experiments are discussed.

Experiments K3-N and K3-O which are reported in Tables B-5 and B-6, respectively, were performed with media containing 4CP but no phenol. Again, the two strains exhibited a completely different behavior. Strain *O* could degrade, and actually mineralize 4CP. There are three pieces of evidence which support this conclusion: increase in optical density (thus, biomass production), essentially complete recovery of chloride, and no indication of intermediates from spectroscopic analysis. These facts can be seen from Table B-6 and Figure B-3. To the contrary, strain *N* could not even utilize 4CP (see second spike in Table B-5).

Using the evidence from experiments K2-N, K2-O, K3-N, and K3-O the following conclusions can be reached. Strain *P. putida O* can utilize and metabolize 4CP regardless of whether 4CP is supplied to the culture as sole carbon and energy source, or in mixture with phenol. This points toward a conclusion that strain *O* follows the *ortho*-cleavage pathway. Since no special acclimation of the culture to 4CP was needed, this culture appears to utilize the *ortho*-cleavage pathway (i.e., 1,2-dioxygenase enzyme

system) towards both phenol and 4CP. This finding is very interesting and puzzling at the same time. It is interesting because it seems to contradict existing reports, mentioned in Chapter 2, which have concluded that the *meta*-cleavage pathway is the one followed. It is puzzling for two reasons. First, the initial origin of the strain is the same as that of *P. putida N*. Second, if both the *ortho*- and the *meta*-cleavage enzymes coexist [Bayly and Barbour (1984)] why did the *ortho*-pathway prevailed especially since Knackmuss (1981) reports that the *ortho*-enzymes are less efficient than the *meta*-cleavage enzymes?

Regarding *P. putida N* the situation seems much more complex. Clearly, it cannot use 4CP alone. However, it can transform it to 2H5CMA in the presence of either phenol (see Figure B-2) or the carbon source present in the nutrient broth (see Table B-5 for the first spike, and the spectra shown in Figure B-3). The results of experiment K3-N seem to indicate that even if some *meta*-cleavage enzymes are present, they get deactivated (or inhibited), as evidenced by the fact that 4CP levels remain constant after the second spike. This seems to agree with the claim of Knackmuss (1981) that 4CP is a "suicide substrate". On the other hand, experiment K2-N does not seem to support the notion of "suicide substrate", unless the continuing addition of phenol induces formation of new quantities of 2,3-dioxygenase which, probably, get subsequently inhibited by 4CP. Furthermore, there is the indication of some chloride recovery in both experiments K2-N and K3-N which does not agree with the results of Knackmuss (1981) although it appears to agree with those of Rochkind et al. (1986). There is no information at this point that could explain this chloride release.

In order to investigate whether the two strains exhibited the same or a different behavior towards 2H5CMA, the following experiments were performed. An amount of the suspension from the end of experiment K2-N was filtered and divided in two equal portions. The two portions were inoculated with amounts of suspensions from the end of either experiment K1-N or K1-O. The amounts of suspension added were such that the two portions of the filtrate from experiment K2-N had approximately the same optical

density after inoculation. The data from these two experiments (K4-N and K4-O) are reported in Tables B-7 and B-8. As expected, strain *N* cannot grow on the accumulated intermediate (2H5CMA). The same is true for strain *O*. This can be seen from the fact that the optical density does not change. The behavior is identical even from the spectroscopic point of view. This can be seen from the spectra shown in Figures B-4 and B-5. Since the spectra shown in Figure B-4 were taken immediately after inoculation, they should be identical since the same medium was used in both experiments. Interesting is the fact that the spectra are identical even 50 h after inoculation, as shown in Figure B-5. From this evidence, one can conclude that once 2H5CMA is formed, it cannot be utilized by either strain *N* or *O*. However, it is very interesting that 2H5CMA seems to be undergoing further transformation. This can be seen from the decrease in the reading from the chloride electrode (chloride recovery) reported in Tables B-7 and B-8, as well as from the decreasing absorbance at 375 nm (Tables B-7 and B-8; comparison of Figures B-4 and B-5). As also discussed earlier, this is contrary to the report of Knackmuss (1981), but in accord with the report of Rochkind et al. (1986). As indicated in Tables B-7 and B-8, 50 h after the original inoculation more biomass and fresh medium was added to the reactors. The intent was to examine whether depletion of some essential nutrients prevented the utilization of 2H5CMA. As the results indicate, through the observed constant optical density, this was not the case.

Results similar to those obtained from experiment K4-N and K4-O were obtained from experiment K5-O. This experiment was performed by inoculating the suspension obtained at the end of experiment K3-N with suspension from experiment K1-O. The results are shown in Table B-9. As can be seen from the table, strain *P. putida O* initially grew by metabolizing 4CP which was present in the medium. However, it showed no action again toward 2H5CMA.

One more experiment, in many ways similar to K4-O, was performed as follows. Originally, an inoculum of *P. putida N* was grown in nutrient broth. At a certain instant of

time the medium was spiked with both phenol and 4CP at a concentration ratio of 2:1. Measurements made 43 h after spiking with phenol and 4CP indicated growth of biomass but essentially no chloride recovery, as was the case with experiment K2-N. At that point, the medium was spiked with a quantity of 4CP which resulted in a concentration of 67 g m^{-3}. Measurements made 22 and 45 h after this second spiking, revealed that 4CP was present at a level very close to the original 67 g m^{-3}, while absorbance at 375 nm decreased. This part of the experiment resembles experiment K3-N. Subsequently, the culture was inoculated with suspension from experiment K1-O. The results from this part of the experiment, which is similar to experiment K4-O, are reported in Table B-10. Again, some biomass growth is observed (in the first 25 h), probably due to the mineralization of 4CP by *P. putida O.* However, the peak at 375 nm remains and indicates no action of the culture towards 2H5CMA. These facts can be also seen from the spectra shown in Figures B-6 and B-7. These spectra were taken immediately, and 25 h after inoculation with *P. putida O.* The samples were scanned at wavelengths reaching lower values than those of spectra discussed earlier. In Figure B-6 one can observe two peaks; one at 375 nm which is indicative of the presence of 2H5CMA, and one at 280 nm which is indicative of the presence of 4CP. Although 4CP is depleted, and thus the peak at 280 nm disappears (Figure B-7), the one at 375 nm remains albeit with a lower intensity.

5.3 Conclusions

Based on the work presented in this chapter, the following conclusions have been reached.

Mere disappearance of a compound does not ensure that it is completely mineralized. While with single pollutants biomass growth can essentially guarantee complete mineralization, this is not true with mixed pollutants. Earlier results of Wang (1991) from SBR experiments with *P. putida N* had shown that both phenol and 4CP

disappeared. However the results of the present study suggest that 4CP was not really completely mineralized. Most probably, the effluent contained 2H5CMA which is toxic and may be unacceptable for discharge. The fact that 4CP was not mineralized can possibly also explain why there was poor agreement between theory and experimental results in the aforementioned study.

The studies with strains *P. putida N* and *P. putida O* performed here have revealed a number of interesting results. Since the origin of *P. putida O* was the same as that of *P. putida N*, the results imply that extensive use of a culture may lead to different biodegradation pathways. Contrary to the seemingly well established belief that *P. putida* follows always the *meta*-cleavage pathway in degrading phenol, the results of the present study have shown that this is not always true. The results also indicate that in cases where 2H5CMA is formed, it appears that it is not a dead-end intermediate. It is further transformed to other compounds with a concomitant release of chloride through a mechanism which is unknown.

If an intermediate which is toxic is formed, it may not be easy to metabolize it by other species. This study for example, has shown that 2H5CMA cannot be degraded by *P. putida O*. However it is worth noticing that 2H5CMA appeared not to affect the activity of *P. putida O* toward 4CP. One could conclude then that accidental releases of new compounds into a system designed to treat certain pollutants may have an effect on process performance ranging from minor (as the present study seems to indicate) to major [as reported by Knackmuss (1981)].

Clearly, the original intent was to perform detailed kinetic studies employing *P. putida O* which was found to be capable of completely mineralizing both phenol and 4CP, and determine the kinetic expressions in explicit mathematical form. However, this was not accomplished because, for some unknown reason, *P. putida O* lost completely its activity towards phenolics (chlorinated or not). Although the culture was eventually revived, adaptation and acclimation took a considerable amount of time. Furthermore, it

never seemed to regain its activity towards 4CP. This could be due to the fact that acclimation was performed in shake-flasks where oxygen may not be as abundant as in an aerated reactor and, as Knackmuss (1981) suggests, under such conditions the mechanism of *ortho*-cleavage of a ring structure is less efficient. After reacclimation, strain *P. putida O* was designated as *P. putida OR* to denote the fact that the two cultures had a different behavior towards 4CP.

CHAPTER 6

KINETIC STUDIES ON THE UTILIZATION OF GLUCOSE AND MIXTURES OF PHENOL AND GLUCOSE BY CULTURE *P. putida OR*

In this chapter the results of the kinetic studies on the utilization of glucose and mixtures of phenol and glucose are presented. The culture employed in this work was *P. putida OR*. The experiments were performed under batch conditions in an aerated reactor so that reaction rates were not limited by the levels of dissolved oxygen in the media. The materials and methods for these experiments have been discussed in Chapter 4. The experiments with media containing glucose as the sole carbon and energy form were performed in order to determine some of the kinetic constants which are valid even in cases where the medium contains phenol in addition to glucose. Some experiments were also performed with media containing phenol but not glucose. The results of these experiments could be perfectly described when the kinetic constants obtained by Dikshitulu (1993) were used. The aforementioned study had used the same culture and media hence, it is no surprise that the values of the kinetic constants were valid here as well. The greatest emphasis for the work presented in this chapter was placed on the experiments with media containing both phenol and glucose as carbon and energy sources. The objective was to determine detailed mathematical expressions for the reaction rates so that they could be subsequently used in reaction engineering studies (discussed in Chapter 7).

6.1 Kinetics of Glucose Utilization

A series of batch kinetic experiments with media containing glucose as the sole carbon and energy source was performed in order to determine the specific growth rate and yield coefficient of species *P. putida OR* on glucose. The raw data from the eight experiments

performed are shown in Tables C1-2 through C1-9 of Appendix C1. The data from each experiment were plotted as shown in Figures 6.1 and C1-1 through C1-7. The lnb versus t (where b is biomass concentration and t is time) graphs allowed determination of the extent of the lag phase and the specific growth rate $\mu_2(s_2)$. The value of $\mu_2(s_2)$ was obtained as the slope of the line to which the initial lnb versus t data (after the lag phase) from each run were regressed. This value of $\mu_2(s_2)$ was attributed to a glucose concentration (s_2) value equal to the average of all s_2-values falling between the initial and final data points used in determining $\mu_2(s_2)$, i.e., the points in the linear regime of lnb versus t. The glucose and biomass concentration values corresponding to the points used in determining $\mu_2(s_2)$ were also plotted against each other on an arithmetic scale as shown in graphs (b) of Figures 6.1 and C1-1 though C1-7. As can be seen from the graphs, the data fall on a straight line. The negative slope of these lines represents the yield coefficient (Y_2) of the culture on glucose.

A summary of the information obtained from the kinetic runs is shown in Table C1-1. As can be seen from that table, it was found that the value of $\mu_2(s_2)$ increases with s_2, while the value of the yield coefficient is essentially independent of the value for the glucose concentration. These findings suggest that *P. putida OR* grows on glucose following Monod-type kinetics and does not have maintenance requirements.

In order to determine the values of the two parameters involved in the Monod expression, the values of $s_2/\mu_2(s_2)$ were plotted against the values of the corresponding s_2. This means that the Hanes-Woolf plot was prepared [Shuler and Kargi (1992)]. A least-squares linear regression was performed, and the slope and intercept of the resulting line revealed the value for μ_{m2} and K_2 based on the expression,

$$\frac{s_2}{\mu_2(s_2)} = \frac{1}{\mu_{m2}} s_2 + \frac{K_2}{\mu_{m2}} \qquad (6.1)$$

The linear regression had a R^2 value of 0.999. It was found that $\mu_{m2} = 0.84\ h^{-1}$ and $K_2 = 29.84\ g\ m^{-3}$. Based on these values, the $\mu_2(s_2)$ curve was generated and plotted in

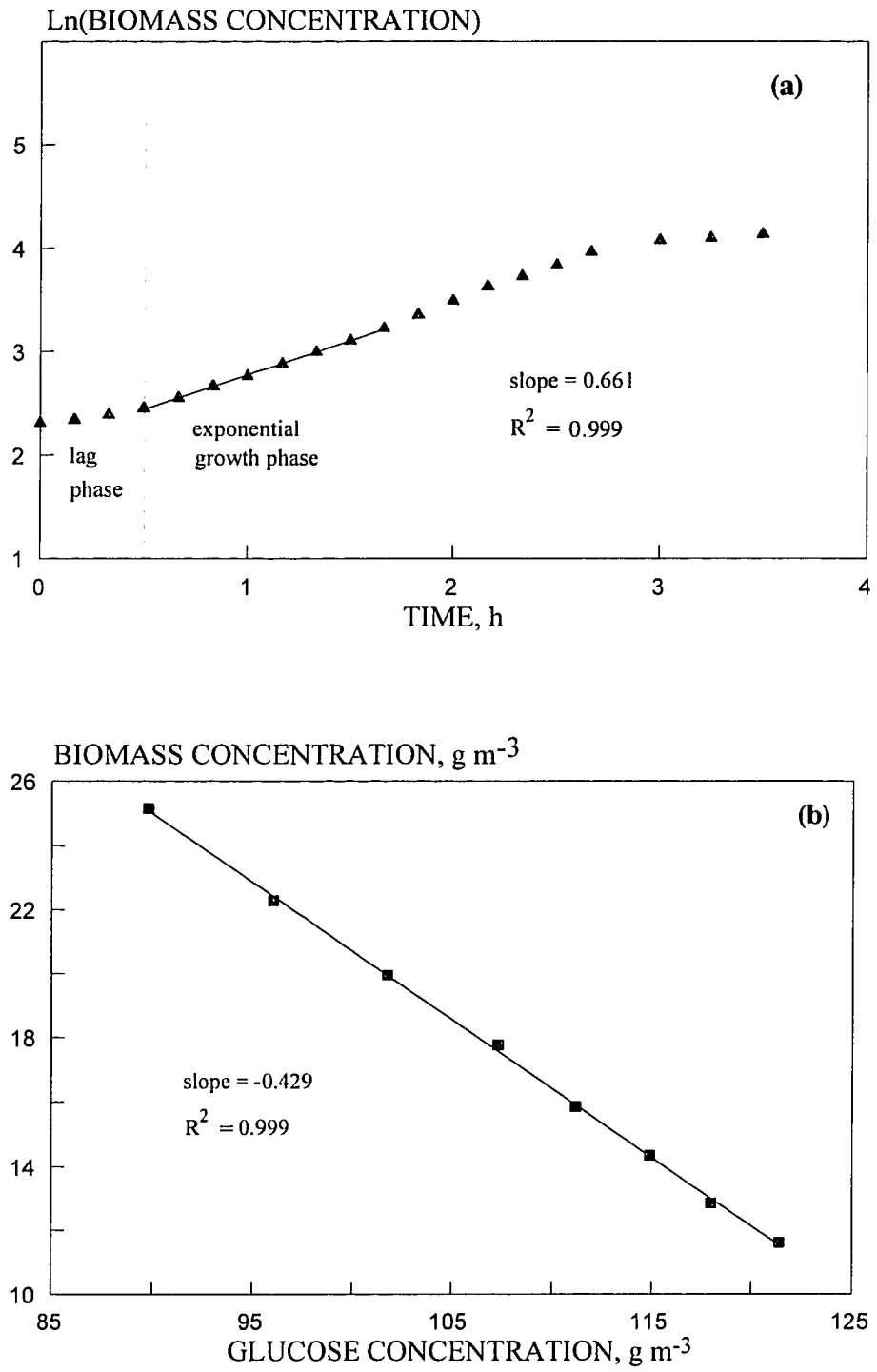

Figure 6.1 Determination of the specific growth rate (a) and yield coefficient (b) of *P. putida OR* on glucose from experiment G-6.

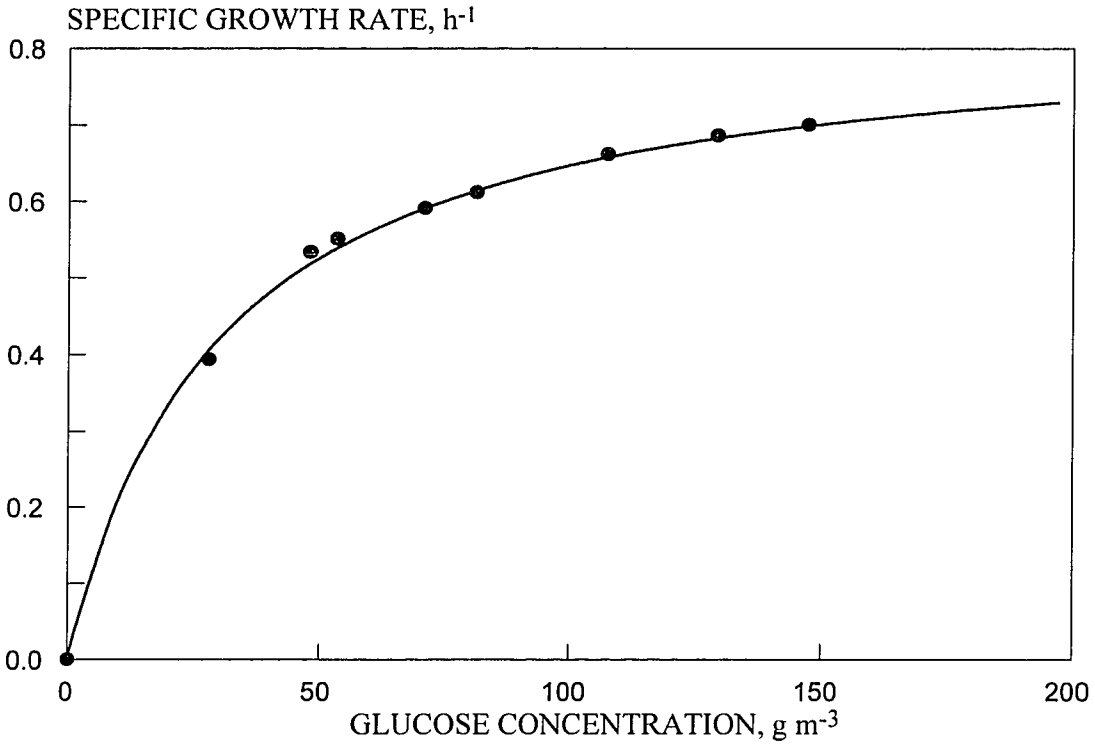

Figure 6.2 Data for the specific growth rate of *P. putida OR* on glucose. The data have been fitted to the Monod expression.

Figure 6.2. As can be seen from the diagram there is an excellent agreement between the data (shown as symbols) and the fitted curve.

The value of the yield coefficient was taken as 0.44 g-biomass/g-glucose which is the average of all values reported in Table C1-1.

While the specific growth rate was determined based on the initial data from the exponential phase of growth, the kinetic parameters determined should allow a good description/prediction of all data in the exponential phase of growth. For this to be tested, the following equations were integrated,

$$\frac{db}{dt} = \frac{\mu_{m2} s_2}{K_2 + s_2} b \qquad (6.2)$$

$$\frac{ds_2}{dt} = -\frac{1}{Y_2} \frac{\mu_{m2} s_2}{K_2 + s_2} b \qquad (6.3)$$

The above two equations imply that,

$$-Y_2\, ds_2 = db \tag{6.4}$$

which upon integration yields the following relationship,

$$Y_2\,(s_{2,o} - s_2) = b - b_o \tag{6.5}$$

When equation (6.5) is used, equation (6.3) can be written as

$$\frac{ds_2}{dt} = -\frac{1}{Y_2}\frac{\mu_{m2} s_2}{K_2 + s_2}[Y_2(s_{2,o} - s_2) + b_o] \tag{6.6}$$

Equation (6.6) can be integrated analytically, and it leads to the following relationship.

$$\frac{b_o + Y_2(K_2 + s_{2,0})}{b_o + Y_2 s_{2,0}} \ln\frac{b_o + Y_2(s_{2,0} - s_2)}{b_o} - \frac{Y_2 K_2}{b_o + Y_2 s_{2,0}} \ln\frac{s_2}{s_{2,o}} = \mu_{m2} t \tag{6.7}$$

A simple computer code based on equations (6.7) and (6.5) was written and is given in Appendix E-1. Using as initial conditions (i.e., $s_{2,o}$ and b_o) the values corresponding to the end of the lag phase of each experiment, this code yielded the time-concentration profiles.

The computed glucose and biomass concentration profiles were plotted versus time as shown in Figures 6.3 and C1-8 through C1-14. On these graphs the actual data are also shown (as symbols) for comparison. As can be seen from the graphs, the agreement between data and predicted curves is good provided that the glucose concentration does not fall below a value of about 20 g m^{-3}. It should be kept in mind that all kinetic experiments were performed with initial glucose concentrations above 30 g m^{-3}. This may explain the discrepancy between predictions and actual data, since experimental values of $\mu_2(s_2)$ were not determined for $s_2 < 20$ g m^{-3} and thus, they have not influenced the values of the parameters in the $\mu_2(s_2)$ expression. It should be also added that in almost all cases [e.g., Dikshitulu (1993), Wang (1994)] predicted concentration profiles fail to follow data at low substrate concentrations. Despite this problem, the determined kinetic parameter values can be used with confidence in predicting concentration profiles over a wide range of values.

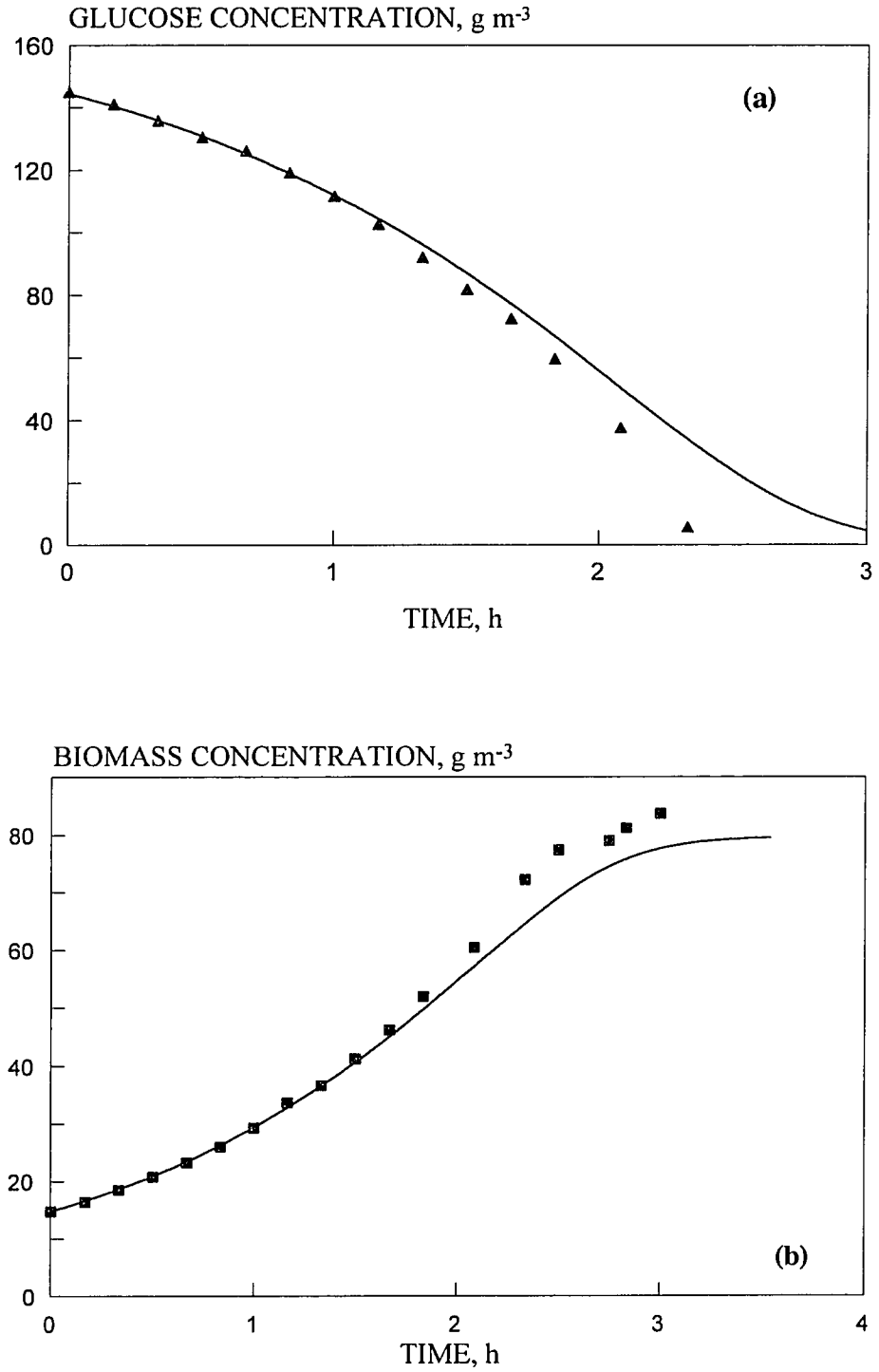

Figure 6.3 Comparison between experimentally obtained and model predicted concentration profiles for glucose (a) and biomass (b) for experiment G-7.

6.2 Kinetics of Simultaneous Utilization of Phenol and Glucose

Once culture *P. putida OR* was acclimated in media containing both glucose and phenol, it was found that it could utilize both carbon sources simultaneously. Subsequently, batch experiments were performed in order to determine the kinetics of glucose utilization in the presence of phenol, and the kinetics of phenol utilization by the culture in the presence of glucose. Information about these experiments, along with the raw data collected, is given in Appendix C2 of this dissertation.

Since it was known that both phenol (substrate S_1) and glucose (substrate S_2) can serve as carbon and energy sources for the culture, the basic equations describing the removal of phenol and glucose mixtures in a batch reactor were written as,

$$\frac{ds_1}{dt} = -\frac{1}{Y_1}\mu_1(s_1,s_2)b \qquad (6.8)$$

$$\frac{ds_2}{dt} = -\frac{1}{Y_2}\mu_2(s_2,s_1)b \qquad (6.9)$$

$$\frac{db}{dt} = [\mu_1(s_1,s_2)+\mu_2(s_2,s_1)]b \qquad (6.10)$$

Equations (6.8)-(6.10) represent mass balances on phenol, glucose, and biomass, respectively. Expression $\mu_1(s_1,s_2)$ represents the specific growth rate of the culture on phenol when glucose is also present. Similarly, expression $\mu_2(s_2,s_1)$ represents the specific growth rate of the culture on glucose when phenol is also present in the medium.

The above model formulation allows for kinetic interactions between the two substrates since the specific growth rates are represented by functions depending on the concentration of both substances. The assumptions involved in the model derivation are that there are no maintenance requirements, and that the yield coefficient on a substrate is unaffected by the presence of any other substrate. Hence, the value of Y_2 is taken as 0.44 g-biomass/g-glucose as was found from experiments with media containing glucose but not phenol (see the preceding section).

In the absence of phenol (i.e., when $s_1 = 0$) expression $\mu_2(s_2,s_1)$ reduces to $\mu_2(s_2)$ which is the expression revealed in the preceding section, i.e.,

$$\mu_2(s_2) = \frac{\mu_{m2} s_2}{K_2 + s_2} \tag{6.11}$$

with $\mu_{m2} = 0.84\ h^{-1}$ and $K_2 = 29.84\ g\ m^{-3}$.

In the absence of glucose (i.e., when $s_2 = 0$) expression $\mu_1(s_1,s_2)$ reduces to $\mu_1(s_1)$ which is the specific growth rate of the culture on phenol, when phenol is the sole carbon and energy source in the medium. As has been discussed in Chapter 4, culture *P. putida OR* was revived from another strain *P. putida O*. The specific growth rate of *P. putida O* on phenol was known [Dikshitulu (1993)] to be,

$$\mu_1(s_1) = \frac{\hat{\mu}_1 s_1}{K_1 + s_1 + \frac{s_1^2}{K_I}} \tag{6.12}$$

with $\hat{\mu}_1 = 0.897\ h^{-1}$, $K_1 = 12.204\ g\ m^{-3}$, and $K_I = 203.678\ g\ m^{-3}$. From the same study it was known that $Y_1 = 0.768$ g-biomass/g-phenol.

If the specific growth rate and yield coefficient of *P. putida OR* on phenol are the same as those of *P. putida O*, then batch experimental data from runs with *P. putida OR* in media containing phenol as the sole carbon source should be predicted by integrating equations (6.8)-(6.10) along with expression (6.12) and setting $s_2 = 0$. The values for the kinetic parameters should be those mentioned earlier from the study of Dikshitulu (1993). In order to test if this was the case, some experiments with *P. putida OR* and phenol as sole carbon and energy source were performed. Three such experiments (PG-4, PG-8, and PG-12) were performed and are reported in Appendix C2. Comparisons between experimental data and model predictions (assuming identical kinetics for *P. putida O* and *P. putida OR* on phenol) are shown in Figure C2-1. As can be seen from the diagrams of this figure, the agreement between data and predictions is very good. Hence, it was

concluded that the specific growth rate of *P. putida OR* on phenol, when glucose is absent from the medium, is the same as that of *P. putida O.*

In order to determine whether there is kinetic interference from phenol on glucose and vice versa, the kinetic experiments were carefully planned as follows. All experiments were performed with essentially the same initial biomass concentration. Initial phenol and glucose concentrations were selected so that experiments could be classified in groups each one of which comprises of runs with the same initial phenol (or glucose) concentration and varying glucose (or phenol) initial concentration. Interference was judged from the values of the (per unit biomass) specific removal rate of phenol (R_1) and glucose (R_2) by the culture. The values of R_1 and R_2 were calculated as time averages of experimental values and thus, one value for R_1 and one for R_2 were determined from each experiment.

The raw data are shown in Appendix C2 while a summary and partial analysis of them is shown in Tables 6-1 and 6-2. In these tables, the initial phenol and glucose concentrations are not the actual ones (see Appendix C2) but the real numbers have been brought to the closest round number to allow easier comparisons. In any case, the deviation between concentration values reported in Tables 6-1 and 6-2, and the actual ones do not exceed 3 g m^{-3}.

As can be seen from Table 6-1 when the initial value of phenol concentration is constant while that of glucose varies among experiments, the value of R_1 decreases as the glucose presence increases. This implies that glucose exerts a negative (inhibitory) effect on the specific rate of phenol removal. Similarly, from Table 6-2 it can be seen that when the initial glucose concentration is constant while that of phenol varies, the value of R_2 decreases as the phenol presence increases. This suggests that phenol exerts an inhibitory (negative) effect on the specific rate of glucose utilization. From the foregoing discussion it can be concluded that phenol and glucose are involved in a cross-inhibitory kinetic interaction.

Table 6-1 Average specific rate of phenol removal (R_1) by *P. putida OR* in the presence of glucose. For all experiments the initial biomass concentration was about 13.7 g m^{-3}.

Experiment[1]	$s^2_{1,o}$ (g m^{-3})	$s^3_{2,o}$ (g m^{-3})	R_1 (g-phenol / h /g-biomass)
PG-1	100	100	0.26
PG-2	100	50	0.37
PG-3	100	33	0.47
PG-4	100	0	0.55
PG-5	50	100	0.31
PG-6	50	50	0.36
PG-7	50	25	0.44
PG-8	50	0	0.65
PG-9	25	100	0.32
PG-10	25	50	0.36
PG-11	25	25	0.42
PG-12	25	0	0.69

[1] Information for these experiments is given in Appendix C2.
[2] Approximate value of the initial phenol concentration for the experiment.
[3] Approximate value of the initial glucose concentration for the experiment.

In order to quantify the cross-inhibitory interaction, two different modifications of kinetic expressions (6.11) and (6.12) were tried. These were as follows,

$$\mu_1(s_1,s_2)=\frac{\hat{\mu}_1 s_1}{K_1+s_1+\dfrac{s_1^2}{K_I}+K_3' s_2},\qquad \mu_2(s_2,s_1)=\frac{\mu_{m2}s_2}{K_2+s_2+K_4' s_1} \tag{6.13}$$

$$\mu_1(s_1,s_2)=\frac{\hat{\mu}_1 s_1}{K_1+s_1+\dfrac{s_1^2}{K_I}+K_3 s_1 s_2},\qquad \mu_2(s_2,s_1)=\frac{\mu_{m2}s_2}{K_2+s_2+K_4 s_2 s_1} \tag{6.14}$$

Using the terminology of enzyme kinetics [Shuler and Kargi (1992)], expressions (6.13) imply that phenol and glucose are involved in a competitive cross-inhibitory

Table 6-2 Average specific rate of glucose removal (R_2) by *P. putida OR* in the presence of phenol. For all experiments the initial biomass concentration was about 13.7 g m^{-3}.

Experiment[1]	$s^3_{2,o}$ (g m^{-3})	$s^2_{1,o}$ (g m^{-3})	R_2 (g-glucose / h /g-biomass)
PG-1	100	100	0.50
PG-5	100	50	0.73
PG-9	100	25	0.84
G-5	100	0	1.03
PG-2	50	100	0.51
PG-6	50	50	0.66
PG-10	50	25	0.74
G-2	50	0	0.84
PG-7	25	50	0.60
PG-11	25	25	0.65
G-1	25	0	0.83

[1] Information for these experiments is given in Appendices C1 and C2.
[2,3] Defined as in Table 6-1.

interaction. On the other hand, expressions (6.14) imply that the two substrates are involved in an uncompetitive cross-inhibitory pattern. Competitive inhibition arises when the substrates are structurally similar molecules and compete for the active sites of the enzyme system. Uncompetitive inhibitors bind to the complexes formed between a substrate and its enzyme system, and have no affinity for the enzymes themselves. Since phenol and glucose are not structurally similar, the likelihood that expressions (6.13) are indeed valid is low. However, both expressions (6.13) and (6.14) were tested against the experimental data.

Testing of the data against expressions (6.13) and (6.14) was performed through integration of equations (6.8)-(6.10) along with either expressions (6.13) or (6.14).

Integration was performed numerically with a code which is based on a fourth-order Runge-Kutta routine. This code is given in Appendix E-2 of this dissertation.

Whether expressions (6.13) or (6.14) are used, there are two kinetic constants $K_3^{'}$ and $K_4^{'}$, or K_3 and K_4 which are unknown. For this reason a fitting approach was used. The experimental sets were first divided in two groups. Data from runs PG-1, PG-2, PG-5, and PG-6 were used in fitting the pair of unknown constants. Use of expression (6.13) yielded very poor results (as anticipated) while a good agreement between data and fitted curves was obtained with expressions (6.14) with values K_3 = 0.038 g^{-1} m^3 and K_4 = 0.022 g^{-1} m^3. The agreement between data and fitted curves can be seen from the diagrams of Figures C2-2 and C2-3. Once the values of K_3 and K_4 were determined, equations (6.8)-(6.10) along with expressions (6.14) were integrated in order to predict the concentration profiles for the experimental sets (PG-3, PG-7, PG-9, PG-10, PG-11) which were not used in the fitting approach. Comparisons between experimentally obtained and model predicted concentration profiles are shown in Figures 6.4 and C2-4. The agreement is good (with the usual exception at low substrate concentrations) which implies that the values of K_3 and K_4 mentioned earlier can be used with confidence in describing the simultaneous removal of any mixture of phenol and glucose by *P. putida OR*. The K_3 to K_4 ratio is 1.75 which suggests that glucose inhibits the specific rate of phenol removal much more than phenol inhibits the specific rate of glucose removal.

The results obtained here regarding substrate interactions agree qualitatively with those of Papanastasiou and Maier (1982), and partially with those of Rozich and Colvin (1986). Both these studies, as discussed in Chapter 2, have shown that glucose hinders the removal of pollutants. On the other hand, the results obtained here, appear to disagree with those of Schmidt et al. (1987) and Hess et al. (1990, 1993). As has been discussed in Chapter 2, these studies have found that the presence of glucose exerts a positive effect on the removal of recalcitrant compounds such as *p*-nitrophenol and 2,4-dinitrophenol.

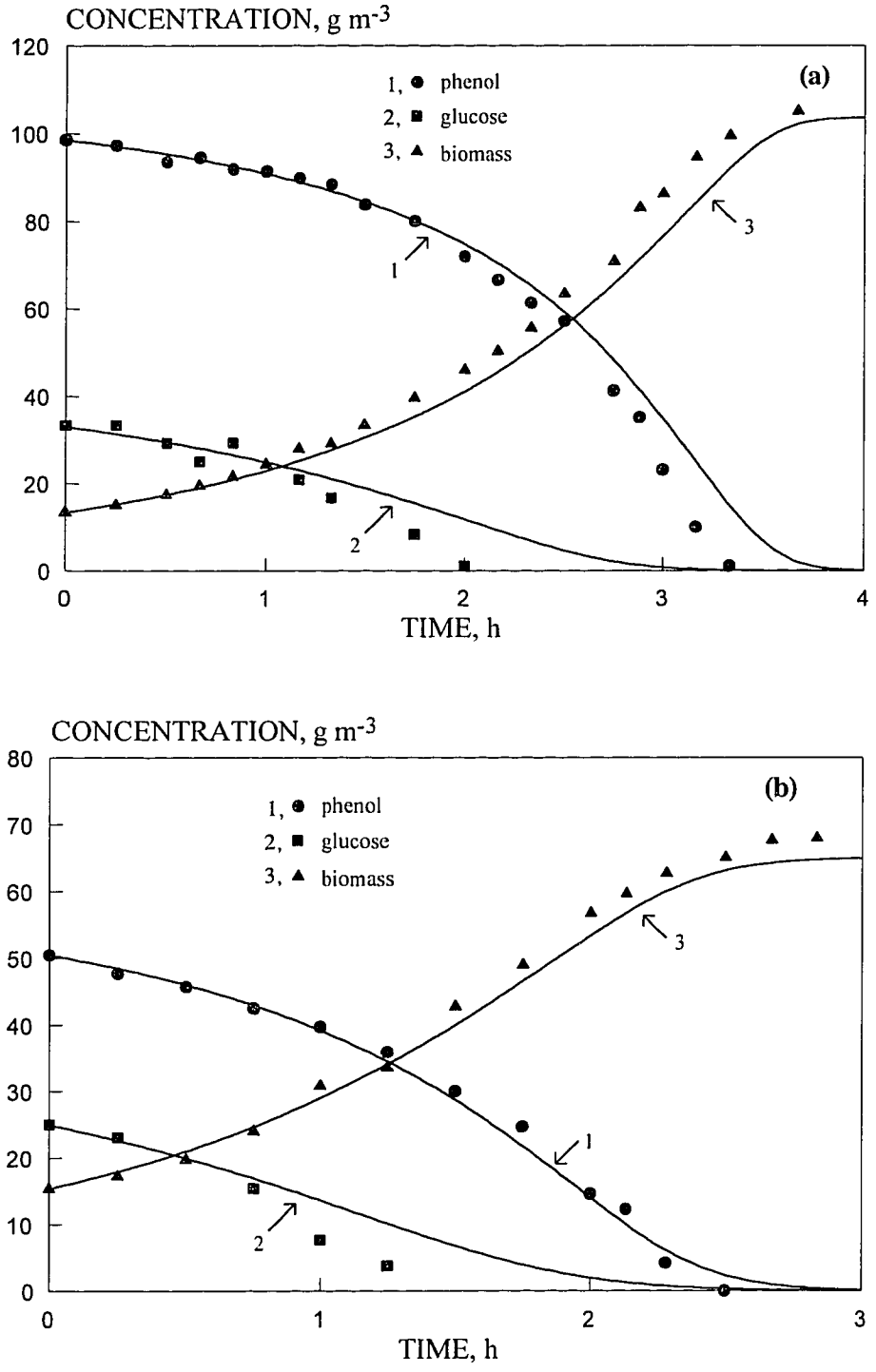

Figure 6.4 Experimentally obtained (symbols) and model-predicted (curves) concentration profiles for experiments PG-3 (a) and PG-7 (b). Information for these experiments is given in Table C2-1.

Cross inhibition between substrates has been also found, as discussed in Chapter 2, between nitrate and nitrite [Wang (1994) and Wang et al. (1995b)] and benzene and toluene [Oh et al. (1994) and Chang et al. (1993)]. The kinetic expressions (specific growth rates) revealed during the course of the work presented in this chapter were subsequently used in reaction engineering studies which are discussed in the following chapter.

CHAPTER 7

REACTION ENGINEERING FOR A CYCLIC REACTOR EMPLOYED IN TREATMENT OF DISSIMILAR LIQUID WASTES

In this chapter the analysis of the dynamics of a continuously operated cyclic reactor employed in treatment of dissimilar liquid wastes is presented. In addition, results of experimental studies performed in order to test/validate the theoretical predictions are shown and discussed. The reasons for examining the behavior of a cyclic reactor have been discussed in Chapters 1 and 2. The model system selected for the experiments as well as the detailed theoretical studies involved media containing mixtures of phenol and glucose. These two substrates simulate mixed liquid wastes of dissimilar structure and origin. Phenol represents wastes of industrial origin while glucose can be viewed as simulating domestic/urban wastes. These two substrates were also used because the detailed kinetics of their biodegradation had been revealed during the course of the study the results of which have been presented in Chapter 6.

7.1 Theory

7.1.1 General Model Development

Consider a vessel which contains at time t = 0 an amount of culture suspension of volume V_o. The concentration of the biomass in the suspension is b_o. The medium contains two substitutable substrates (carbon sources) S_1 and S_2 at growth-limiting concentrations $s_{1,0}$ and $s_{2,0}$, respectively. At t = 0, the vessel starts being fed with a medium carrying substrates S_1 and S_2 at concentrations s_{1f} and s_{2f}, respectively. The externally fed stream carries no biomass, while all required nutrients except S_1 and S_2 are present in it in excess quantities. The medium is fed at a constant flowrate Q_f^* for a period up to time $t = t_1$. This is the first period of the cycle and during it, there is no output from the vessel.

Consequently, the volume of the suspension increases linearly with time and at time $t = t_1$ reaches a maximum value of V_m. During this first phase of the cycle, the contents of the reactor are aerated and thus, reaction occurs. At time $t = t_1$ feeding of the vessel stops while there is still no outlet for the reactor contents. This lasts up to time $t = t_2$. Hence, for a period of time, the extent of which is given by $t_2 - t_1$, the vessel operates as a batch reactor with a constant volumetric hold-up equal to V_m. The period of time from $t = t_1$ to $t = t_2$ constitutes the second phase of the cycle. At time $t = t_2$ a pump is activated and reactor contents start being drawn from the vessel at a constant flowrate Q, while there is still no external feeding of the vessel. During this third phase of the cycle, which lasts up till time $t = t_3$, the volume of the reactor contents decreases linearly with time and at time $t = t_3$ it becomes V_0 which was the value of the suspension at the beginning of the cycle (i.e., $t = 0$). At that instant of time, the discharge pump is deactivated while the feed pump is activated and a second cycle starts for the reactor. This cyclic pattern is repeated continuously. The variation of the volume of the reactor contents during the cyclic operation is shown schematically in Figure 7.1.

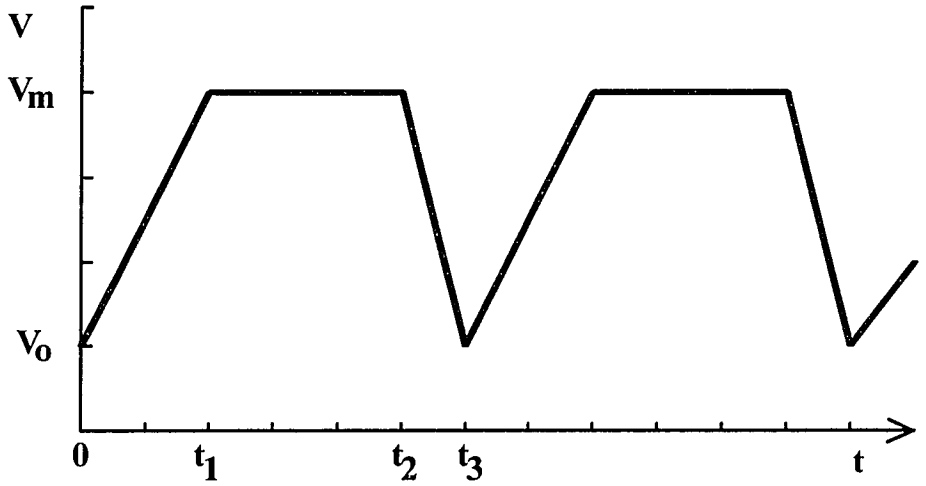

Figure 7.1 Schematic representation of the variation of the volume of the reactor contents during the cyclic operation. It is assumed that the flowrates during feeding and discharging are constant.

Assuming that the liquid (suspension) density is constant at all times and that the two substitutable substrates, which are fed to the reactor at growth-limiting concentrations, can be simultaneously used by the culture, the process can be described by four equations. These equations represent the total mass balance, mass balances on substrates S_1 and S_2, and balance on the biomass. Their form is, correspondingly, as follows.

$$\frac{dV}{dt} = Q_f - Q \tag{7.1}$$

$$\frac{ds_j}{dt} = \frac{Q_f}{V}(s_{jf} - s_j) - \frac{b\mu_j(s_1, s_2)}{Y_j}, \qquad j = 1,2 \tag{7.2}$$

$$\frac{db}{dt} = \left[-\frac{Q_f}{V} + \mu_1(s_1, s_2) + \mu_2(s_1, s_2) \right] b \tag{7.3}$$

The specific form of the equations above depends on what phase of the cycle the system is at. For example, $Q_f = Q_f^*$ during the first phase while $Q_f = 0$ during the following two phases. Symbols which appear in equations (7.1) - (7.3) and have not yet been defined are: V, volume of reactor contents; s_j, concentration of substrate j (j = 1, 2) in the reactor; b, biomass concentration in the reactor; Y_j, yield coefficient of the culture on substrate j; $\mu_j(s_1,s_2)$, specific growth rate of the culture on substrate j. Observe that $\mu_j(s_1,s_2)$ is indicated to be a function of the concentrations of both substrates, which is true when substrate interactions are present.

Equations (7.1)-(7.3) are generally true for any system involving two substitutable rate-limiting substrates. Their form changes depending on the kinetics of the specific system. Unless the kinetic expressions are known, the analysis of the model equations cannot be performed. However, the general methodology of the analysis is independent of the particular kinetic expressions.

7.1.2 Mathematical Formulation for the Case of Phenol/Glucose Mixtures

Equations (7.1)-(7.3) can be further modified when the particular functional expressions of $\mu_1(s_1,s_2)$ and $\mu_2(s_2,s_1)$ for the system of interest are introduced. For the case of phenol/glucose mixtures the kinetic studies (discussed in Chapter 6) have shown that the culture has no (or negligible) maintenance requirements and that the following kinetic expressions are valid,

$$\mu_1(s_1,s_2)=\frac{\hat{\mu}_1 s_1}{K_1+s_1+\frac{s_1^2}{K_1}+K_3 s_1 s_2}; \qquad \mu_2(s_2,s_1)=\frac{\mu_{m2} s_2}{K_2+s_2+K_4 s_2 s_1} \tag{7.4}$$

The analysis of the model equations is substantially facilitated when the following dimensionless quantities are introduced,

$$V'=\frac{V}{V_m},\quad \theta=\frac{tQ_f^*\sigma_1}{V_m},\quad Q_f'=\frac{Q_f}{Q_f^*\sigma_1},\quad Q'=\frac{Q}{Q_f^*\sigma_1},\quad u=\frac{s_1}{K_1},\quad u_f=\frac{s_{1f}}{K_1},$$

$$z_f=\frac{s_{2f}}{K_2},\quad z=\frac{s_2}{K_2},\quad x=\frac{b}{Y_1K_1},\quad \gamma=\frac{Y_1K_1}{Y_2K_2},\quad \eta=\frac{\mu_{m2}}{\hat{\mu}_1},\quad \omega=\frac{K_1}{K_1},$$

$$\lambda_1=K_2K_3,\quad \lambda_2=K_1K_4,\quad \delta=\frac{V_o}{V_m},\quad \sigma_1=\frac{t_1}{t_3},\quad \sigma_2=\frac{t_2-t_1}{t_3},\quad \sigma_3=\frac{t_3-t_2}{t_3},\quad \beta=\frac{\hat{\mu}_1 V_m}{Q_f^*\sigma_1}$$

Using the dimensionless quantities defined above, equations (7.1)-(7.3) along with expressions (7.4) can be brought into the following dimensionless form.

$$\frac{dV'}{d\theta}=Q_f'-Q' \tag{7.5}$$

$$\frac{du}{d\theta}=\frac{Q_f'}{V'}(u_f-u)-x\beta f(u,z) \tag{7.6}$$

$$\frac{dz}{d\theta}=\frac{Q_f'}{V'}(z_f-z)-x\beta\gamma\eta g(z,u) \tag{7.7}$$

$$\frac{dx}{d\theta}=-\frac{Q_f'}{V'}+[f(u,z)+\eta g(z,u)]\beta x \tag{7.8}$$

where, $f(u,z) = \dfrac{u}{1+u+\omega u^2+\lambda_1 uz}$ and $g(z,u) = \dfrac{z}{1+z+\lambda_2 uz}$ (7.9)

The following steps of the analysis have been already used by others [Dikshitulu et al. (1993), Lenas et al. (1994), Wang et al. (1995a)] and can be more easily understood when the schematic of the volume variation during a cycle, shown in Figure 7.1, is kept in mind.

When a cycle starts, i.e., $t = \theta = 0$, the following equalities hold.

$$Q_f = Q = 0 \; ; \qquad Q_f' = Q' = 0 \; ; \qquad V = V_0 \; ; \qquad V' = \delta \tag{7.10}$$

During feeding of the reactor (first phase of the cycle), i.e., for $0 < \theta < \theta_1$, the following equalities are valid.

$$Q_f = Q_f^* \; ; \qquad Q = 0 \; ; \qquad Q_f' = \frac{1}{\sigma_1} \; ; \qquad Q' = 0 \tag{7.11}$$

Equation (7.5) is a linear one and can be easily integrated subject to the initial condition given by (7.10). When equalities (7.11) are also used, the result of the integration leads to,

$$V' = \delta + \frac{1}{\sigma_1}\theta \tag{7.12}$$

When $t = t_1$ (or $\theta = \theta_1$) the end of the filling phase of the cycle is reached and $V = V_m$ or $V' = 1$. This fact, in conjunction with equation (7.12), yields the following.

$$\theta_1 = \sigma_1(1-\delta) \tag{7.13}$$

During the second phase of a cycle, the reactor operates in a batch mode. Hence, the volume of its contents is constant and equal to the value reached at the end of the first phase of the cycle. Consequently, for $\theta_1 \le \theta \le \theta_2$ the following equalities hold.

$$Q_f' = Q' = 0 \; ; \qquad V' = 1 \tag{7.14}$$

Cyclic operation of a reactor cannot be done continuously unless the amount of mass fed to the reactor during the first phase of a cycle is equal to the amount of mass discharged from the vessel during the third phase of the cycle. If this is not true, the

reactor will eventually either overflow or run dry. Hence, continuous operation which can lead to steady periodicity requires that,

$$Q_f t_1 = Q_f^* t_1 = Q(t_3 - t_2) \quad \text{and} \quad Q' = \frac{1}{\sigma_3} \tag{7.15}$$

During the third and final phase of a cycle, $Q_f = 0$ while Q' is dictated by equation (7.15). Using this equation to substitute for Q' in equation (7.5) and integrating the resulting expression subject to the initial condition (7.14) one gets the following for $\theta_2 \le \theta \le \theta_3$,

$$V' = 1 - \frac{1}{\sigma_3}(\theta - \theta_2) \tag{7.16}$$

As the schematic of Figure 7.1 indicates, the volume of the reactor contents at the beginning and end of a cycle is the same. Hence, for $\theta = 0$ and $\theta = \theta_3$, $V' = \delta$. When this is considered, equation (7.16) yields,

$$\sigma_3(1-\delta) = \theta_3 - \theta_2 \tag{7.17}$$

By looking at the definition of the various dimensionless quantities, one can easily see that $\theta_3 - \theta_2 = \sigma_3 \theta_3$ which, in conjunction with equation (7.17) leads to

$$\theta_3 = 1 - \delta \tag{7.18}$$

When the results of the foregoing analysis are used, equation (7.5) can be eliminated and incorporated into equations (7.6)-(7.8) which now take the following form.

$$\frac{du}{d\theta} = \frac{(u_f - u)M}{\delta\sigma_1 + \theta} - x\beta f(u,z) \tag{7.19}$$

$$\frac{dz}{d\theta} = \frac{(z_f - z)M}{\delta\sigma_1 + \theta} - x\beta\gamma\eta g(z,u) \tag{7.20}$$

$$\frac{dx}{d\theta} = \frac{-xM}{\delta\sigma_1 + \theta} + [f(u,z) + \eta g(z,u)]\beta x \tag{7.21}$$

$$\text{with} \qquad M = \begin{cases} 1, & \text{if } 0 \le \theta \le \sigma_1(1-\delta) \\ 0, & \text{if } \sigma_1(1-\delta) \le \theta \le 1-\delta \end{cases} \tag{7.22}$$

The system is now described by three mass balances given by equations (7.19)-(7.21) the specific form of which, is determined by the phase of the cycle. What phase of a cycle the system is at, depends on time and is dictated by equation (7.22).

Equations (7.19)-(7.21), along with expressions (7.9) and (7.22), constitute a three-dimensional non-autonomous dynamical system. The system is non-autonomous due to the forcing described by equations (7.22), which in physical terms means that forcing occurs due to the variation of the inlet flow rate between a constant non-zero value during the first phase of a cycle and a constant but zero value for the remaining two phases of a cycle.

No forced system can reach a steady-state (equilibrium point). Instead, after the decay of transients, the state variables enter a sustained oscillatory pattern (or orbit). The eventual, or steady, orbit is also called a limit cycle.

The system examined here can have up to two qualitatively different solutions (limit cycles or outcomes). The first is the unwanted culture washout solution. This outcome is possible due to the fact that biomass is not fed to the reactor while it is drawn from it during the third phase of a cycle. Consequently, unless the amount of biomass drawn from the vessel during the third phase of a cycle is made-up for during the first two phases, the culture washes out. The second outcome is one of culture survival and thus, one which allows continuous treatment of a waste stream. It should be also mentioned that due to the highly non-linear form of the kinetic expressions (7.9), there may be more than one state of culture survival. This implies multiplicity of qualitatively similar limit cycles. In addition, there is nothing which excludes the possibility of two qualitatively different outcomes (survival and washout of the culture) arising under the same operating conditions. This is another form of solution multiplicity. Multiplicity and multistability of

limit cycles have been found by Dikshitulu (1993), Dikshitulu et al. (1993), Ko (1988), Lenas et al. (1994), Wang (1994), and Wang et al. (1995a) all of whom have studied systems similar to the one examined here.

In order to investigate what types of solutions the system has, their stability, and the operating conditions under which they arise, one needs to analyze equations (7.19)-(7.22) and (7.9). When the kinetic parameters are known, the model equations contain the following five operating parameters: β, δ, σ_1, u_f, and z_f. Consequently, a complete analysis of the dynamics of the system needs to be performed in the five-dimensional space. The work presented here was based on studies where three of the five operating parameters were fixed at various values. Hence, at least the graphical representation of the results constitutes projections of the five-dimensional diagram on to two-dimensional planes.

One more thing needs to be added in order to complete the problem formulation before numerical methodologies are discussed.

Using equations (7.19)-(7.21) one can easily see that,

$$\frac{d}{d\theta}(x+u+\frac{z}{\gamma}) = \frac{M}{\delta\sigma_1+\theta}(-x+u_f-u+\frac{z_f-z}{\gamma}) \tag{7.23}$$

For given (fixed values) of u_f and z_f, equation (7.23) can be written as

$$\frac{d}{d\theta}(u_f-u+\frac{z_f-z}{\gamma}-x) = \frac{-M}{\delta\sigma_1+\theta}(u_f-u+\frac{z_f-z}{\gamma}-x) \tag{7.24}$$

Let's call,

$$y = u_f-u+\frac{z_f-z}{\gamma}-x \tag{7.25}$$

Hence, equation (7.24) becomes

$$\frac{dy}{d\theta} = \frac{-My}{\delta\sigma_1+\theta} \tag{7.26}$$

For $\sigma_1(1-\delta) \le \theta \le 1-\delta$, according to equation (7.22), M=0. Thus, equation (7.26) implies that,

$$y = C = \text{constant} \tag{7.27}$$

For $0 \le \theta \le \sigma_1(1-\delta)$, equation (7.22) dictates that M=1. Hence, integration of equation (7.26) yields,

$$\ln y = -\ln(\delta\sigma_1 + \theta) + C_1 \tag{7.28}$$

or $$y(\delta\sigma_1 + \theta) = C_1' \tag{7.28a}$$

where C_1 and C_1' are constants.

Assume that the system has reached its limit cycle. Then, $y(\theta_3) = y(0)$. In addition, using equation (7.27) one gets

$$y(\theta) = y(0), \quad \text{for } \sigma_1(1-\delta) \le \theta \le 1-\delta \tag{7.29}$$

From equation (7.28a) and for $\theta = 0$ one gets,

$$y(0)\delta\sigma_1 = C_1' \tag{7.30}$$

From equation (7.28a) again, but for $\theta = \sigma_1 (1 - \delta) = \theta_1$ one also gets

$$y(\theta_1)\delta = C_1' \tag{7.31}$$

However, according to equation (7.29), $y(\theta_1) = y(0)$. Taking this into account, equations (7.30) and (7.31) imply that,

$$y(0)\delta\sigma_1 = y(0)\delta \tag{7.32}$$

Equation (7.32) cannot be satisfied unless $y(0) = 0$. From the foregoing last part of the analysis, it becomes now clear that when the system has reached its limit cycle, the following equality holds,

$$x(\theta) + u(\theta) + \frac{z(\theta)}{\gamma} = u_f + \frac{z_f}{\gamma} \tag{7.33}$$

Equation (7.33) implies that the state variables as determined by equations (7.19)-(7.21) lie on a surface of dimension two in the three dimensional space when the limit cycle is reached. Physically speaking, equation (7.33) is a balance between amounts of

reactants (substrates) consumed and amounts of products (biomass) formed. There are arguments in the literature, recently reviewed by Baltzis and Wu (1994), which imply that the original three-dimensional system of equations (7.19)-(7.21) is asymptotically dynamically equivalent to a two-dimensional system. This system is produced by any two of the three original equations when the state variable associated with the deleted equation is substituted for by equation (7.33). This means that although equation (7.33) strictly speaking is valid only at the limit cycle, it can be also used during transient cycles. This reduction in the dynamical dimensionality of the system reduces substantially the computational time needed for studying the dynamics of the system.

7.2 Numerical Methodologies and Studies

The analysis of the model equations was done numerically following the methodologies discussed by Dikshitulu (1993), Dikshitulu et al. (1993), Wang (1994), Wang et al. (1995a), and Lenas et al. (1994). The codes used are adaptations of those originally developed by Doedel (1986), Pavlou et al. (1990), Pavlou and Kevrekidis (1992), and Lenas et al. (1994). These codes are based on the bifurcation theory for forced systems. The basic idea is that the periodic solutions are computed as fixed points of the Poincare' map and their stability is determined from the magnitude of the Floquet multipliers. These multipliers are the eigenvalues of the Jacobian matrix of the map. This Jacobian (evaluated at the fixed point) is actually a matrix which is consisted of the solutions to the variational equations of the original system, when evaluated at time equal to the period of the cycle. This methodology leads to the preparation of bifurcation diagrams such as those shown in Figures 7.2 and 7.3. Once a bifurcation point is found, the codes allow for one- and two-parameter continuation which traces the curves which separate regimes in the operating parameter space where the system exhibits a different behavior (i.e., it has different solutions). This methodology leads to the preparation of operating diagrams such as those shown in Figures 7.4 and 7.5.

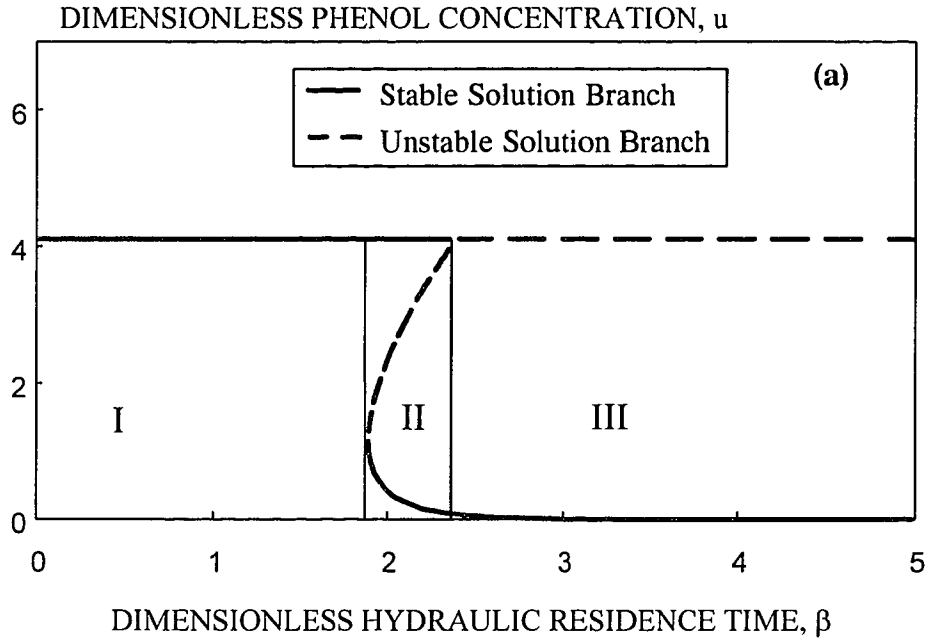

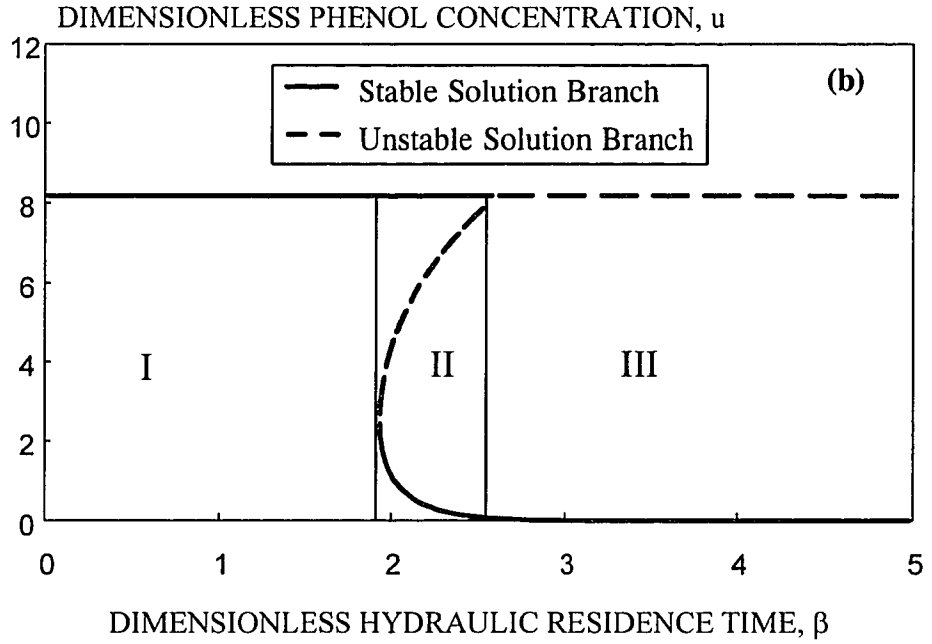

Figure 7.2 Bifurcation diagrams of periodic states. These plots indicate the phenol concentration at the end of a limit cycle as a function of β when $\sigma_1 = \delta = 0.5$. The values of s_{1f} and s_{2f} (in g m^{-3}) are, respectively, 50 and 100 in (a) and 100 and 50 in (b).

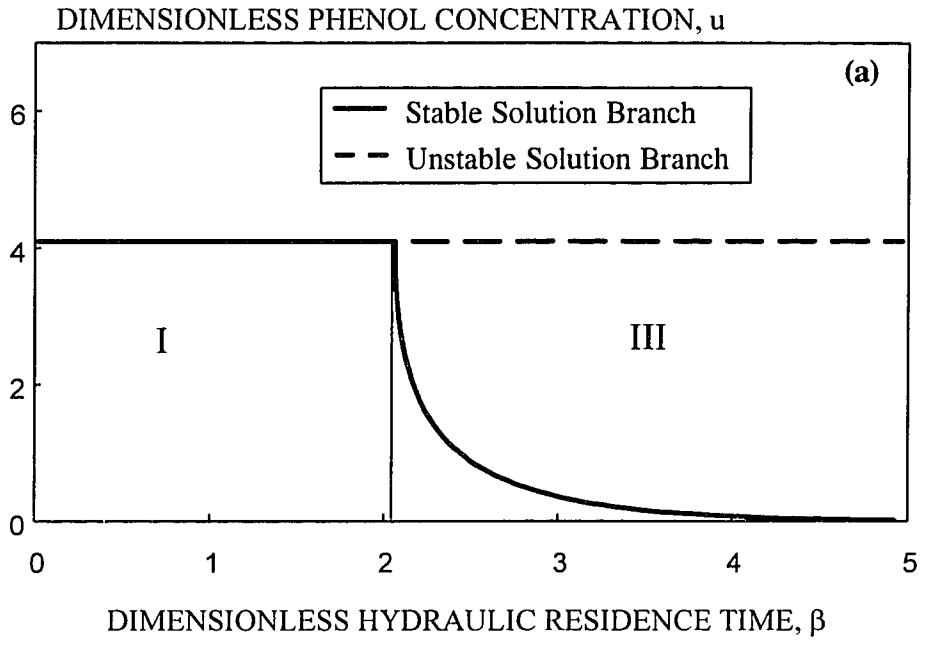

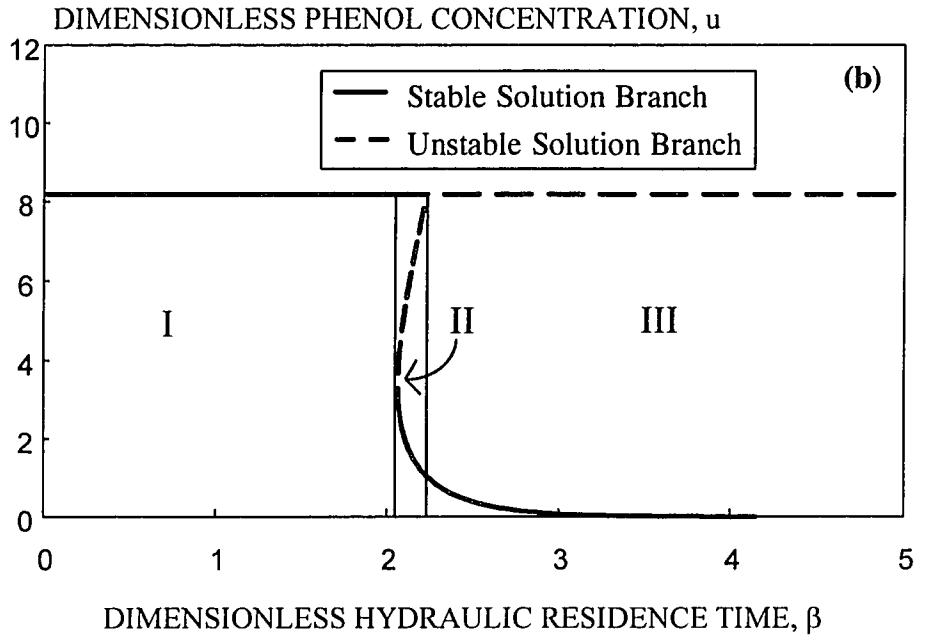

Figure 7.3 Bifurcation diagrams of periodic states for the case where $\sigma_1 = \delta = 0.5$ and the medium contains phenol only at levels 50 g m^{-3} (a) and 100 g m^{-3} (b). These plots indicate the phenol concentration at the end of a limit cycle as a function of β.

The system considered in the present study has been found to have the same two types of bifurcations as those found by Lenas et al. (1994) and Dikshitulu et al. (1993). One is a transcritical and the other is a limit point bifurcation. These are shown in the diagrams of Figure 7.2. Transcritical bifurcations occur at values of β separating regions II and III while limit point bifurcations occur at values of β separating regions I and II in the diagrams of Figure 7.2. In these diagrams, thick solid lines represent branches of stable solutions while thick dotted lines represent branches of unstable solutions. As has been discussed in earlier studies [e.g. Wang et al. (1995a)] unstable solutions are not physically realizable unless appropriate control algorithms are applied to the process. The vertical thin lines in Figure 7.2 represent boundaries between regimes of β-values where the system exhibits a different behavior. In region I the culture cannot survive in the reactor. Thus, the value of β where a limit point bifurcation occurs represents the minimum β (or maximum volumetric flow rate of the feed stream) value allowable if the culture is to have any chance of establishing itself in the reactor. In region III, culture washout is excluded. Thus, the value of β where a transcritical bifurcation occurs represents the minimum β value which guarantees culture survival. Finally in region II the system exhibits multistability. This means that depending on the start-up conditions the culture will either survive or wash-out. It also means that even if the culture establishes itself, the operation is not globally stable and temporary operational upsets may cause the culture to wash-out.

As can be seen from the diagrams of Figure 7.2 (and this also true for other parameter values) these are no regimes in which the survival state exhibits multiplicity. Such multiplicities have been found by Wang et al. (1995a), but not by either Dikshitulu et al. (1993) or Lenas et al. (1994).

The bifurcation diagrams shown in Figure 7.3 are for cases where the waste (medium) contains phenol but not glucose. The features of these graphs are similar to those shown in Figure 7.2 and are given here for comparison purposes. The meaning of

curves, lines, and regions in Figure 7.3 is the same with the corresponding ones in Figure 7.2. It is interesting to observe that diagram (a) in Figure 7.3 shows that it is possible to have cases where a limit point bifurcation cannot arise and thus, there is no region II. This can happen even in cases where the feed stream contains both phenol and glucose. Comparing the diagrams of Figures 7.2(a) and 7.3(a) one can see that - although this is not generally true - the presence of glucose leads to the formation of region II of multistability. Furthermore, comparing Figures 7.2(b) and 7.3(b) one can see that the presence of glucose increases the extent of region II when this region exits even in the absence of glucose. Hence, one can conclude that glucose may have a destabilizing effect (in the general sense) on the dynamics of phenol biodegradation.

The diagrams of Figures 7.2 and 7.3 are for cases where all but one of the operating parameters are fixed. The results of the analysis can be shown also in the form of two-dimensional operating diagrams such as those of Figures 7.4 and 7.5. The meaning of regions I, II, and III in these diagrams is the same with the corresponding ones in Figures 7.2 and 7.3. The boundary between regions I and II in Figures 7.4 and 7.5 is the locus of points where a limit point bifurcation occurs. The boundary between regions II and III or I and III is the locus of points where a transcritical bifurcation occurs. From the diagrams of Figure 7.4 one can see that region II exists even in the absence of glucose in the feed but expands as the presence of glucose increases. One can also see, on the other hand, that the extent of region III also expands at low u_f-values with the increase of glucose presence. This means that when the medium contains low phenol quantities the presence of glucose allows culture survival at lower β-values. This is expected because glucose allows the biomass to grow and reduces the certitude of culture wash-out when β (or the residence time) is low.

Figure 7.5 shows operating diagrams on the β-z_f plane at three inlet phenol concentrations. Whatever was earlier discussed regarding the effect of glucose presence on the dynamics of the system can be now repeated for the effect of phenol presence on

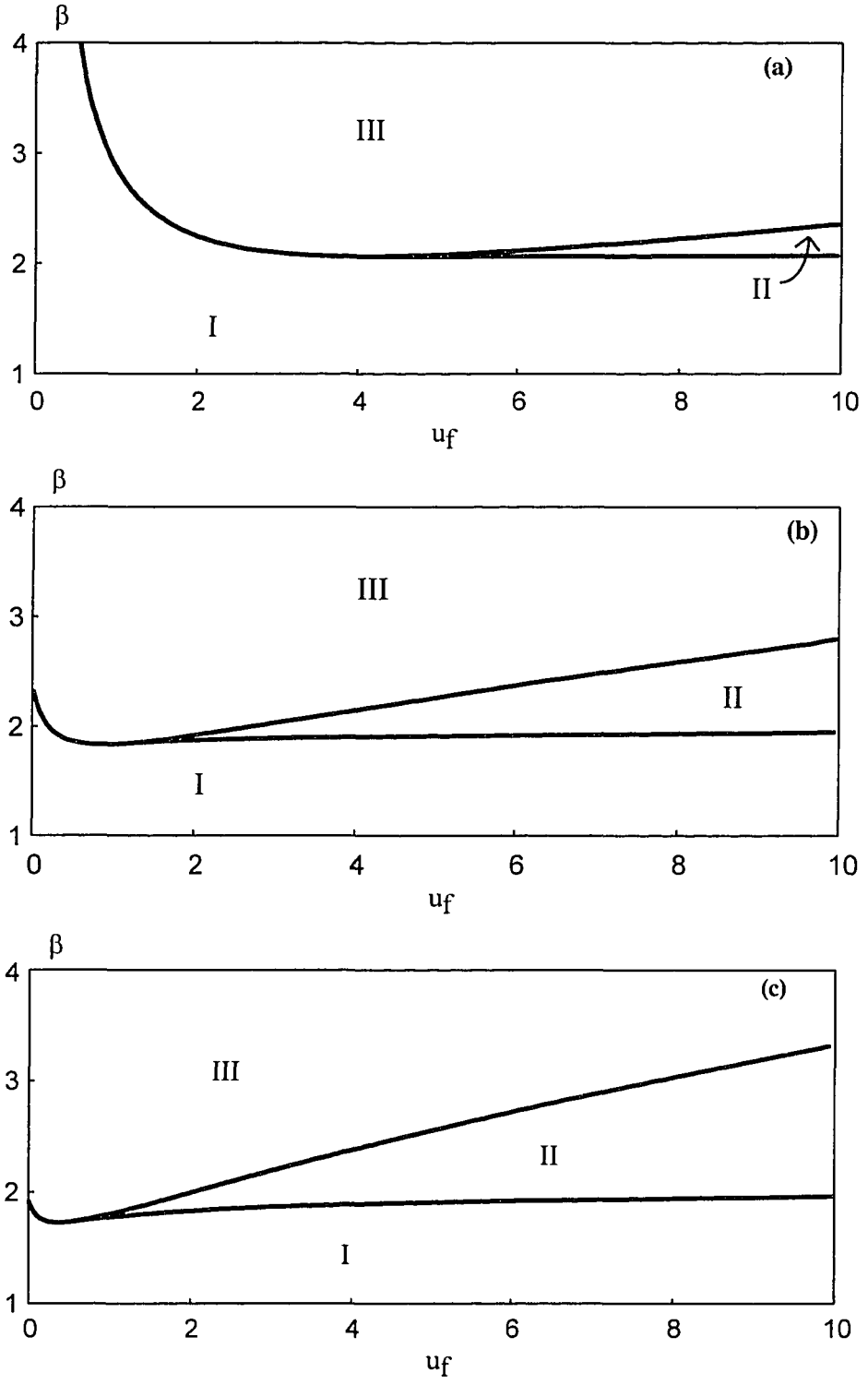

Figure 7.4 Operating diagrams on the $\beta - u_f$ plane when $\sigma_1 = \delta = 0.5$ and s_{2f} (in g m^{-3}) is 0 (a), 50 (b), or 100 (c).

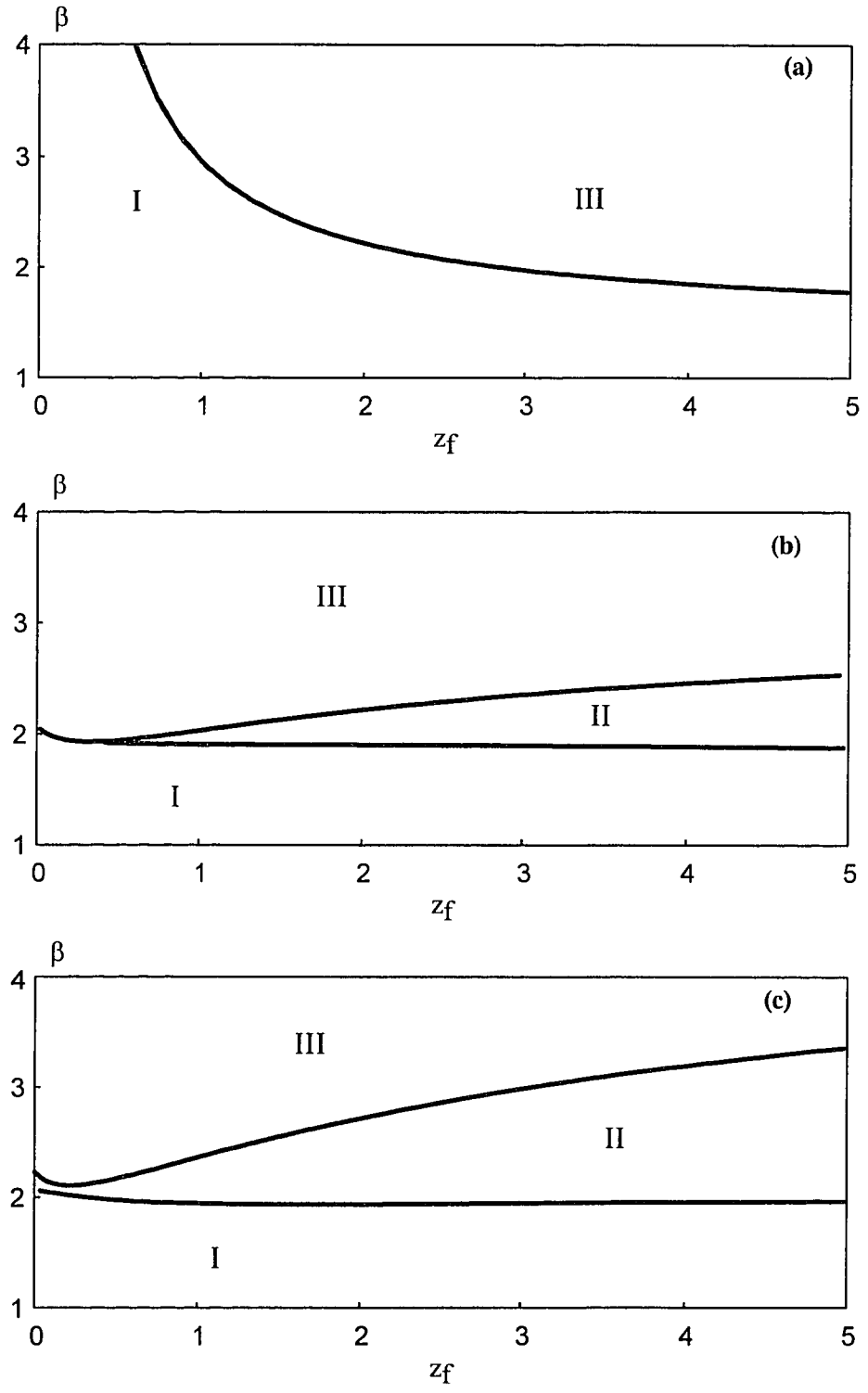

Figure 7.5 Projection of operating diagrams on the $\beta - z_f$ plane when $\sigma_1 = \delta = 0.5$ and s_{1f} (in g m^{-3}) is 0 (a), 50 (b), or 100 (c).

the system dynamics. The only difference is between diagrams (a) in Figures 7.4 and 7.5. In absence of phenol, glucose follows classical Monod kinetics and region II does not arise. On the other hand, in the absence of glucose, phenol follows Andrews kinetics and region II arises. When one deals with glucose/phenol mixtures, further non-linearities are introduced through the cross-inhibition terms in the denominators of the specific growth rate terms [expressions (7.9)]. As the non-linear character of the model intensifies, region II of multistability becomes larger in the operating parameter space.

A final point which needs to be made is that in region II, in addition to one stable washout and one stable survival state, there is also an unstable survival state. This state can be physically realized through control actions, but is of no practical importance because when reached, it will lead to phenol removal lower than the other survival state [as can be seen from Figures 7.2 and 7.3(b)].

7.3 Experimental Results and Validation of the Theory

In order to verify the key-predictions of the theoretical analysis of the system, experiments were performed with a unit the schematic of which is shown in Figure A-4. The procedures for the experiments have been discussed in Chapter 4 of this dissertation.

The operating and start-up conditions for the experiments are given in Table D-1 of Appendix D. On the same table the region in Figure 7.4 and/or Figure 7.5 where the conditions fall (within experimental error) is also indicated. The raw data from these experiments, designated as experiments C-1 through C-5, are given in Tables D-2 through D-6. The same experimental data along with the theoretically predicted concentration profiles are shown in the diagrams of Figures 7.6, 7.7, D-1, D-2, and D-3. Due to the manual collection of samples and the need for their immediate processing, samples were only collected for a few of the cycles run for each experiment. Wherever data are not reported in Tables D-2 though D-6, or symbols (data points) are not shown in the corresponding graphs the implication is that data were not collected. As the operation of

the unit was automated, the experiments -in most instances- were allowed to run for cycles during which samples were not collected. Data were always collected for a full cycle before each experiment was terminated. The concentration profiles have been predicted through integration of equations (7.19)-(7.22) along with expressions (7.9). Integration was performed through the use of a simple computer code which is based on the 4-th order Runge-Kutta method. This code is given in Appendix E-3. Integration was subject to the start-up conditions of each experiment (Table D-1). These profiles are predicted based on the kinetics revealed in the studies discussed in Chapter 6. There is no curve-fitting involved in any of the graphs of Figures 7.6, 7.7, D-1, D-2, or D-3.

Since one of the objectives of the experiments was to verify the existence of an eventual repeated pattern (limit cycle) the start-up conditions for each experiment were selected based on the theory. By using the operating parameter values selected for a particular experiment, the expected limit cycle was calculated as a fixed point of the Poincare' map as discussed in an earlier section of this chapter. A full integration was then performed for time equal to the period of the cycle; the glucose, phenol, and biomass concentration profiles were generated and initial (start-up) conditions were selected so that the system would be close to its eventual cycle right from the beginning. This methodology, also used earlier by Dikshitulu (1993) and Wang (1994), significantly reduces the required time for experimentation. It should be mentioned that computer simulations predict that transients may last for hundreds or even thousands of cycles if the start-up is under random conditions.

In selecting the operating parameters for the experiments, one of the objectives was to validate the theoretical prediction of the existence of regimes in the operating parameter space where the outcome (i.e., survival or wash-out) depends on the start-up conditions. Validation of this prediction was accomplished via experiments C-2 and C-3. As can be seen from Table D-1 the operating conditions for these experiments are identical while the start-up conditions are different. The results shown in Figures 7.6 and

7.7 prove that in fact the system reaches a different limit cycle depending on the start-up conditions. The actual way experiment C-3 was performed was as follows. After the last cycle of experiment C-2, the system was temporarily perturbed through discharge of an amount of reactor contents larger than that used during experiment C-2 and subsequent dilution of the remaining reactor contents with medium (waste) before operation was restored to the previous level of operating parameters. This methodology also proves the theoretical prediction that culture survival under operating conditions falling in region II of the operating diagrams is not globally stable.

From the data and theoretically predicted profiles shown in Figures 7.6, 7.7, D-1, D-2, and D-3 one can see that the agreement between theory and experiments is remarkably good, almost perfect. There are some discrepancies at low values of the substrate concentrations but they can be safely attributed to inaccuracies of the analytical techniques at very low concentrations.

In all cases where culture survival is reached (experiments C-1, C-2, C-4, and C-5) the data show that it is in fact possible to have a continuous and simultaneous removal of both phenol and glucose. In addition, when the operating parameters are properly selected one can achieve a practically zero concentration for both phenol and glucose at the end of each steady (limit) cycle (see Figures D-1 and D-2 for experiments C-1 and C-4, respectively).

It is also interesting to compare the results of experiments C-1 and C-2. The only difference between the two experiments in terms of operating parameters is in the value of β. The two experiments fall actually on a line vertical to the x-axis of Figure 7.4(b). The point for experiment C-1 is in region III while that for experiment C-2 is in region II of Figure 7.4(b). Given that theoretically only the conditions of experiment C-1 lead to complete removal of both substrates one could argue that it is fortunate that in this case complete removal is achieved under conditions falling in the safest operating region (III). This is not generally true though. Even here, the data suggest that complete removal of

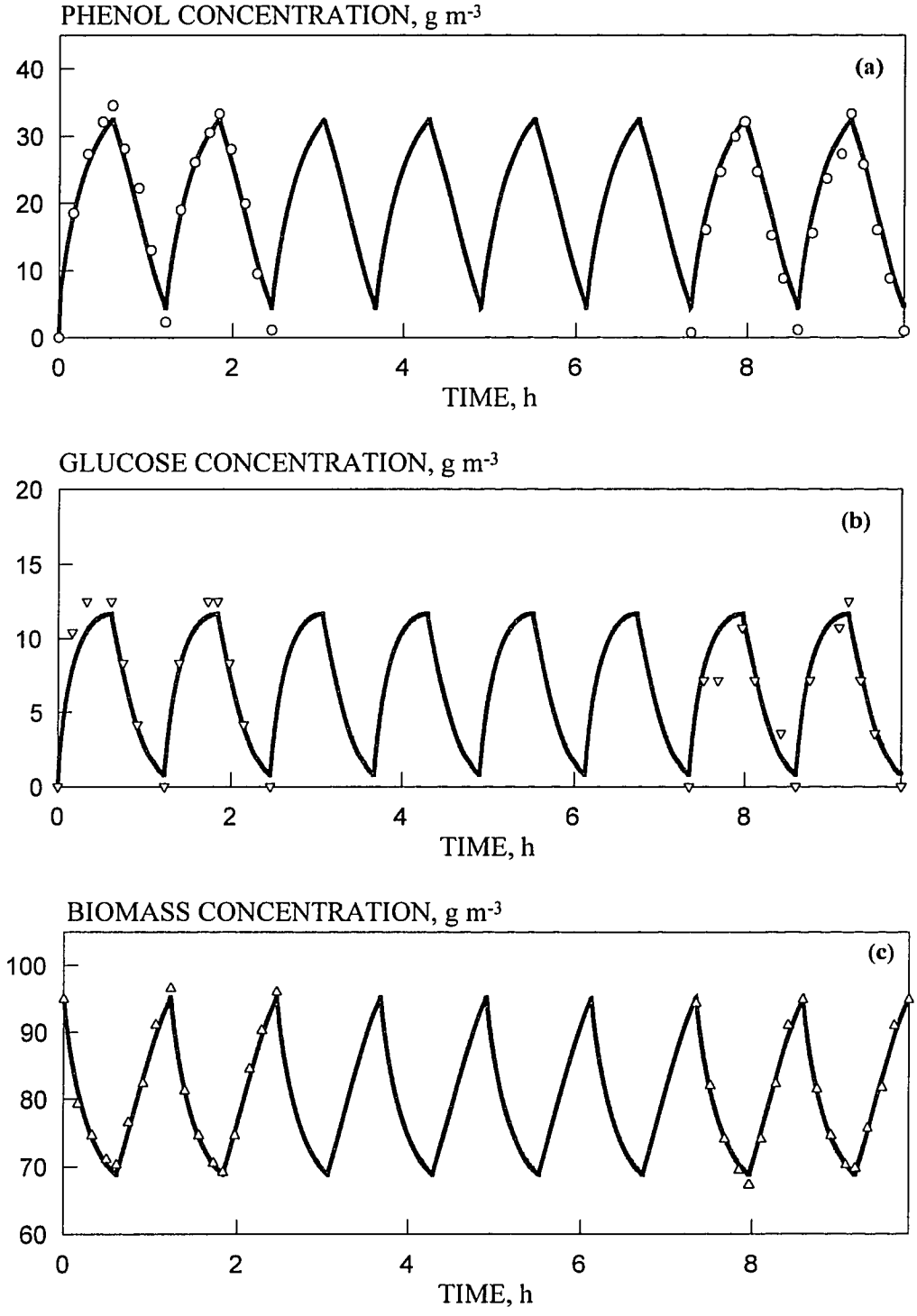

Figure 7.6 Experimentally obtained and model-predicted concentration profiles for phenol (a), glucose (b), and biomass (c) for experiment C-2. Conditions for this experiment are given in Table D-1. The system reaches a survival periodic state.

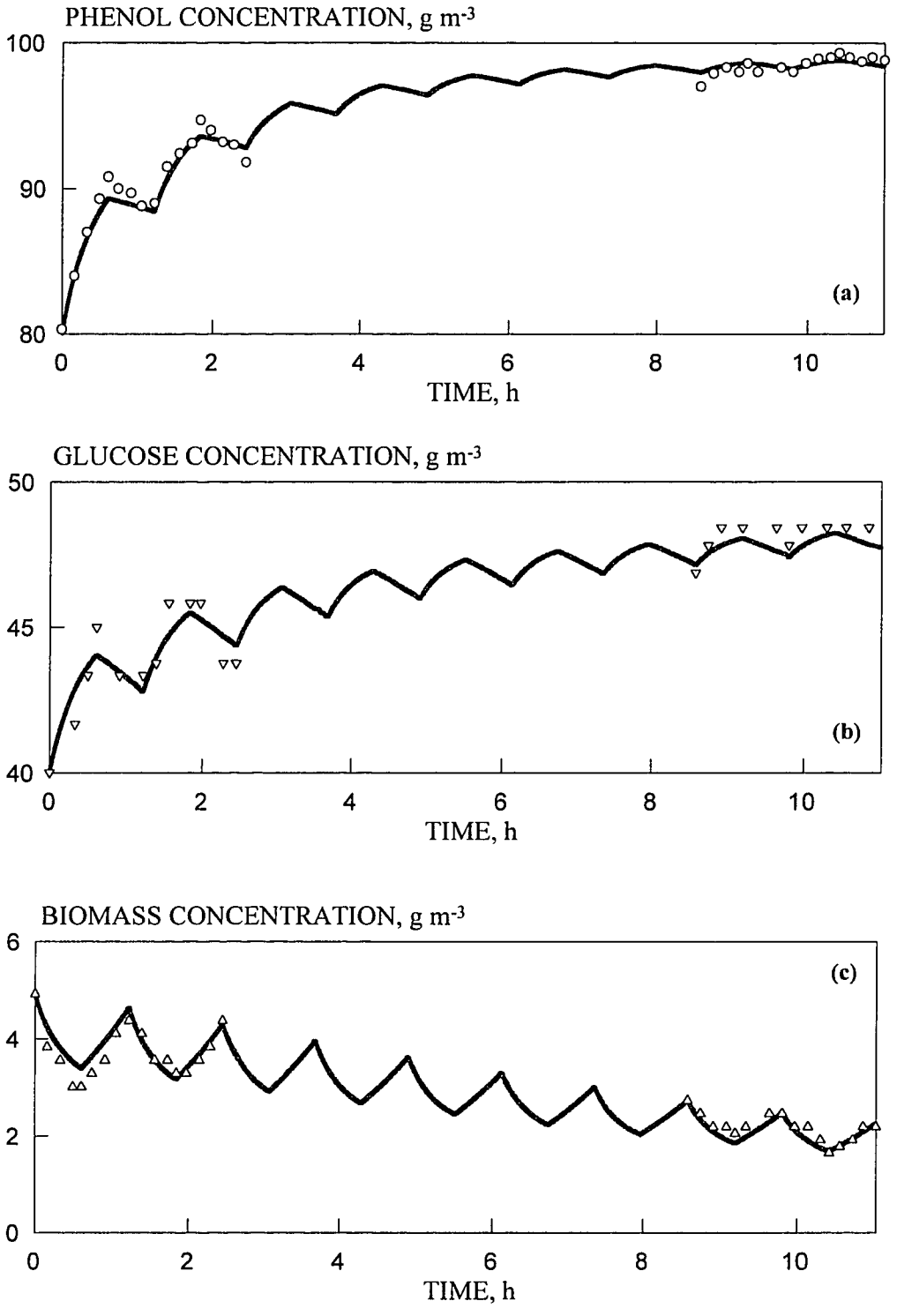

Figure 7.7 Experimentally obtained and model-predicted concentration profiles for phenol (a), glucose (b), and biomass (c) for experiment C-3. Conditions for this experiment are given in Table D-1. In this case the system reaches a washout state.

both glucose and phenol is achieved both in experiments C-1 and C-2. Hence, operation in region II may be the rule rather than the exception unless one uses suboptimal conditions of higher β (meaning lower feed flowrate or larger reactor size) just in order to avoid multistability. This is an expensive solution to a problem which could be addressed in terms of process control.

The work presented here shows that the process of simultaneous treatment of two dissimilar substrates can be successfully described with a mathematical model. This model can be now used in computational studies for finding the optimal operating conditions. This could probably be achieved by using a methodology similar to that of Lenas et al. (1994). The objectives of optimization should be to achieve conversion of pollutants to environmentally acceptable levels with the minimum reactor volume.

CHAPTER 8

CONCLUSIONS AND RECOMMENDATIONS

Fundamental kinetic studies with mixtures of phenol/4-chlorophenol and phenol/glucose were performed with three strains of *Pseudomonas* species. The results have shown that the kinetics of biodegradation are quite complex.

Studies with strains *P. putida O* and *P. putida N* have shown that, although both cultures had the same origin, their behavior toward phenol and 4-chlorophenol (4-CP) is different. While both strains could use phenol as sole carbon and energy source, only *P. putida O* could completely degrade 4-CP by using it as carbon and energy source. Species *P. Putida N* could transform 4-CP, in the presence of phenol, to 2-hydroxy-5-chloromuconic semialdehyde (2H5CMA). The results suggest that *P. putida O* follows the *ortho*-cleavage pathway while *P. putida N* follows the *meta*-cleavage pathway. The behavior of *P. putida O* is interesting because it seems to contradict claims in the literature that *Pseudomonas* species always follow the *meta*-cleavage pathway. The results from the experiments with *P. putida N* are also interesting due to the fact that, based on UV-spectra taken after long periods of time, it appears that 2H5CMA is not a "dead-end" intermediate as claimed in the literature. Spectra, as well as chloride ion recovery, have shown that 2H5CMA gets transformed to some other, non-chlorinated, intermediate albeit without concomitant biomass formation. The results from these studies have not been quantified in the sense of deriving mathematical functional expressions for the rates of biodegradation, biotransformation, or mineralization. It appears that when complete mineralization of chlorinated phenols is desired, one has to -most probably- use microbial consortia rather than pure cultures. This implies that detailed reaction engineering studies with such systems have to take into consideration population interactions, something which further complicates the kinetic studies as well

as the dynamics of the reactors eventually employed. This is a potential direction for future studies.

Kinetic studies with phenol and glucose and with culture *P. putida OR* have led to the following conclusions. In the absence of phenol, the culture utilizes glucose following classical Monod-type kinetics. In the absence of glucose, the culture biodegrades phenol following Andrews, inhibitory, kinetics. It was found that the yield on glucose (0.44 g-biomass/g-glucose) is substantially lower than that on phenol (0.768 g-biomass/g-phenol). This may be explained by the fact that phenol is in a more reduced state relative to glucose. However, one could possibly also argue that cultures are using more efficiently substrates which are not very easy to degrade. Studies with mixtures of phenol and glucose have shown that the culture utilizes, even under batch conditions, both substrates simultaneously and without any sign of diauxic growth. However, the two substrates have been found to be involved in a cross-inhibitory uncompetitive interaction. It was found that glucose inhibits the rate of phenol removal more than phenol reduces the rate of glucose utilization. This cross-inhibition can be also interpreted as a degree of preference of a culture towards substitutable resources. One could argue then that, although both substances were simultaneously utilized as carbon/energy sources, the culture used in the experiments exhibits a preference towards glucose. The results of cross-inhibition appear to be in agreement with some earlier studies which have shown that the presence of glucose inhibits the removal of hazardous/toxic substances. On the other hand, the results obtained here contradict the claims of some other investigators that glucose helps the removal of pollutants. Although phenol may not be really comparable to substances such as nitro-phenols, it seems that if two substrates can be used as substitutable resources by a culture, these substances will be involved in some type of inhibitory interaction. Positive effects are more likely to happen only within the context of cometabolism. It is clear however that, in describing the biodegradation of mixed wastes, one cannot simply use additive expressions for the removal rates of individual

pollutants. Kinetic interactions need to be taken into account and quantified, especially if one is interested in reaction engineering, control, and optimization studies.

Further work in terms of kinetics of dissimilar compounds would be interesting to focus on mixtures such as aromatic and aliphatic hydrocarbons.

The detailed kinetic expressions revealed from the batch experiments with phenol/glucose mixtures were subsequently used in reaction engineering studies. The reactor studied operated in a continuous cyclic mode. This type of reactor operation protocol had been also used in earlier studies on other substrate and/or microbial population systems. The dynamics of this reactor were studied through the analysis of differential equations describing the variation of volume, and concentrations of phenol, glucose and biomass. Using computer codes, which have been derived based on the bifurcation theory for forced systems, it was found that the system has two qualitatively different solutions. One is the unwanted culture wash-out state and the other is the culture survival state. The latter has not been found to exhibit any multiplicity. The numerical analysis of the dynamics of the system have determined the maximum feed flow rate which can be used if the culture is to have any chance to survive and thus, treat the (synthetic) waste stream. In addition, the maximum allowable flow rate which can be used during the reactor feeding phase in order to exclude any chance for culture wash-out has been also found. These values of the two aforementioned flowrates have been found to be, in most cases, different from one another. This implies that there are extensive regimes in the operating parameter space where both the culture survival and the culture wash-out state are possible. In such cases of multistability, the process start-up conditions determine the final state of the system. For cases where the waste stream contains phenol only, the aforementioned results were already known. What has been found in the present study is that the presence of glucose does not qualitatively alter the dynamics of the system. It has been also found that the region of multistability becomes wider in the operating parameter space as the glucose presence in the feed-stream (untreated waste)

increases. It could be claimed then that from the point of view of dynamics, glucose destabilizes a cyclically operated reactor used in treatment of phenol. From the practical point of view, this implies that either different operating regimes have to be used depending on the composition of the feed stream, or that process control should be applied more often than is usually anticipated in order to ensure stable operation.

The results of the analysis of the system dynamics were subsequently validated with a 7-liter capacity reactor. The experimental results have been found to be in qualitative as well as remarkable quantitative agreement with the theoretical/numerical predictions. These results imply that an accurate and robust model for describing cyclic reactor operation used in treatment of two substitutable substrates has been derived in this study.

Two of the five operating parameters which are important for cyclic operation, namely the ratio of minimum to maximum volume of reactor contents and the fraction of the cycle time allocated to filling the reactor, were kept constant (at a value of 0.5 both) during the course of this study. Since the model has been experimentally validated, these two parameters should be varied in future computational optimization studies. The intent of optimization should be to determine the values of the operating parameters which allow for a desired conversion of a waste of given strength with the minimum reactor volume and/or processing time.

This study if viewed in conjunction with earlier ones which dealt with phenol only and a pure culture [Ko (1988), Lenas et al. (1994)], phenol and two competing microbial species [Dikshitulu (1993), Dikshitulu et al. (1993)], and nitrate/nitrite with a pure culture [Wang (1994), Wang et al. (1995a)] seems to be concluding the study of relatively simple systems under cyclic reactor operation. Further studies should deal with other issues such as biomass settling, cometabolism of substrates, and possibly the use of immobilized (in the form of biofilms) rather than suspended biomass. Cyclic bioreactor operation appears to be very promising for optimal treatment of liquid waste streams.

APPENDIX A

CALIBRATION CURVES AND SCHEMATIC OF THE EXPERIMENTAL APPARATUS

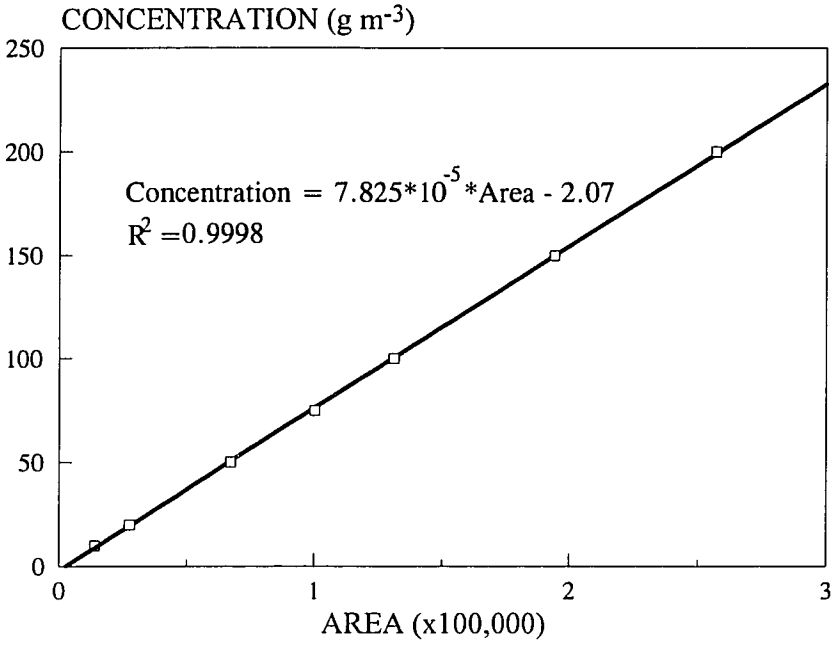

Figure A-1 HPLC calibration curve for phenol concentration measurements.

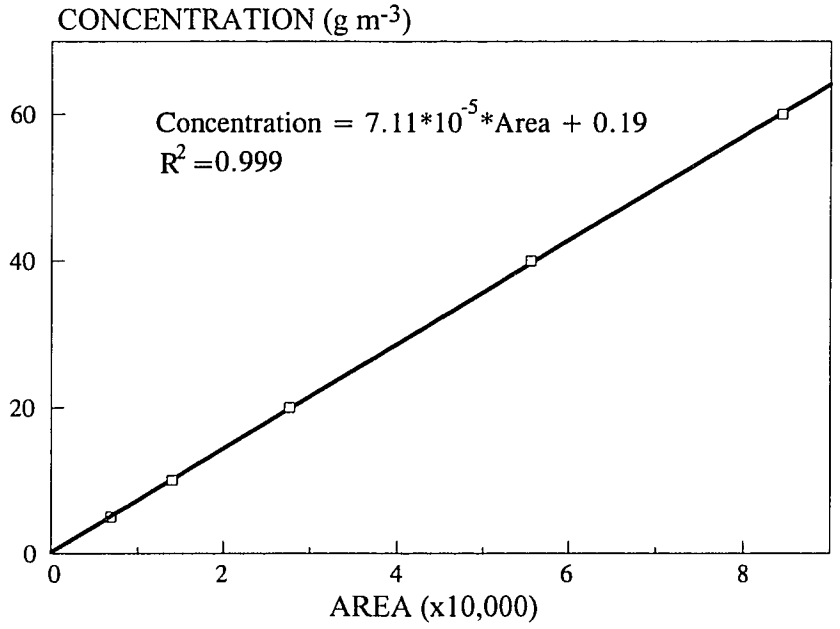

Figure A-2 HPLC calibration curve for 4-chlorophenol concentration measurements.

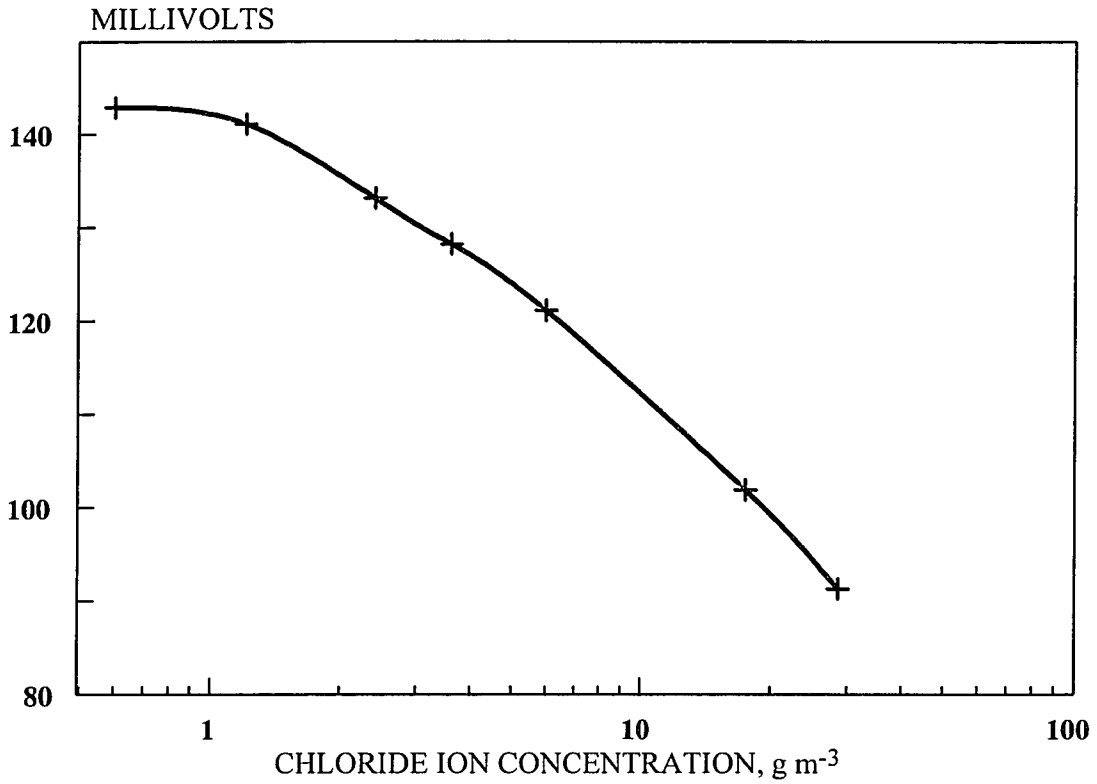

Figure A-3 Calibration curve for chloride concentration measurement by the use of a special electrode.

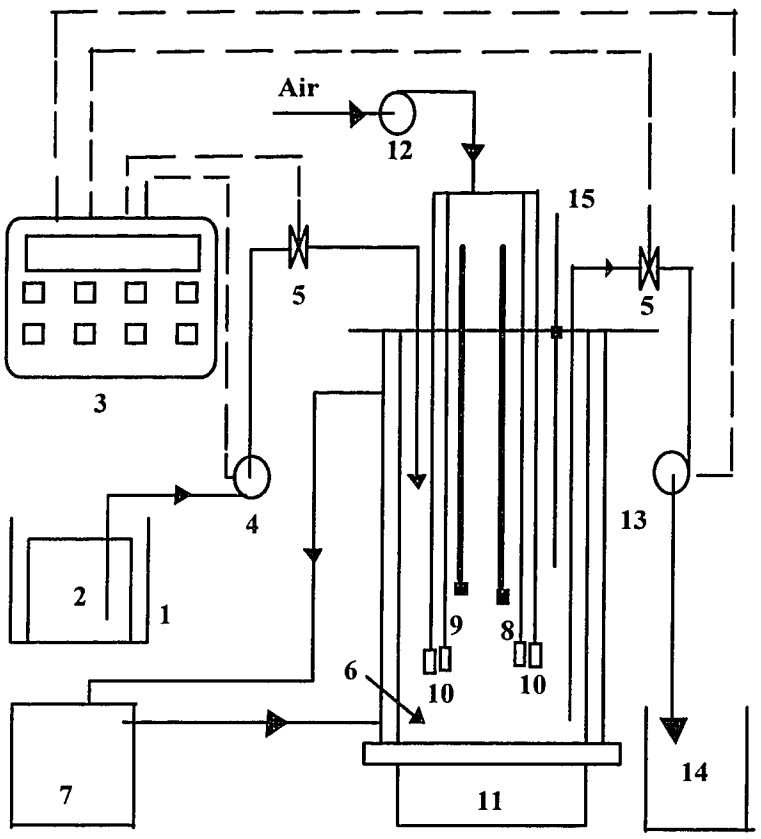

Figure A-4 Schematic of the experimental cyclically operating reactor unit: (1) constant temperature water bath for feed tank; (2) feed tank, i.e., closed tank containing the untreated waste; (3) programmable sequence controller which is used for automating the cyclic operation; (4) peristaltic feed pump; (5) solenoid valve; (6) jacketed reactor; (7) circulating water bath; (8) thermometer; (9) dissolved oxygen probe; (10) air diffusion tube; (11) magnetic stirrer; (12) air pump; (13) peristaltic discharge pump; (14) discharge tank; (15) sampling port.

APPENDIX B

DATA AND UV-SPECTRA FROM THE BIODEGRADATION EXPERIMENTS WITH PHENOL AND 4-CHLOROPHENOL

Table B-1 Data from experiment K1-N. This experiment was performed with phenol only, and strain *P. putida N* under batch conditions.

Time[1] (h)	OD[2]	Ph[3] (g m^{-3})	MV[4]	R[5]
0	0.031	120.8	138	
24	0.316	0	137	
46	0.415	0	141	0
0	0.415	71.3	141	
25	0.504	0	141	
43	0.505	0	140	0

[1] indicates time elapsed after the culture has been spiked with phenol.
[2] optical density, measured at 540 nm; indicates biomass concentration.
[3] phenol concentration.
[4] millivolt reading obtained by using the combined chloride electrode.
[5] % chloride ion recovery from the start-up of experiment to the time at which a value for R is given; the way R is calculated is discussed in Chapter 5.

Table B-2 Data from experiment K1-O. This experiment was performed with phenol only, using strain *P. putida O* under batch conditions.

Time[1] (h)	OD[2]	Ph[3] (g m^{-3})	MV[4]	R[5]
0	0.103	110.8	144	
24	0.282	0	144	
46	0.269	0	142	0
0	0.269	96.7	142	
25	0.412	0	144	
43	0.408	0	142	0

[1-5] defined as in Table B-1.

Table B-3 Data from experiment K2-N. This experiment was performed with a mixture of phenol and 4CP, and strain *P. putida N* under batch conditions.

Time[1] (h)	OD[2]	Ph[3] (g m^{-3})	4CP[6] (g m^{-3})	MV[4]	R[5]
0	0.047	109	37	129	
24	0.358	0	0	123	
46	0.586	0	0	121	26
0	0.586	65	24	121	
25	0.622	0	0	118	
43	0.622	0	0	113	38.6
73	0.622	0	0	109	57

[1-5] defined as in Table B-1.
[6] 4CP concentration.

Table B-4 Data from experiment K2-O. This experiment was performed, under batch conditions, with a mixture of phenol and 4CP, and strain *P. putida O.*

Time[1] (h)	OD[2]	Ph[3] (g m^{-3})	4CP[6] (g m^{-3})	MV[4]	R[5]
0	0.123	94	21	137	
24	0.158	52	9	129	
46	0.251	0	0	119	90
0	0.251	86	32	119	
25	0.272	58	24	119	
43	0.374	0	0	106	97
0	0.062	49	31	135	
29	0.162	0	0	113	91

[1-6] defined as in Tables B-1 and B-3.
Note : Readings immediately before and after the third spike are different due to an intentional dilution with medium.

Table B-5 Data from experiment K3-N. This experiment was performed, under batch conditions, with 4CP only and strain *P. putida N.*

Time[1] (h)	OD[2]	4CP[6] (g m^{-3})	MV[4]	R[5]
0	0.037	29	132	
24	0.128	0	129	
46	0.270	0	127	15
0	0.270	29.2	127	
25	0.257	28.3	123	
43	0.260	28.2	121	40
73	0.236	28	116	64

[1,2,4-6] defined as in Tables B-1 and B-3.

Table B-6 Data from experiment K3-O. This experiment was performed, under batch conditions, with 4CP only and strain *P. putida O.*

Time[1] (h)	OD[2]	4CP[6] (g m^{-3})	MV[4]	R[5]
0	0.122	29	132	
24	0.136	0	114	
46	0.136	0	110	111
0	0.136	38.5	110	
25	0.178	0	98	
43	0.178	0	97.5	104
0	0.050	30	128	
29	0.072	0	112	78

[1,2,4-6] defined as in Tables B-1 and B-3.
Note: the culture suspension was diluted with medium before the third spike with 4CP. See also note in Table B-4.

Table B-7 Data from experiment K4-N. This experiment was performed, under batch conditions, with filtrate from experiment K2-N inoculated with suspension from the end of experiment K1-N.

Time[1] (h)	OD[2]	A[7]	MV[4]
0	0.277	1.845	136
26	0.267	1.241	129
50	0.270	0.832	123
0[8]	0.109	0.282	114
20	0.096	0.115	114
45	0.098	0.069	112

[1,2,4] defined as in Table B-1.
[7] absorbance at 375 nm.
[8] at this instant the reactor (flask) contents were diluted with more suspension from the end of experiment K1-N, and fresh medium.

Table B-8 Data from experiment K4-O. This experiment was performed, under batch conditions, with filtrate from experiment K2-N inoculated with suspension from the end of experiment K1-O.

Time[1] (h)	OD[2]	A[7]	MV[4]
0	0.256	1.858	135
26	0.257	1.16	129
50	0.255	0.769	123
0[9]	0.108	0.251	116
20	0.087	0.095	114
45	0.089	0.053	111

[1,2,4] defined as in Table B-1.
[7] same as in Table B-7.
[9] at this instant the reactor (flask) contents were diluted with more suspension from the end of experiment K1-O, and fresh medium.

Table B-9 Data from experiment K5-O. This experiment was performed, under batch conditions, by adding suspension from the end of experiment K1-O to the reactor contents at the end of experiment K3-N.

Time[1] (h)	OD[2]	4CP[6] (g m^{-3})	A[7]	MV[4]
0	0.124	26.5	0.599	138
26	0.147	0	0.522	117
50	0.140	0	0.333	113.5
0[9]	0.085	0	0.171	117
20	0.068	0	0.094	115
45	0.070	0	0	112

[1,2,4] defined as in Table B-1.
[6] defined as in Table B-3.
[7] defined as in Table B-7.
[9] same as in Table B-8.

Table B-10 Data from experiment K6-O. This experiment was performed, under batch conditions, by adding suspension from the end of experiment K1-O to the reactor contents at the end of an experiment similar to K3-N.

Time[1] (h)	OD[2]	4CP[6] (g m^{-3})	A[7]	MV[4]	ACP[10]
0	0.348	23.3	0.511	107	0.538
25	0.363	0	0.408	96	0
49	0.330	0	0.310	95	0

[1,2,4] defined as in Table B-1.
[6] defined as in Table B-3.
[7] defined as in Table B-7.
[10] absorbance at 280 nm, indicative of the presence of 4CP.

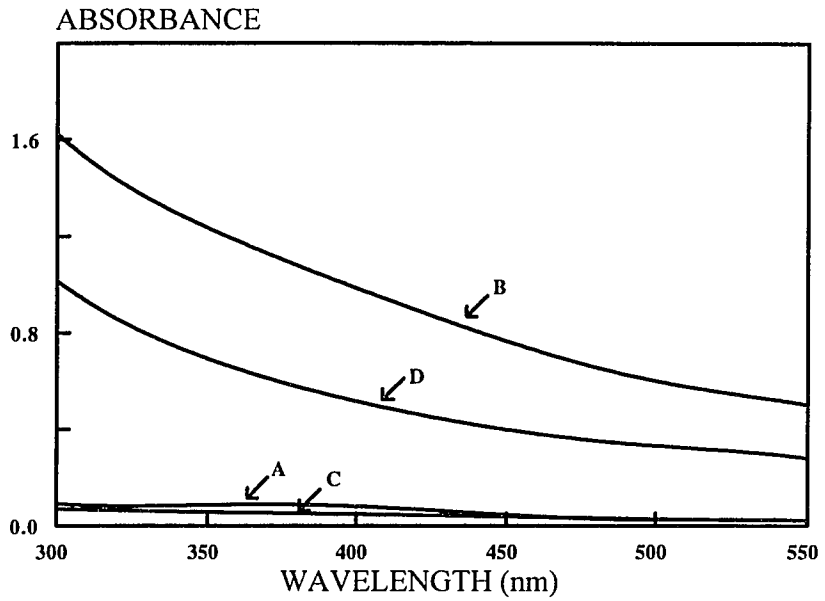

Figure B-1 UV-visible spectra indicating absorbance at various wavelengths. Curves A and B are for samples taken 24 and 46 h, respectively, after initiation of experiment K1-N. Curves C and D are for samples taken 24 and 46 h, respectively, after initiation of experiment K1-O. Samples taken at 24 h were filtered before scanning, while those taken at 46 h were not.

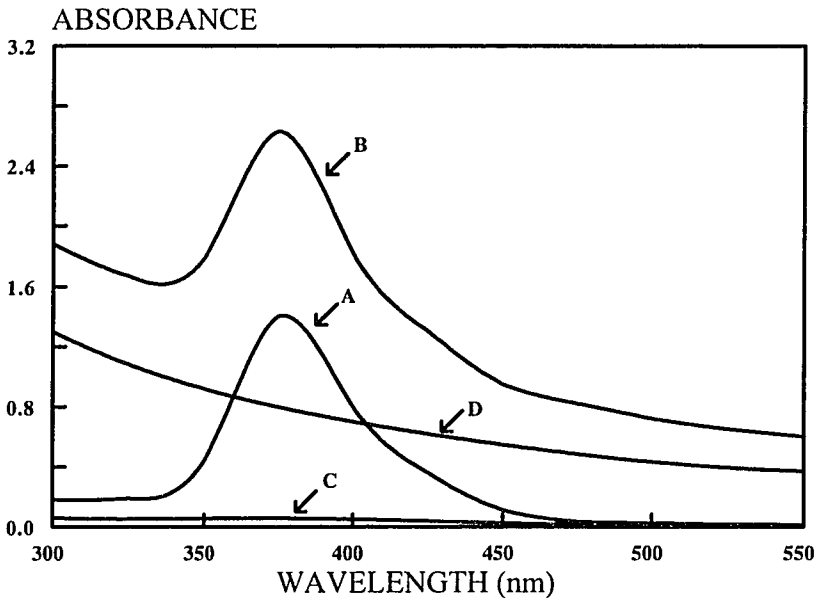

Figure B-2 UV-visible spectra indicating absorbance of samples at various wavelengths. Curves A and B are for samples from experiment K2-N taken 24 and 46 h, respectively, after the experiment started. Curves C and D are for samples from experiment K2-O taken 24 and 46 h, respectively, after initiation of the experiment. Samples taken at 24 h were filtered before scanning, while those taken at 46 h were not.

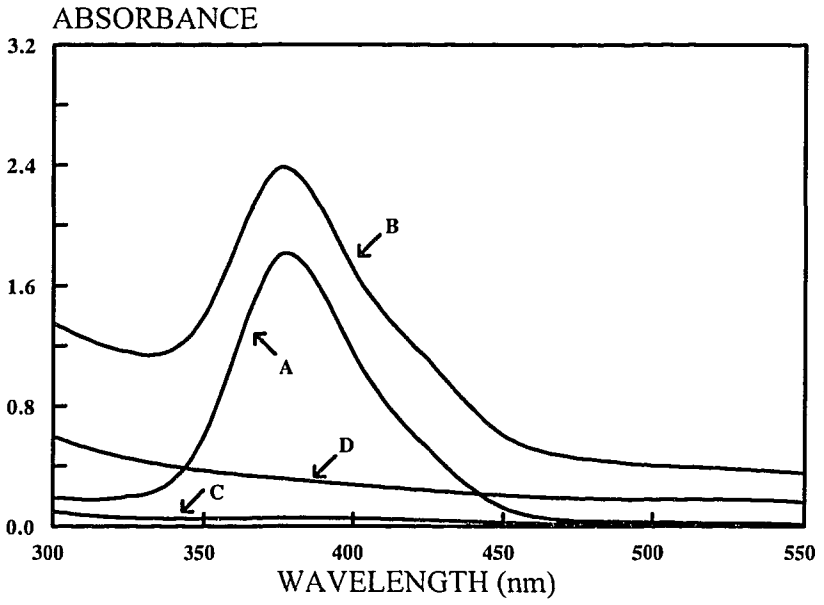

Figure B-3 UV-visible spectra indicating absorbance of samples at various wavelengths. Curves A and B are for samples from experiment K3-N taken 24 and 46 h, respectively, after initiation of the experiment. Curves C and D are for samples from experiment K3-O taken 24 and 46 h, respectively, after the experiment started. Samples taken at 24 h were filtered before scanning, while those taken at 46 h were not.

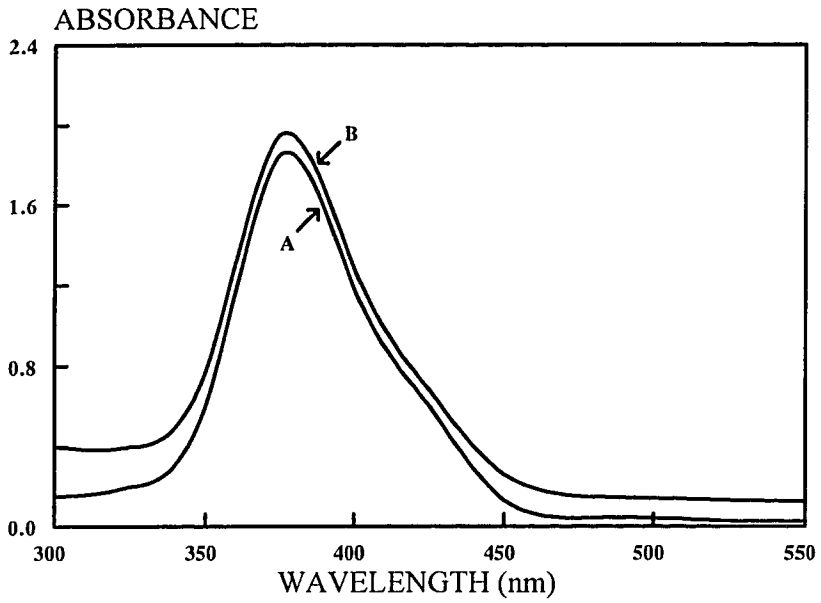

Figure B-4 UV-visible spectra of samples taken at the beginning of experiments K4-N (curve A) and K4-O (curve B). The samples were filtered before scanning.

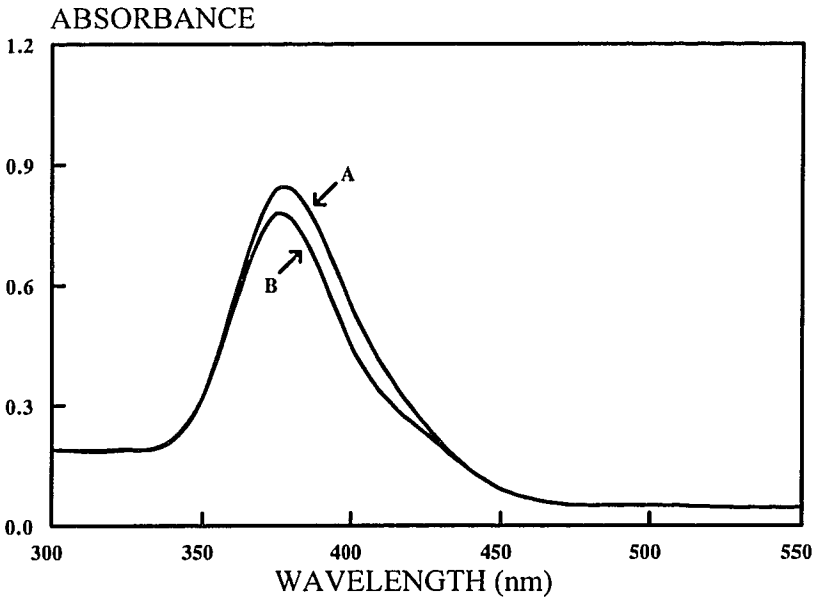

Figure B-5 UV-visible spectra of samples taken 50h after the initiation of experiments K4-N (curve A) and K4-O (curve B). The samples were filtered before scanning.

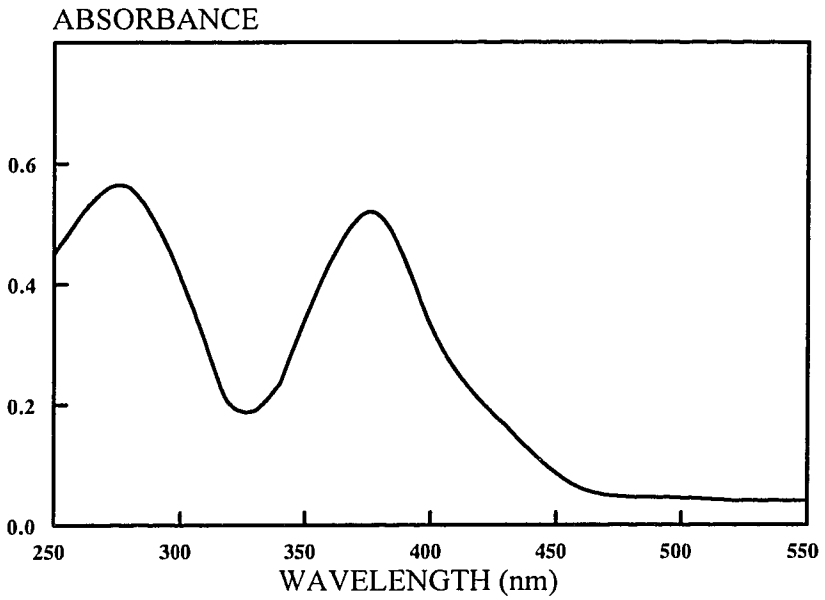

Figure B-6 UV-visible spectrum of a sample taken in the beginning of experiment K6-O. The sample was filtered before scanning.

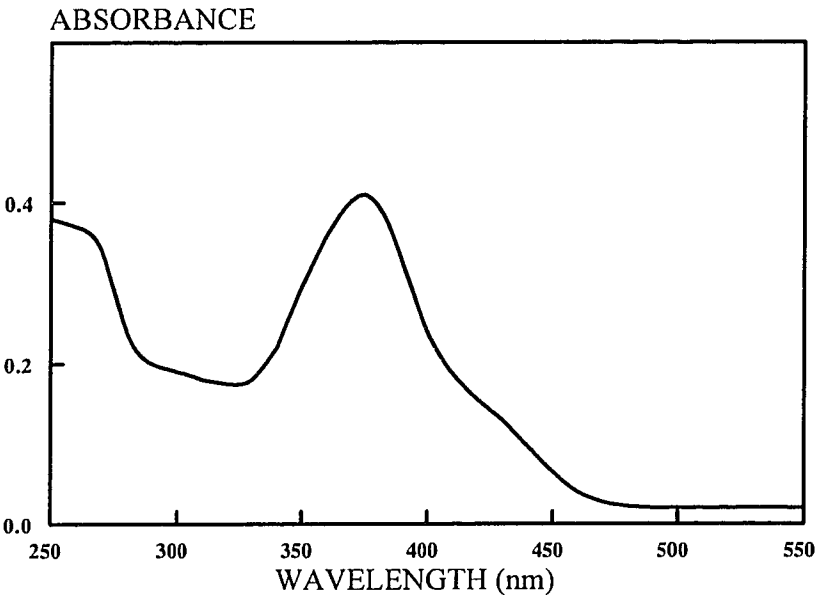

Figure B-7 UV-visible spectrum of a sample taken 25h after initiation of experiment K6-O. The sample was filtered before scanning.

APPENDIX C1

DATA AND THEIR ANALYSIS FOR DETERMINING THE KINETICS OF GLUCOSE UTILIZATION BY *P. putida OR*

Table C1-1 Summary of key information obtained from the kinetic experiments on glucose utilization by *P. putida OR.*

Experiment	Table[1]	Specific growth rate, $\mu_2(s_2)$ (h^{-1})	Glucose[2] concentration ($g\ m^{-3}$)	Yield coefficient	Lag[3] phase (h)	Data points[4] used
G-1	C1-2	0.394	27.9	0.40	0.5	4 - 9
G-2	C1-3	0.533	48.1	0.49	0.5	4 - 10
G-3	C1-4	0.551	53.4	0.44	0.67	5 - 11
G-4	C1-5	0.591	70.8	0.43	0.33	3 - 9
G-5	C1-6	0.612	81.1	0.44	0.5	4 - 11
G-6	C1-7	0.661	107.6	0.43	0.5	4 - 11
G-7	C1-8	0.686	129.3	0.44	0.5	4 - 10
G-8	C1-9	0.700	147.4	0.45	0.5	4 - 11

[1] Table number where detailed data are shown.
[2] Glucose concentration to which the $\mu_2(s_2)$ value shown in column 3 is attributed.
[3] Extent of the observed lag-phase.
[4] Numbers of sample points in the table indicated in column 2 used for determining $\mu_2(s_2)$.

Table C1-2 Data for kinetic experiment G-1.

Sample No.	Time (h)	Optical density	Biomass concentration ($g\ m^{-3}$)	Ln (Biomass concentration)	Glucose concentration ($g\ m^{-3}$)
1	0	0.016	4.374	1.476	32
2	0.167	0.0165	4.511	1.506	31.2
3	0.333	0.017	4.647	1.536	30.5
4	0.5	0.017	4.647	1.536	30
5	0.667	0.018	4.921	1.593	29.3
6	0.833	0.019	5.194	1.648	28.5
7	1	0.0205	5.604	1.723	27.7
8	1.167	0.022	6.014	1.794	26.5
9	1.333	0.0235	6.424	1.860	25.6
10	1.5	0.025	6.835	1.922	24.6
11	1.667	0.0275	7.518	2.017	23.3
12	1.833	0.0305	8.338	2.121	21.8
13	2	0.033	9.022	2.199	19.5
14	2.167	0.036	9.842	2.287	17.9
15	2.333	0.039	10.662	2.367	15.3
16	2.5	0.043	11.755	2.464	12
17	2.75	0.049	13.396	2.595	8
18	3	0.055	15.036	2.711	2
19	3.25	0.062	16.950	2.830	0
20	3.5	0.066	18.043	2.893	0
21	3.75	0.068	18.590	2.923	0

Table C1-3 Data for kinetic experiment G-2.

Sample No.	Time (h)	Optical density	Biomass concentration ($g\ m^{-3}$)	Ln (Biomass concentration)	Glucose concentration ($g\ m^{-3}$)
1	0	0.03	8.201	2.104	54.5
2	0.167	0.031	8.475	2.137	53.8
3	0.333	0.032	8.748	2.169	53
4	0.5	0.033	9.022	2.199	52.7
5	0.667	0.036	9.842	2.287	51
6	0.833	0.039	10.662	2.367	49.5
7	1	0.0425	11.619	2.453	47.3
8	1.167	0.047	12.849	2.553	45
9	1.333	0.0515	14.079	2.645	42.9
10	1.5	0.056	15.309	2.728	39.7
11	1.667	0.062	16.950	2.830	36.7
12	1.833	0.068	18.590	2.923	33
13	2	0.075	20.504	3.021	28.5
14	2.167	0.082	22.417	3.110	23
15	2.333	0.09	24.604	3.203	18.7
16	2.5	0.099	27.0650	3.298	13
17	2.75	0.111	30.345	3.413	6.2
18	3	0.122	33.353	3.507	4
19	3.25	0.125	34.173	3.531	0.5

Table C1-4 Data for kinetic experiment G-3.

Sample No.	Time (h)	Optical density	Biomass concentration ($g\ m^{-3}$)	Ln (Biomass concentration)	Glucose concentration ($g\ m^{-3}$)
1	0	0.021	5.741	1.748	62.1
2	0.167	0.021	5.741	1.748	61.2
3	0.333	0.022	6.014	1.794	60.5
4	0.5	0.0235	6.424	1.860	59.5
5	0.667	0.025	6.835	1.922	58.5
6	0.833	0.027	7.381	1.999	57.2
7	1	0.03	8.201	2.104	55.5
8	1.167	0.033	9.022	2.200	54
9	1.333	0.036	9.842	2.287	52.1
10	1.5	0.0395	10.799	2.379	49.5
11	1.667	0.043	11.755	2.464	47.1
12	1.833	0.048	13.122	2.574	45.3
13	2	0.053	14.489	2.673	42
14	2.167	0.059	16.130	2.781	39.5
15	2.333	0.065	17.770	2.878	36
16	2.5	0.073	19.957	2.994	31.5
17	2.667	0.082	22.417	3.110	26.2
18	2.833	0.092	25.151	3.225	20.4
19	3	0.101	27.612	3.318	14.6
20	3.167	0.107	29.252	3.376	8.9
21	3.333	0.111	30.345	3.413	1.2

Table C1-5 Data for kinetic experiment G-4.

Sample No.	Time (h)	Optical density	Biomass concentration ($g\ m^{-3}$)	Ln (Biomass concentration)	Glucose concentration ($g\ m^{-3}$)
1	0	0.025	6.835	1.922	79.3
2	0.167	0.027	7.381	1.999	78.2
3	0.333	0.029	7.928	2.070	77.9
4	0.5	0.032	8.748	2.169	75.3
5	0.666	0.035	9.568	2.258	73.9
6	0.833	0.0385	10.525	2.354	71.3
7	1	0.042	11.482	2.441	68.9
8	1.166	0.047	12.849	2.553	66
9	1.333	0.053	14.489	2.673	62.4
10	1.5	0.06	16.403	2.797	59.4
11	1.666	0.066	18.043	2.893	56
12	1.833	0.073	19.957	2.994	52.2
13	2	0.08	21.871	3.085	48
14	2.166	0.089	24.331	3.192	43.3
15	2.333	0.099	27.065	3.298	38.3
16	2.5	0.111	30.345	3.413	32.5
17	2.666	0.125	34.173	3.531	26.3
18	2.833	0.138	37.727	3.630	18.5
19	3.083	0.147	40.187	3.694	10.8
20	3.333	0.155	42.374	3.747	1
21	3.583	0.16	43.741	3.778	0

Table C1-6 Data for kinetic experiment G-5.

Sample No.	Time (h)	Optical density	Biomass concentration ($g\ m^{-3}$)	Ln (Biomass concentration)	Glucose concentration ($g\ m^{-3}$)
1	0	0.048	13.122	2.574	101
2	0.167	0.05	13.669	2.615	99.8
3	0.333	0.052	14.216	2.654	98
4	0.5	0.055	15.036	2.710	96.6
5	0.667	0.06	16.403	2.797	93
6	0.833	0.066	18.043	2.893	89.9
7	1	0.073	19.957	2.994	85.5
8	1.167	0.081	22.144	3.098	80.3
9	1.333	0.09	24.604	3.203	74.1
10	1.5	0.1	27.338	3.308	68
11	1.667	0.112	30.619	3.422	61.6
12	1.833	0.123	33.626	3.515	53.9
13	2	0.137	37.453	3.623	45.3
14	2.167	0.155	42.374	3.747	36.5
15	2.333	0.175	47.842	3.868	25
16	2.5	0.196	53.583	3.981	12.3
17	2.75	0.215	58.777	4.074	2.7
18	3	0.22	60.144	4.097	0.7
19	3.25	0.228	62.331	4.132	0

Table C1-7 Data for kinetic experiment G-6.

Sample No.	Time (h)	Optical density	Biomass concentration ($g\ m^{-3}$)	Ln (Biomass concentration)	Glucose concentration ($g\ m^{-3}$)
1	0	0.037	10.115	2.314	128.6
2	0.167	0.038	10.389	2.341	125.9
3	0.333	0.04	10.935	2.392	123
4	0.5	0.0425	11.619	2.453	121.4
5	0.667	0.047	12.849	2.553	118
6	0.833	0.0525	14.353	2.664	114.9
7	1	0.058	15.856	2.764	111.2
8	1.167	0.065	17.770	2.878	107.3
9	1.333	0.073	19.957	2.994	101.8
10	1.5	0.0815	22.281	3.104	96
11	1.667	0.092	25.151	3.225	89.8
12	1.833	0.105	28.705	3.357	82.3
13	2	0.12	32.806	3.491	73.5
14	2.167	0.138	37.727	3.630	62
15	2.333	0.152	41.554	3.727	51.5
16	2.5	0.169	46.202	3.833	37.6
17	2.667	0.192	52.489	3.961	22.1
18	3	0.215	58.777	4.074	2.6
19	3.25	0.22	60.144	4.097	0
20	3.5	0.228	62.331	4.132	0

Table C1-8 Data for kinetic experiment G-7.

Sample No.	Time (h)	Optical density	Biomass concentration ($g\ m^{-3}$)	Ln (Biomass concentration)	Glucose concentration ($g\ m^{-3}$)
1	0	0.045	12.302	2.510	153
2	0.167	0.047	12.849	2.553	150.2
3	0.333	0.05	13.669	2.615	147.5
4	0.5	0.054	14.763	2.692	144.4
5	0.667	0.06	16.403	2.797	140.4
6	0.833	0.0675	18.453	2.915	135.2
7	1	0.076	20.777	3.034	129.9
8	1.167	0.085	23.238	3.146	125.5
9	1.333	0.095	25.971	3.257	118.6
10	1.5	0.107	29.252	3.376	111.1
11	1.667	0.123	33.626	3.515	102.1
12	1.833	0.134	36.633	3.601	91.4
13	2	0.151	41.281	3.720	81.2
14	2.167	0.169	46.202	3.833	71.8
15	2.333	0.19	51.943	3.950	59
16	2.583	0.221	60.418	4.101	37
17	2.833	0.264	72.173	4.279	5.1
18	3	0.283	77.367	4.349	0
19	3.25	0.289	79.008	4.370	0
20	3.333	0.297	81.195	4.397	0
21	3.5	0.306	83.655	4.427	0

Table C1-9 Data for kinetic experiment G-8.

Sample No.	Time (h)	Optical density	Biomass concentration ($g\ m^{-3}$)	Ln (Biomass concentration)	Glucose concentration ($g\ m^{-3}$)
1	0	0.043	11.755	2.464	173.6
2	0.167	0.045	12.302	2.510	171.2
3	0.333	0.048	13.122	2.574	168.3
4	0.5	0.052	14.216	2.654	165.5
5	0.667	0.0585	15.993	2.772	161.3
6	0.833	0.066	18.043	2.893	157
7	1	0.074	20.230	3.007	151.5
8	1.167	0.083	22.691	3.122	145.2
9	1.333	0.093	25.425	3.236	140
10	1.5	0.105	28.705	3.357	133
11	1.667	0.118	32.259	3.474	125.5
12	1.833	0.132	36.087	3.586	114.1
13	2	0.147	40.187	3.694	105.1
14	2.167	0.163	44.561	3.797	90.9
15	2.333	0.181	49.482	3.902	76
16	2.5	0.202	55.223	4.011	60.6
17	2.667	0.227	62.058	4.128	45.4
18	2.833	0.255	69.713	4.244	25
19	3	0.285	77.914	4.356	2.5
20	3.167	0.297	81.195	4.397	0
21	3.5	0.302	82.562	4.414	0

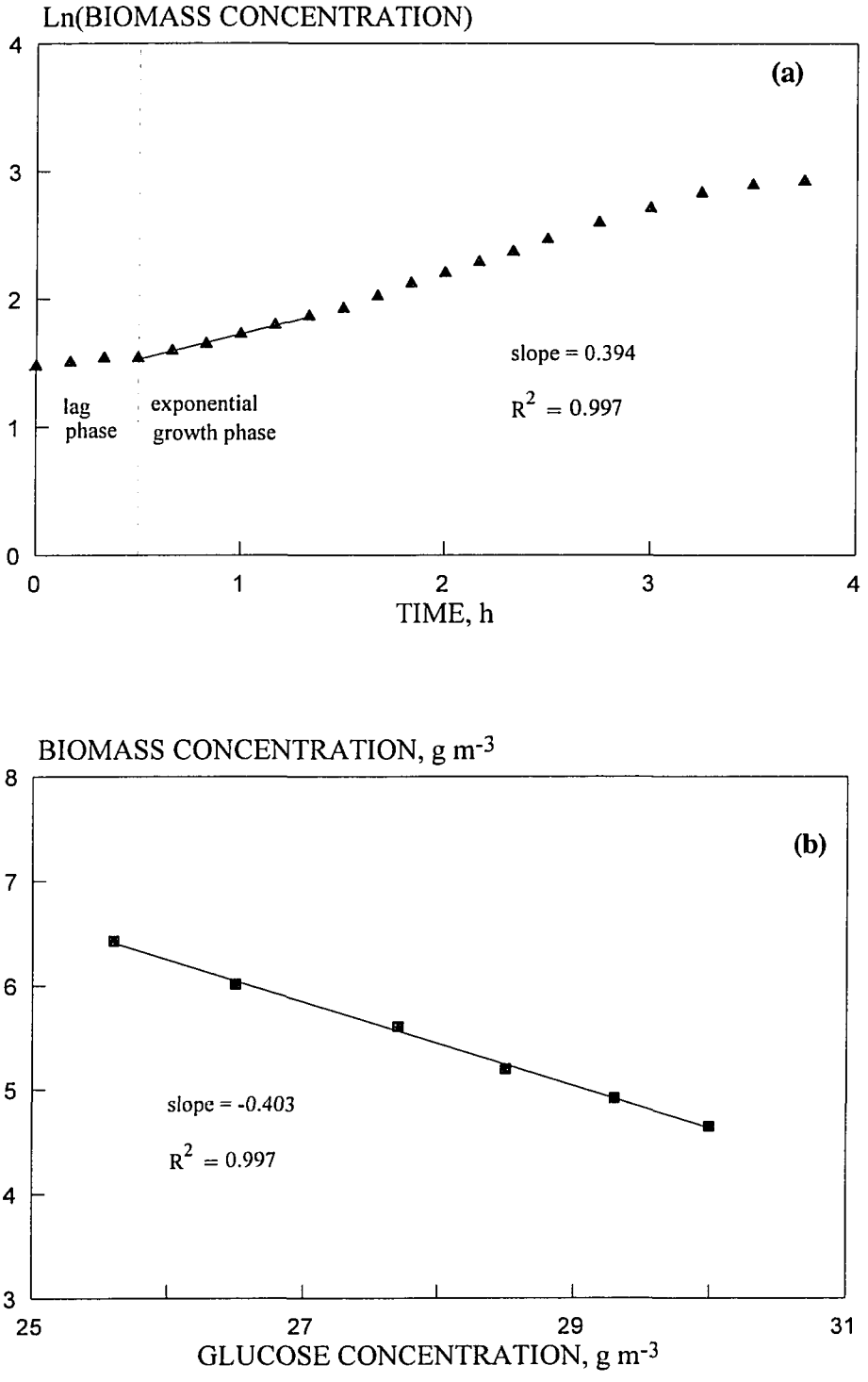

Figure C1-1 Determination of the specific growth rate (a) and yield coefficient (b) of *P. putida OR* on glucose from experiment G-1.

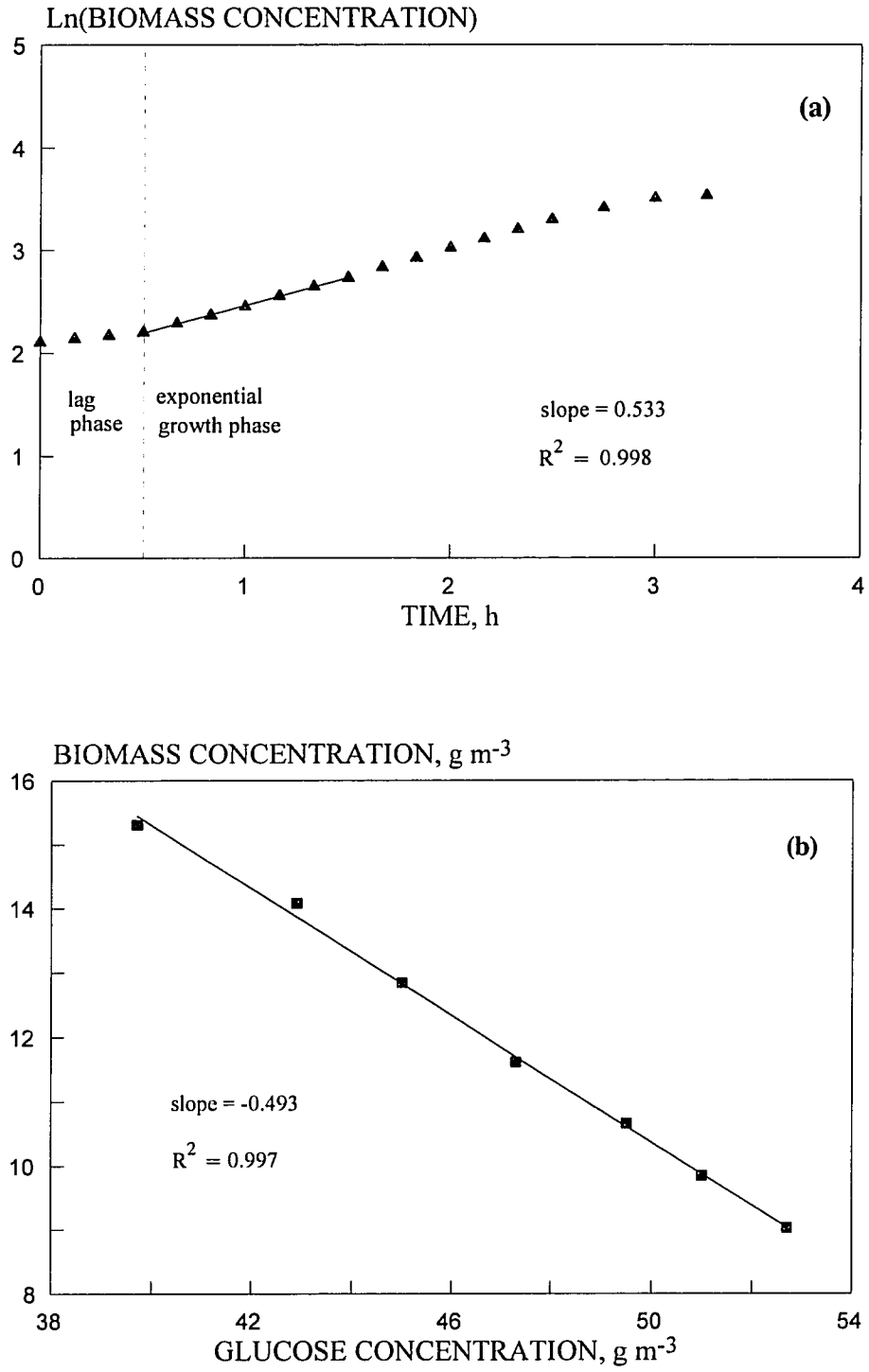

Figure C1-2 Determination of the specific growth rate (a) and yield coefficient (b) of *P. putida OR* on glucose from experiment G-2.

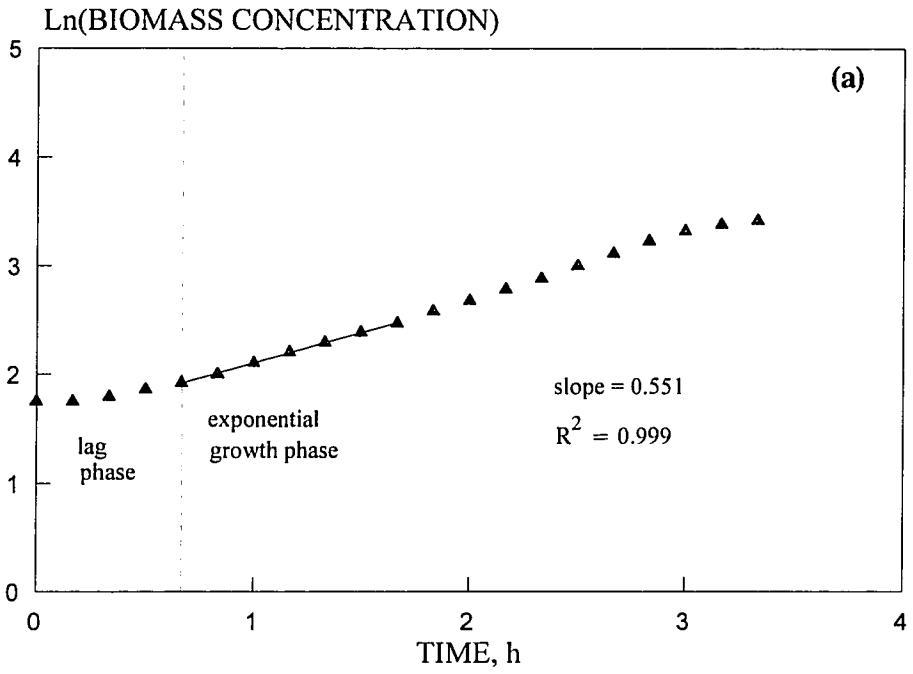

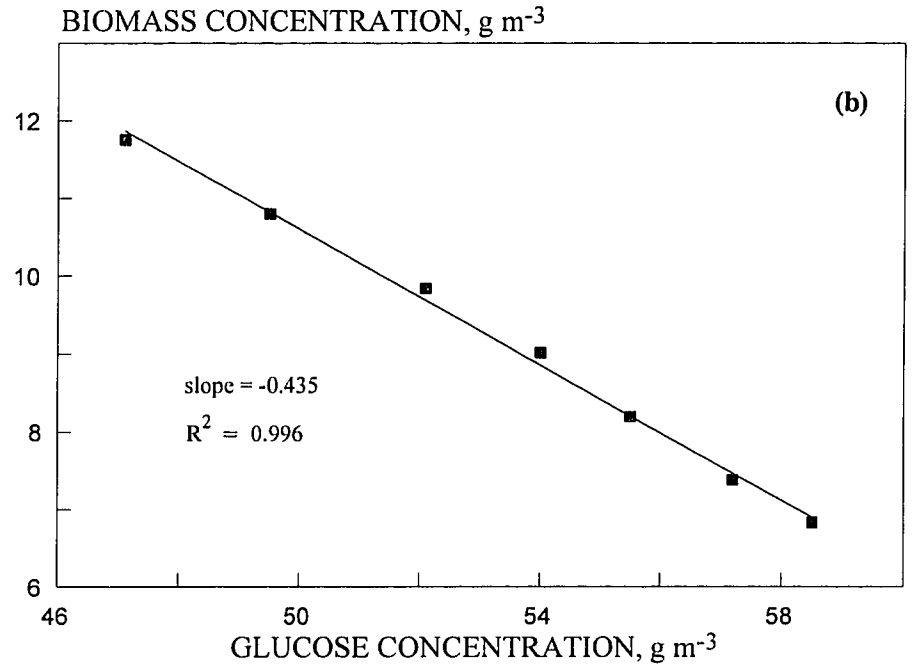

Figure C1-3 Determination of the specific growth rate (a) and yield coefficient (b) of *P. putida OR* on glucose from experiment G-3.

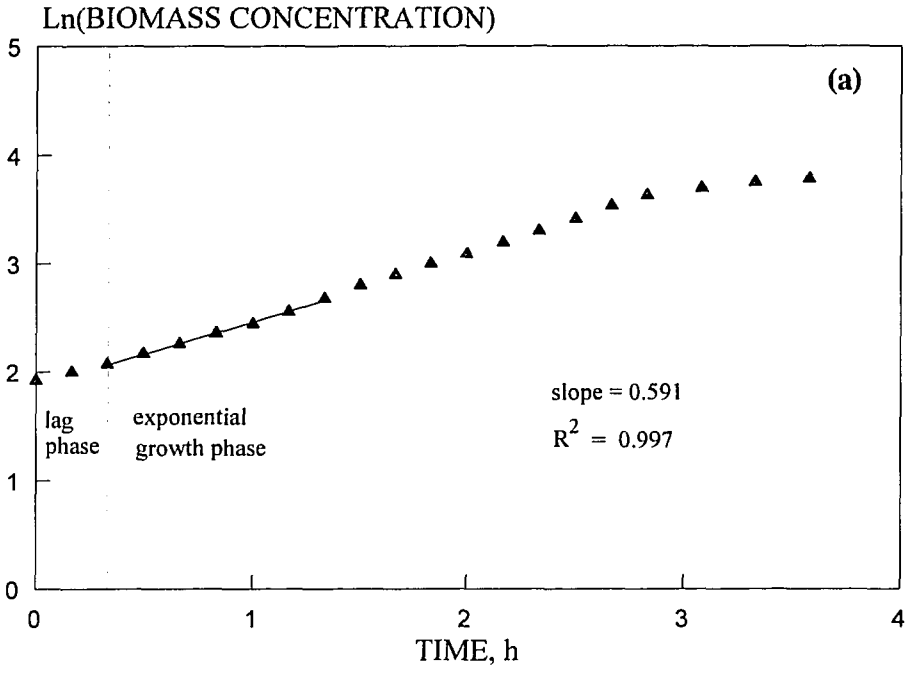

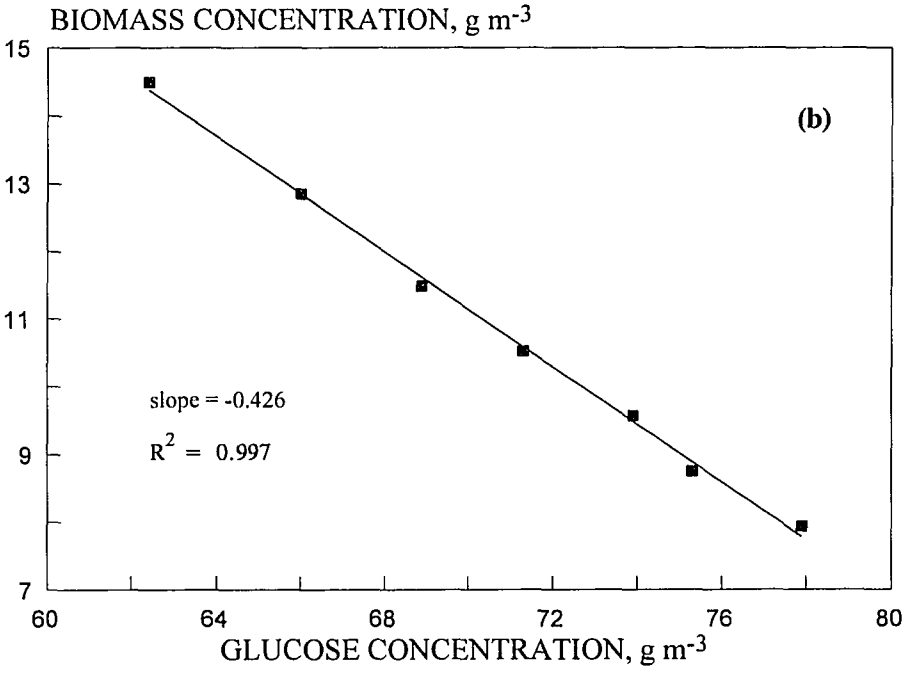

Figure C1-4 Determination of the specific growth rate (a) and yield coefficient (b) of *P. putida OR* on glucose from experiment G-4.

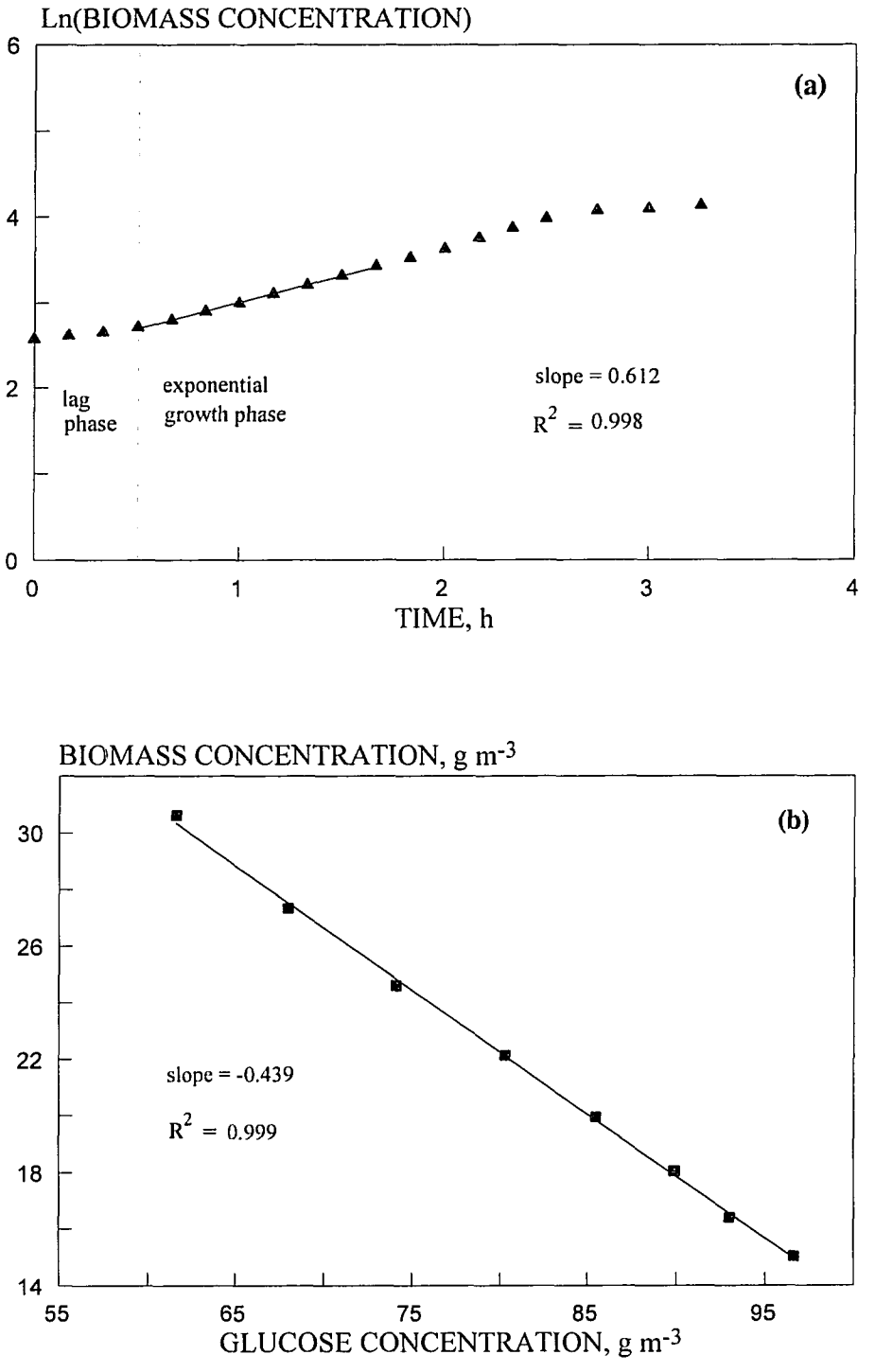

Figure C1-5 Determination of the specific growth rate (a) and yield coefficient (b) of *P. putida OR* on glucose from experiment G-5.

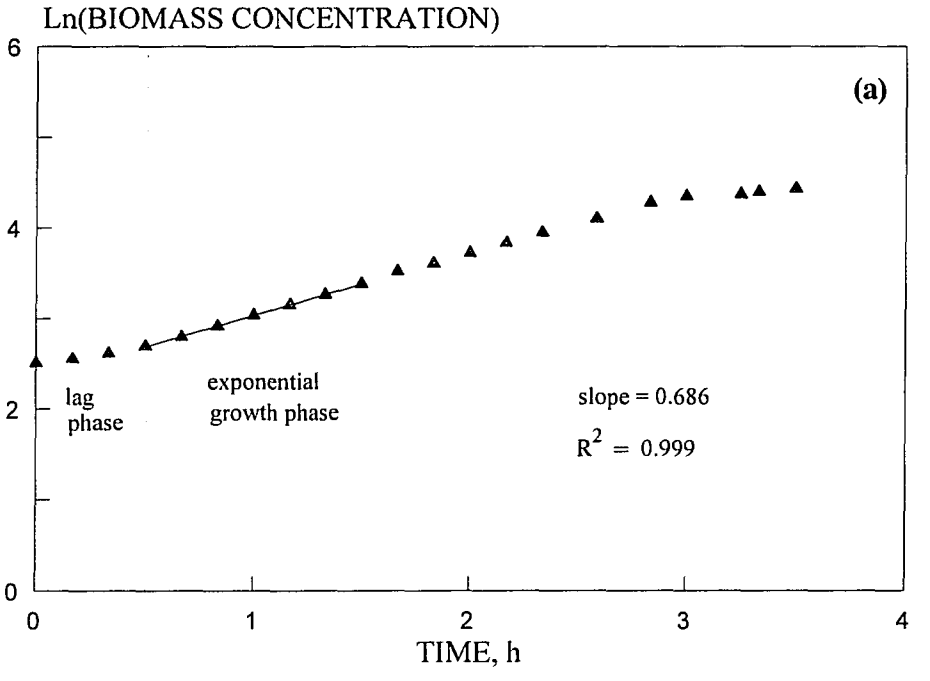

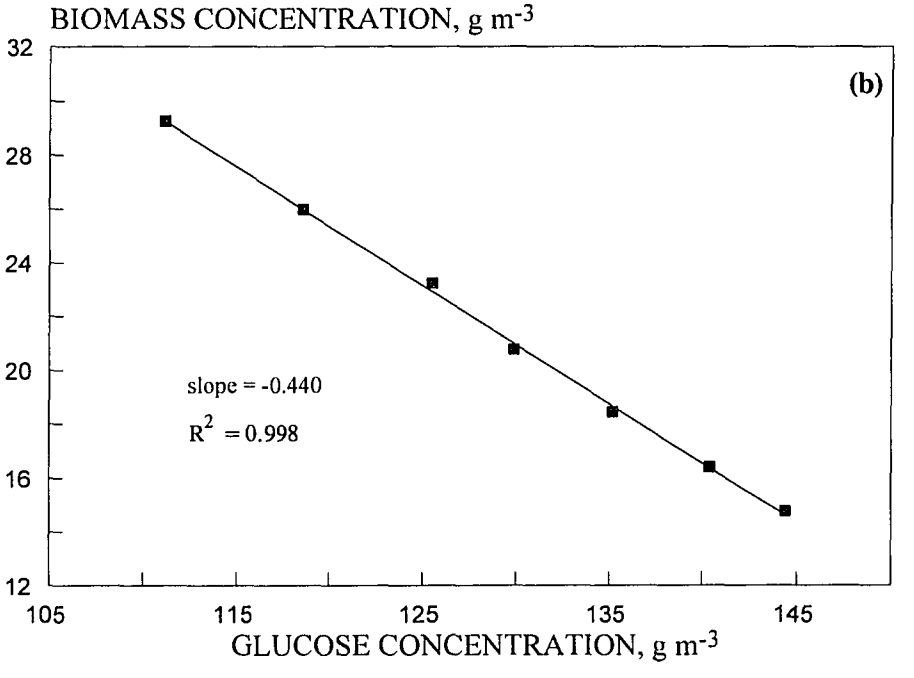

Figure C1-6 Determination of the specific growth rate (a) and yield coefficient (b) of *P. putida OR* on glucose from experiment G-7.

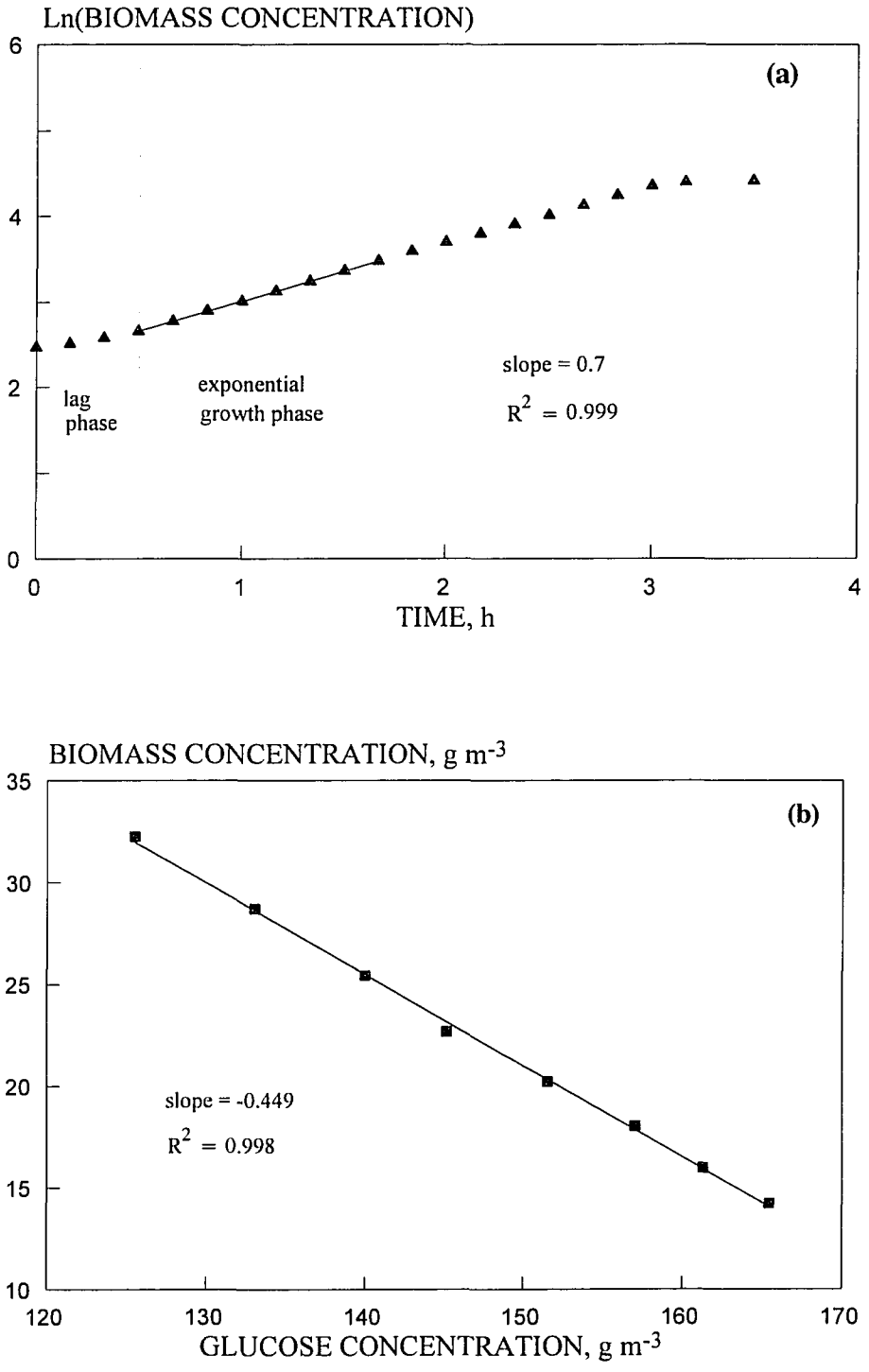

Figure C1-7 Determination of the specific growth rate (a) and yield coefficient (b) of *P. putida OR* on glucose from experiment G-8.

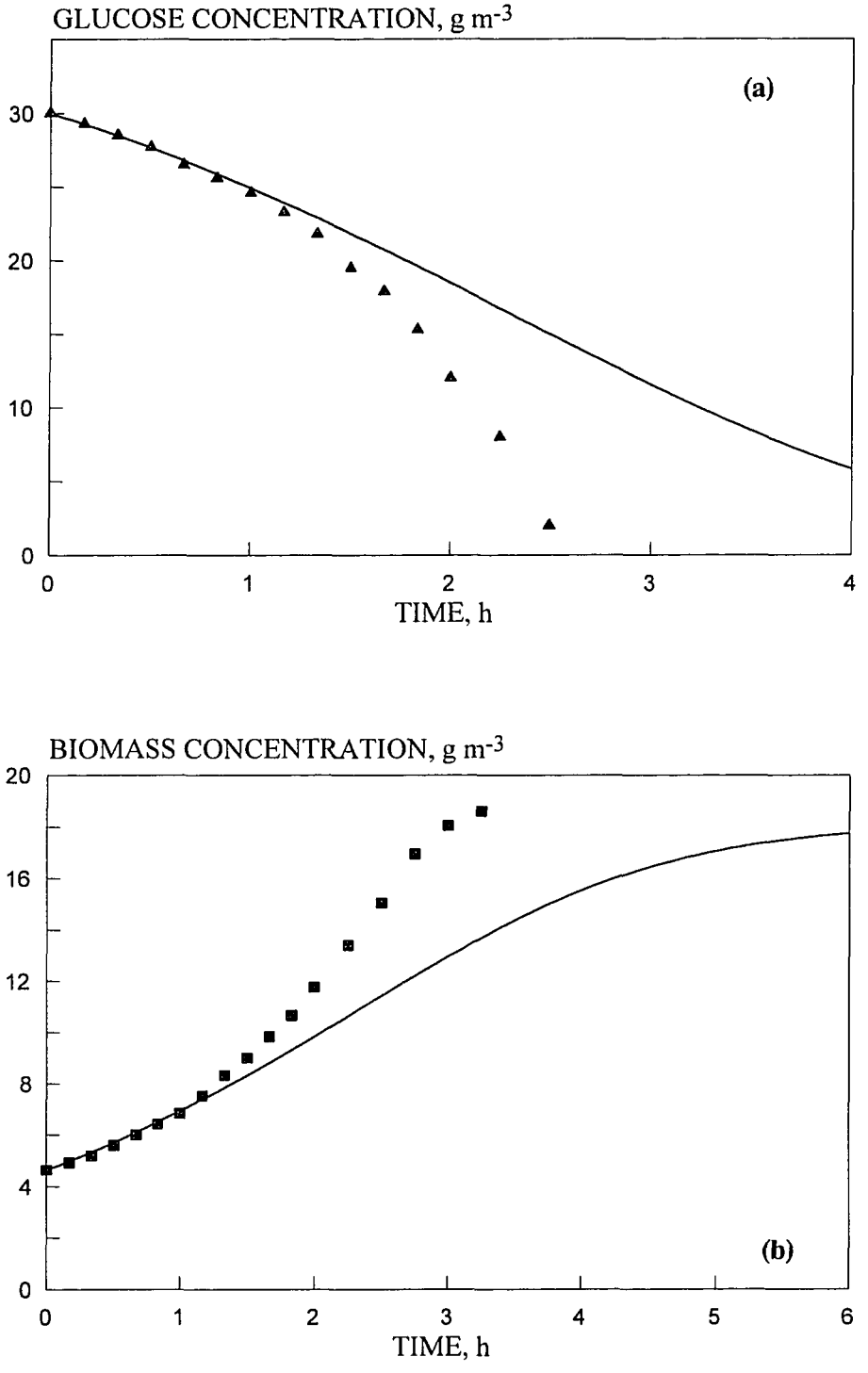

Figure C1-8 Comparison between experimentally obtained and model predicted concentration profiles for glucose (a) and biomass (b) for experiment G-1.

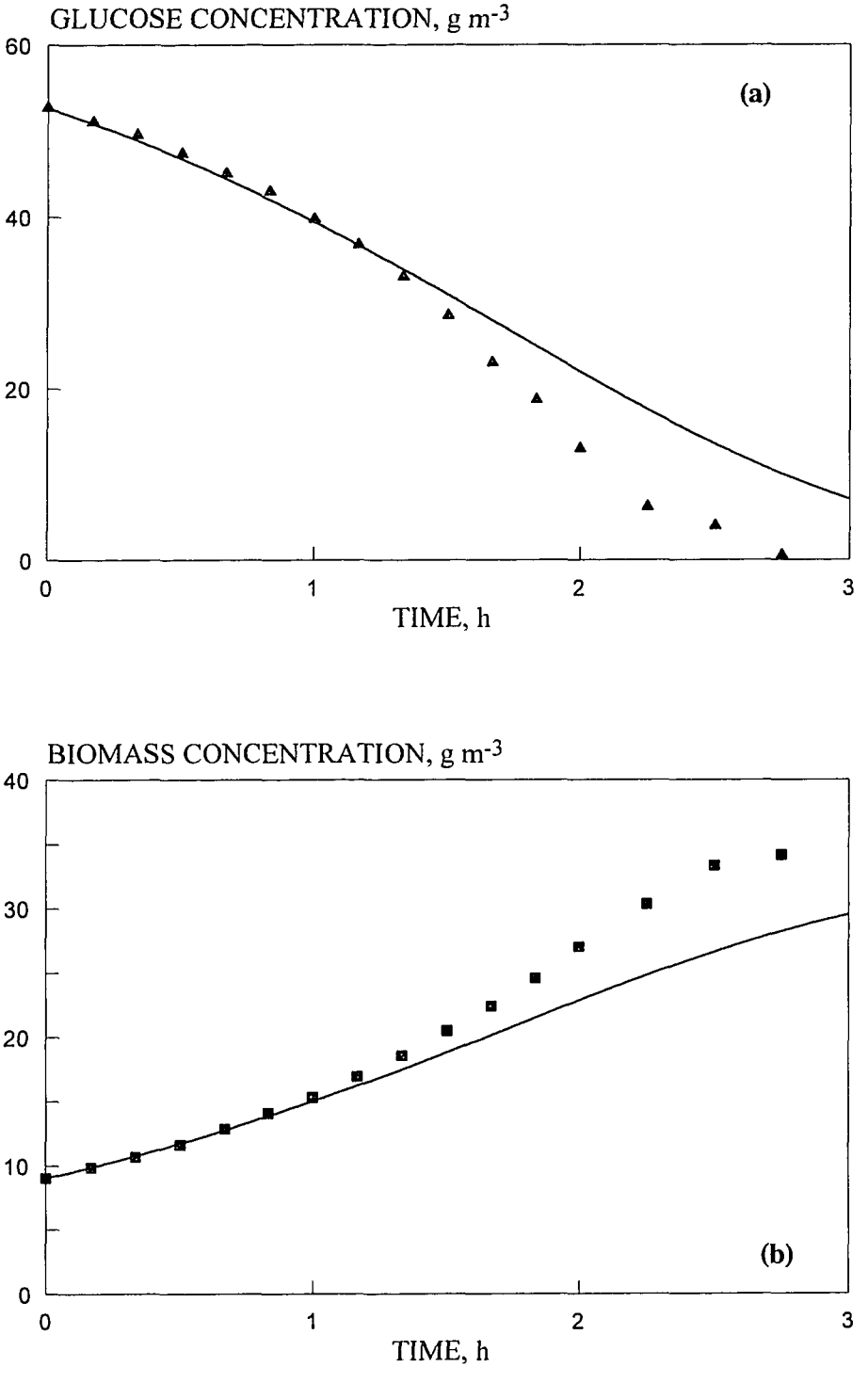

Figure C1-9 Comparison between experimentally obtained and model predicted concentration profiles for glucose (a) and biomass (b) for experiment G-2.

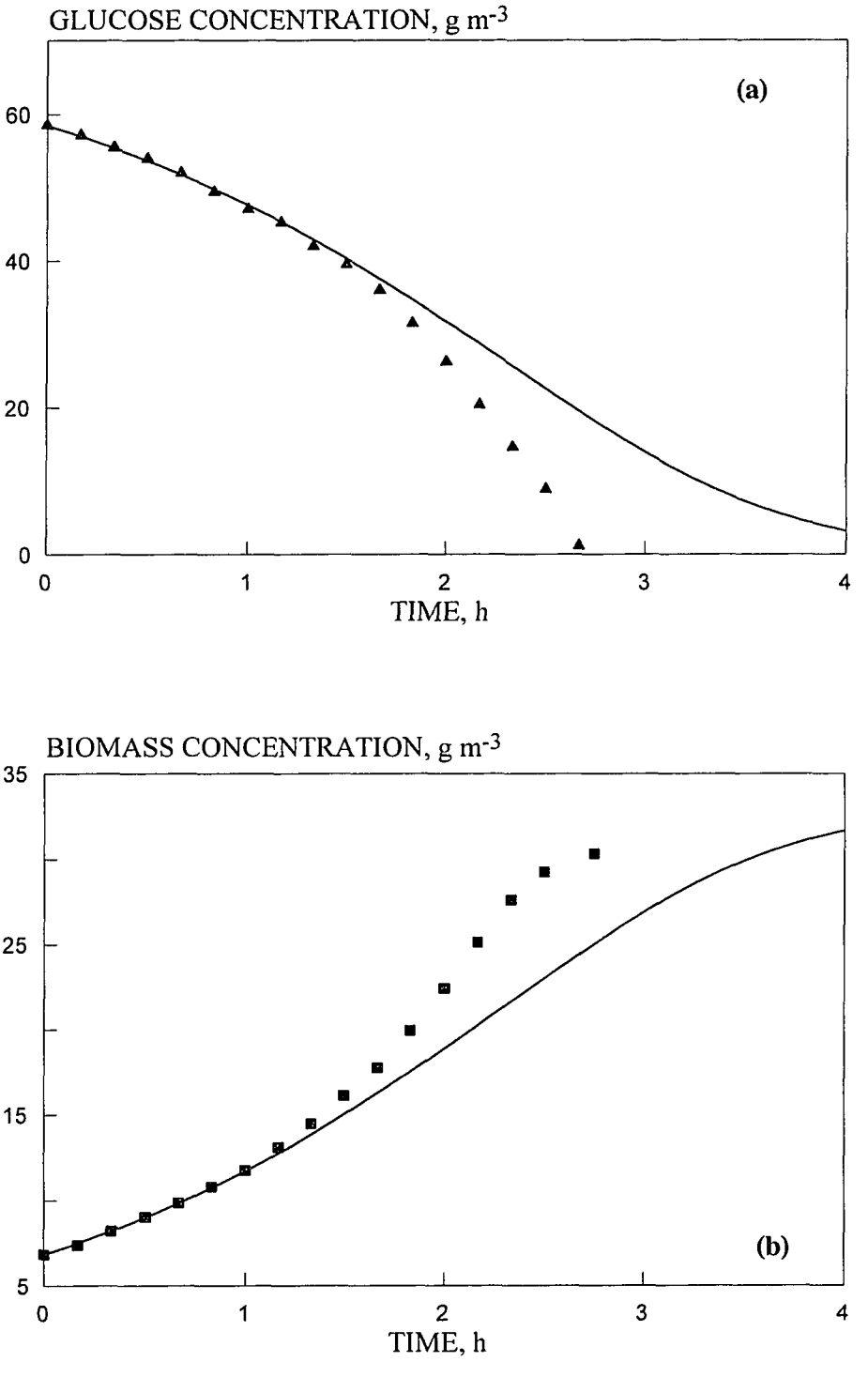

Figure C1-10 Comparison between experimentally obtained and model predicted concentration profiles for glucose (a) and biomass (b) for experiment G-3.

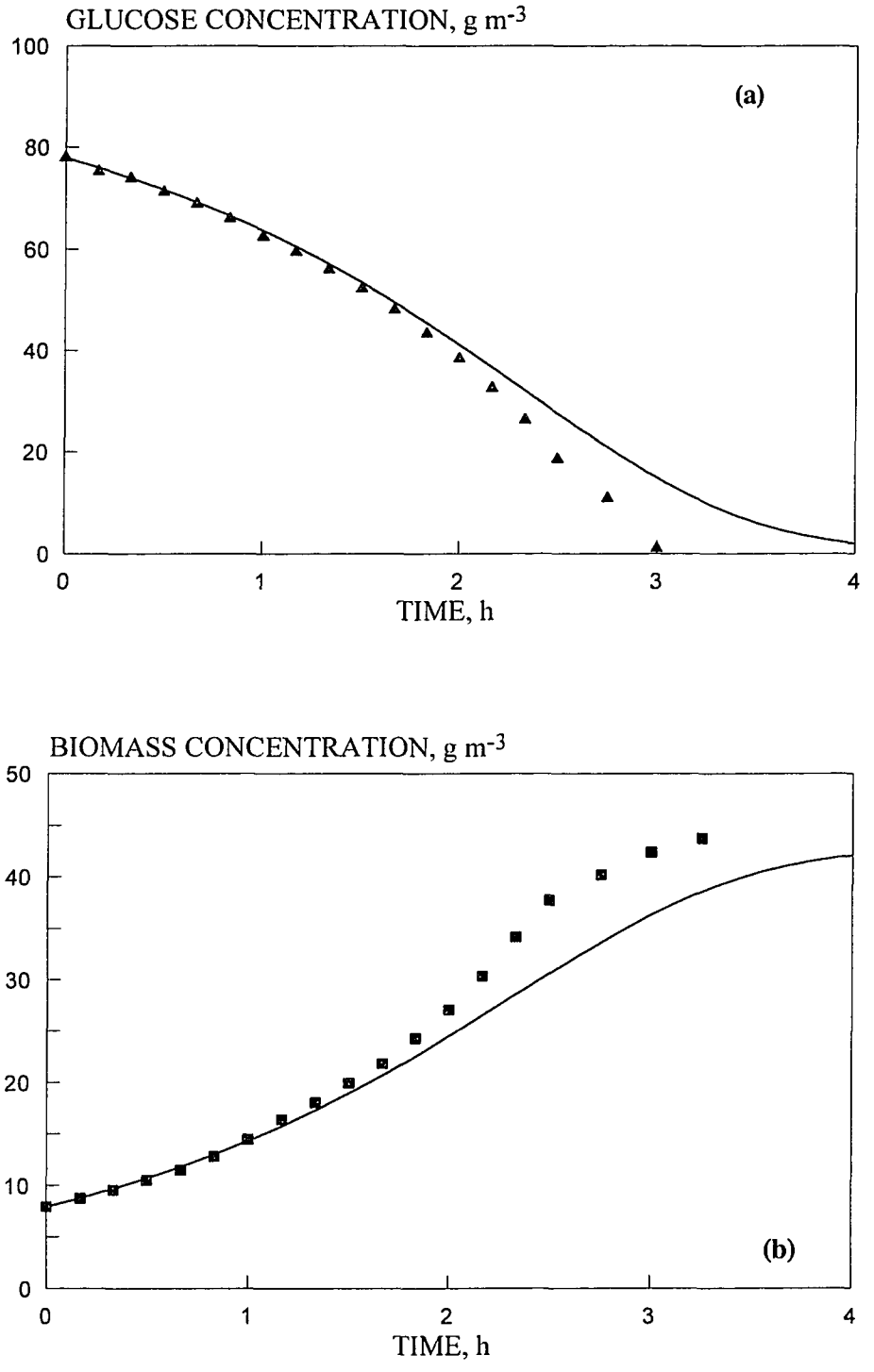

Figure C1-11 Comparison between experimentally obtained and model predicted concentration profiles for glucose (a) and biomass (b) for experiment G-4.

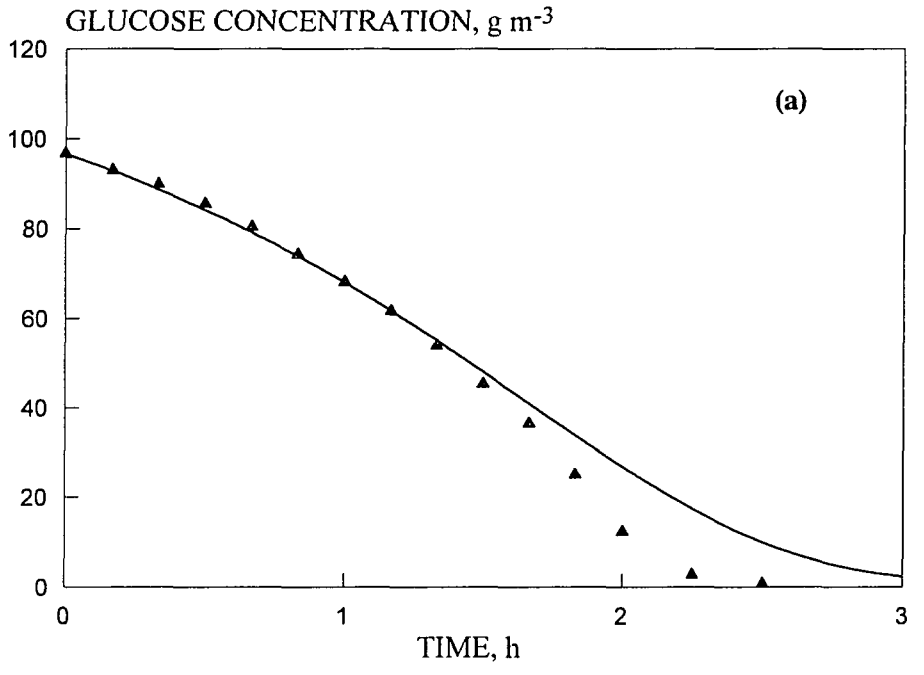

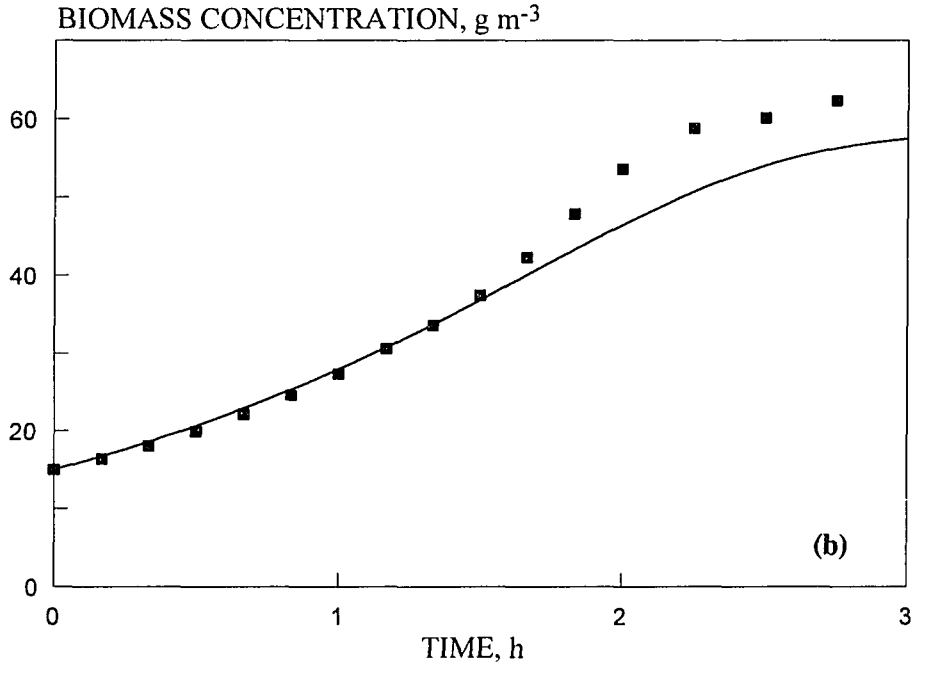

Figure C1-12 Comparison between experimentally obtained and model predicted concentration profiles for glucose (a) and biomass (b) for experiment G-5.

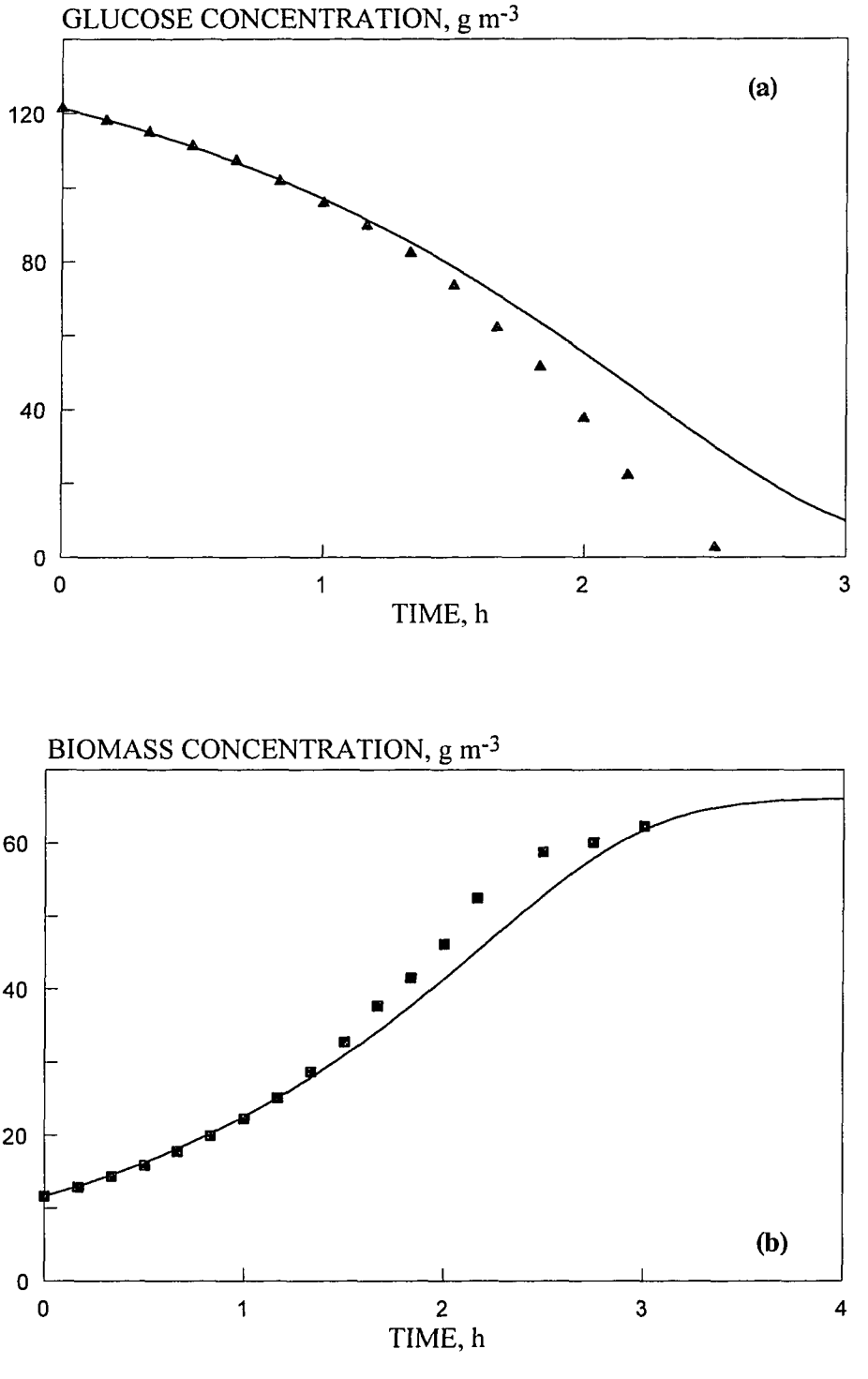

Figure C1-13 Comparison between experimentally obtained and model predicted concentration profiles for glucose (a) and biomass (b) for experiment G-6.

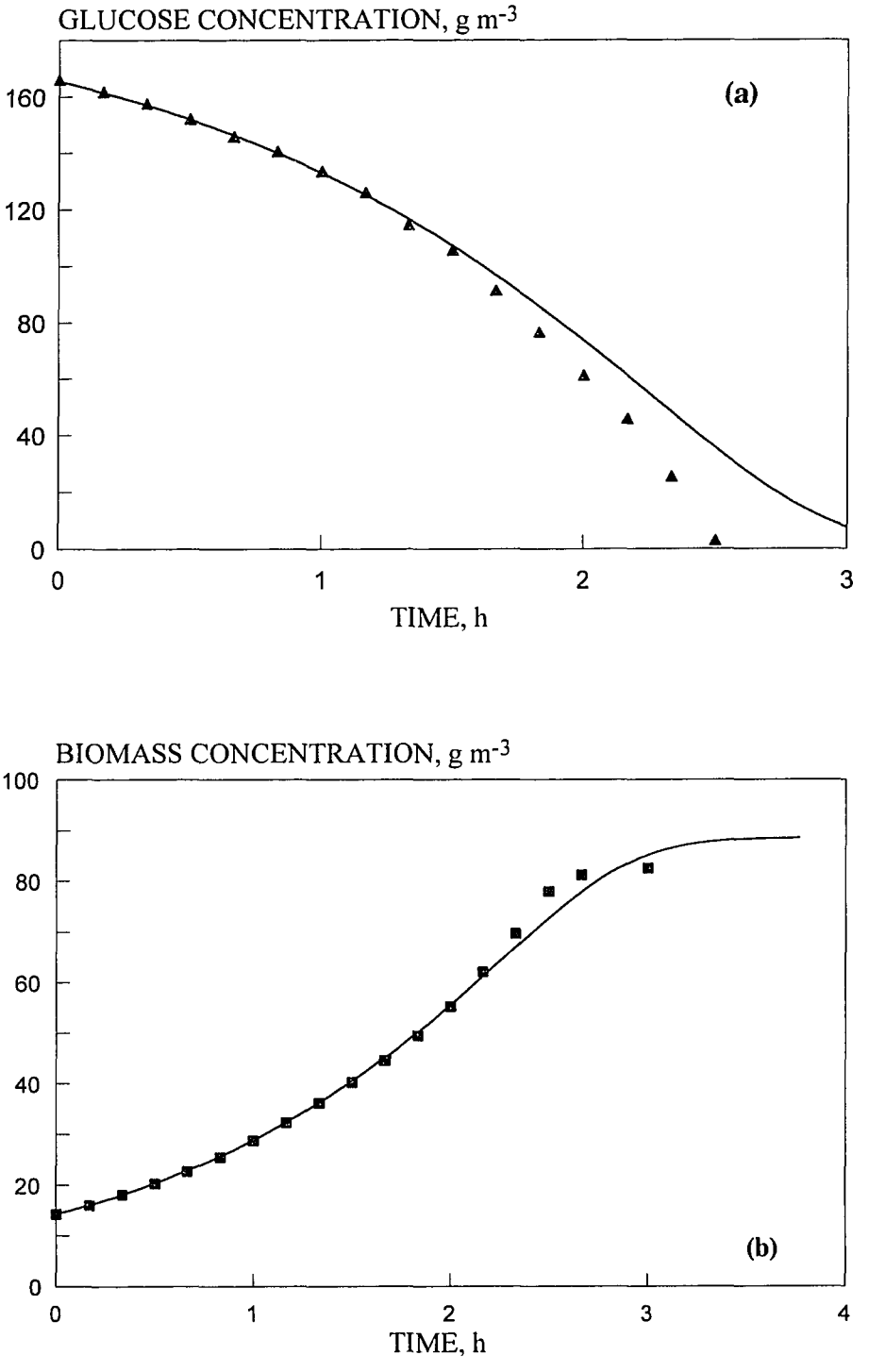

Figure C1-14 Comparison between experimentally obtained and model predicted concentration profiles for glucose (a) and biomass (b) for experiment G-8.

APPENDIX C2

DATA FROM BATCH EXPERIMENTS WITH MIXTURES OF PHENOL AND GLUCOSE UTILIZED BY *P. putida OR*

Table C2-1 Summary of conditions for the batch experiments with mixtures of phenol and glucose utilized by culture *P. putida OR.*

Experiment	Table[1]	$s^{2}_{1,o}$ (g m^{-3})	$s^{3}_{2,o}$ (g m^{-3})	$b^{4}_{1,o}$ (g m^{-3})	R^{5}_{1}	R^{5}_{2}
PG-1	C2-2	98.5	100	14.2	0.26	0.50
PG-2	C2-3	98.6	50	14.5	0.37	0.51
PG-3	C2-4	98.6	33.3	13.4	0.47	0.51
PG-4	C2-5	110.4	0	13.7	0.55	——
PG-5	C2-6	51.8	104.2	13.9	0.31	0.73
PG-6	C2-7	47.6	46	14.2	0.36	0.66
PG-7	C2-8	50.5	25	15.3	0.44	0.60
PG-8	C2-9	54.4	0	13.9	0.65	——
PG-9	C2-10	24.9	100	13.9	0.32	0.84
PG-10	C2-11	25.2	52	13.4	0.36	0.74
PG-11	C2-12	23.6	26.7	12.3	0.42	0.65
PG-12	C2-13	27.1	0	13.7	0.69	——

[1] Table number where detailed data are reported.
[2] Initial phenol concentration.
[3] Initial glucose concentration.
[4] Initial biomass concentration.
[5] Average specific rate of phenol removal (g-phenol / h /g-biomass).
[6] Average specific rate of glucose removal (g-glucose / h /g-biomass).

Table C2-2 Data from batch experiment PG-1.

Sample No.	Time (h)	Phenol concentration ($g\ m^{-3}$)	Glucose concentration ($g\ m^{-3}$)	Biomass concentration ($g\ m^{-3}$)
1	0	98.5	100.0	14.216
2	0.25	97.6	95.8	14.763
3	0.5	97.6	91.7	16.676
4	0.75	94.7	95.8	18.590
5	1	93.0	91.7	21.050
6	1.25	94.1	87.5	24.604
7	1.5	91.0	79.2	28.158
8	1.75	89.4	75.0	33.079
9	2	87.1	75.0	35.540
10	2.333	82.9	66.7	40.187
11	2.583	80.6	58.3	48.115
12	2.833	75.3	45.8	54.677
13	3.083	71.2	41.7	63.972
14	3.25	65.9	29.2	70.533
15	3.5	61.2	20.8	76.547
16	3.667	54.1	4.2	90.216
17	3.833	44		105.526
18	4	33		112.907
19	4.167	20		124.116
20	4.333	5		131.224

Table C2-3 Data from batch experiment PG-2.

Sample No.	Time (h)	Phenol concentration (g m^{-3})	Glucose concentration (g m^{-3})	Biomass concentration (g m^{-3})
1	0	98.6	50.0	14.489
2	0.25	97.6	45.8	15.856
3	0.5	95.5	41.7	17.496
4	0.75	96.2	41.7	20.230
5	1	91.3	37.5	23.238
6	1.25	88.1	29.2	26.518
7	1.5	87.7	33.3	31.166
8	1.75	86.2	25.0	37.453
9	2	79.5	16.7	43.194
10	2.25	74.7	8.3	52.489
11	2.5	60.8		66.705
12	2.75	58.6		71.353
13	2.917	47.4		80.375
14	3.167	38.6		93.497
15	3.333	20.7		101.698
16	3.5	5		110.720
17	3.583	0		112.360
18	3.75			114.547

Table C2-4 Data from batch experiment PG-3.

Sample No.	Time (h)	Phenol concentration ($g\ m^{-3}$)	Glucose concentration ($g\ m^{-3}$)	Biomass concentration ($g\ m^{-3}$)
1	0	98.6	33.3	13.396
2	0.25	97.3	33.3	15.036
3	0.5	93.6	29.2	17.496
4	0.667	94.6	25.0	19.410
5	0.833	92	29.2	21.597
6	1	91.5	29.2	24.331
7	1.167	89.9	20.8	27.885
8	1.333	88.5	16.7	28.979
9	1.5	83.8	8.3	33.353
10	1.75	80	8.3	39.640
11	2	72		45.928
12	2.167	66.6		50.302
13	2.333	61.3		55.497
14	2.5	57.1		63.425
15	2.75	41.2		70.806
16	2.883	35		83.108
17	3	23		86.116
18	3.167	10		94.590
19	3.333	1		99.511

Table C2-5 Data from batch experiment PG-4.

Sample No.	Time (h)	Phenol concentration ($g\ m^{-3}$)	Biomass concentration ($g\ m^{-3}$)
1	0	110.4	13.669
2	0.25	105.5	14.763
3	0.5	102.0	16.950
4	0.75	98.3	19.137
5	1	95.6	22.417
6	1.25	90.2	25.971
7	1.5	84.0	31.166
8	1.75	77.1	36.633
9	2	71.6	43.468
10	2.167	67.0	50.029
11	2.333	60.0	55.770
12	2.5	53.0	59.871
13	2.667	42.9	67.526
14	2.917	34.8	78.187
15	3	22.0	80.921
16	3.167	11.3	89.396
17	3.333	0	95.411
18	3.5		94.044

Table C2-6 Data from batch experiment PG-5.

Sample No.	Time (h)	Phenol concentration ($g\ m^{-3}$)	Glucose concentration ($g\ m^{-3}$)	Biomass concentration ($g\ m^{-3}$)
1	0	51.8	104.2	13.943
2	0.25	50.2	95.8	15.309
3	0.5	49.6	87.5	17.770
4	0.75	46.3	91.7	21.324
5	1	45.6	83.3	25.425
6	1.25	43.6	75.0	27.612
7	1.5	40	70.8	31.439
8	1.717	38.2	62.5	34.173
9	1.883	36	66.7	42.101
10	2.033	34.9	54.2	47.022
11	2.167	28.8	45.8	50.302
12	2.417	25	33.3	59.871
13	2.667	14	12.5	71.626
14	2.917	3.1		85.022
15	3			88.576
16	3.25			99.785
17	3.62			104.432
18	3.85			106.893

Table C2-7 Data from batch experiment PG-6.

Sample No.	Time (h)	Phenol concentration ($g\ m^{-3}$)	Glucose concentration ($g\ m^{-3}$)	Biomass concentration ($g\ m^{-3}$)
1	0	47.6	46.0	14.216
2	0.25	45.8	50.0	16.676
3	0.5	44.4	41.7	19.137
4	0.75	43.1	41.7	21.871
5	1	38.5	33.3	25.151
6	1.25	36.2	25.0	30.619
7	1.5	31.5	20.8	36.360
8	1.833	26.9	8.3	46.202
9	2.083	19.3		55.497
10	2.333	10.6		68.072
11	2.417	0		70.259
12	2.583			73.540
13	2.75			75.454
14	2.833			77.641

Table C2-8 Data from batch experiment PG-7.

Sample No.	Time (h)	Phenol concentration ($g\ m^{-3}$)	Glucose concentration ($g\ m^{-3}$)	Biomass concentration ($g\ m^{-3}$)
1	0	50.5	25.0	15.309
2	0.25	47.7	23.1	17.223
3	0.5	45.7	15.4	19.684
4	0.75	42.5	15.4	24.058
5	1	39.7	7.7	30.892
6	1.25	35.9	3.8	33.626
7	1.5	30		42.921
8	1.75	24.7		48.936
9	2	14.6		56.864
10	2.133	12.3		59.597
11	2.283	5		62.605
12	2.5	0		65.065
13	2.667			67.799
14	2.833			68.072

Table C2-9 Data from batch experiment PG-8.

Sample No.	Time (h)	Phenol concentration ($g\ m^{-3}$)	Biomass concentration ($g\ m^{-3}$)
1	0	54.4	13.943
2	0.25	50.2	15.309
3	0.5	48.1	17.496
4	0.75	43.5	20.230
5	1	38.0	24.058
6	1.25	32.9	28.705
7	1.417	28.6	31.986
8	1.583	25.2	36.360
9	1.75	19.2	40.187
10	1.917	14.4	44.835
11	2.115	8.0	50.302
12	2.25		54.403
13	2.417		56.317
14	2.667		60.691

Table C2-10 Data from batch experiment PG-9.

Sample No.	Time (h)	Phenol concentration (g m^{-3})	Glucose concentration (g m^{-3})	Biomass concentration (g m^{-3})
1	0	24.9	100.0	13.943
2	0.25	23.7	95.8	15.583
3	0.5	20.7	87.5	18.317
4	0.666	18.7	91.7	20.777
5	0.833	18	87.5	23.511
6	1	15.7	75.0	26.245
7	1.166	13.1	75.0	29.799
8	1.333	8	66.7	33.899
9	1.5	4	66.7	38.547
10	1.75	0	50.0	47.022
11	2		37.5	56.590
12	2.333		16.7	71.080
13	2.5			78.734
14	3.166			79.281

Table C2-11 Data from batch experiment PG-10.

Sample No.	Time (h)	Phenol concentration ($g\ m^{-3}$)	Glucose concentration ($g\ m^{-3}$)	Biomass concentration ($g\ m^{-3}$)
1	0	25.2	52.0	13.396
2	0.25	23.5	45.8	15.309
3	0.5	21.1	41.7	18.043
4	0.75	20.4	41.7	21.597
5	1	18	33.3	25.971
6	1.167	15.1	29.2	29.252
7	1.333	12.5	33.3	33.353
8	1.5	9.1	20.8	38.000
9	1.667	5.5	12.5	42.921
10	1.833	1	4.2	47.842
11	2			50.302
12	2.167			53.310
13	2.333			55.223
14	2.5			56.590
15	2.667			58.777
16	2.75			58.504

Table C2-12 Data from batch experiment PG-11.

Sample No.	Time (h)	Phenol concentration ($g\ m^{-3}$)	Glucose concentration ($g\ m^{-3}$)	Biomass concentration ($g\ m^{-3}$)
1	0	23.6	26.7	12.302
2	0.25	22.5	26.7	14.216
3	0.5	20.9	20.0	16.676
4	0.667	19	13.3	17.223
5	0.833	17	16.7	21.871
6	1	15	13.3	25.698
7	1.167	12.6	6.7	27.338
8	1.333	9.9		30.072
9	1.5	6.4		34.446
10	1.667	2.4		36.087
11	1.833			38.000
12	2			40.461
13	2.083			42.101
14	2.417			44.015
15	2.583			45.108

Table C2-13 Data from batch experiment PG-12.

Sample No.	Time (h)	Phenol concentration ($g\ m^{-3}$)	Biomass concentration ($g\ m^{-3}$)
1	0	27.1	13.669
2	0.167	24.8	13.943
3	0.333	23.0	15.309
4	0.5	20.7	16.676
5	0.667	18.0	18.590
6	0.833	16.5	21.050
7	1.083	12.0	24.878
8	1.185	9.6	26.792
9	1.333	7.1	27.612
10	1.5	2.0	30.072
11	1.667		32.259
12	1.833		34.173
13	2.083		39.640
14	2.333		

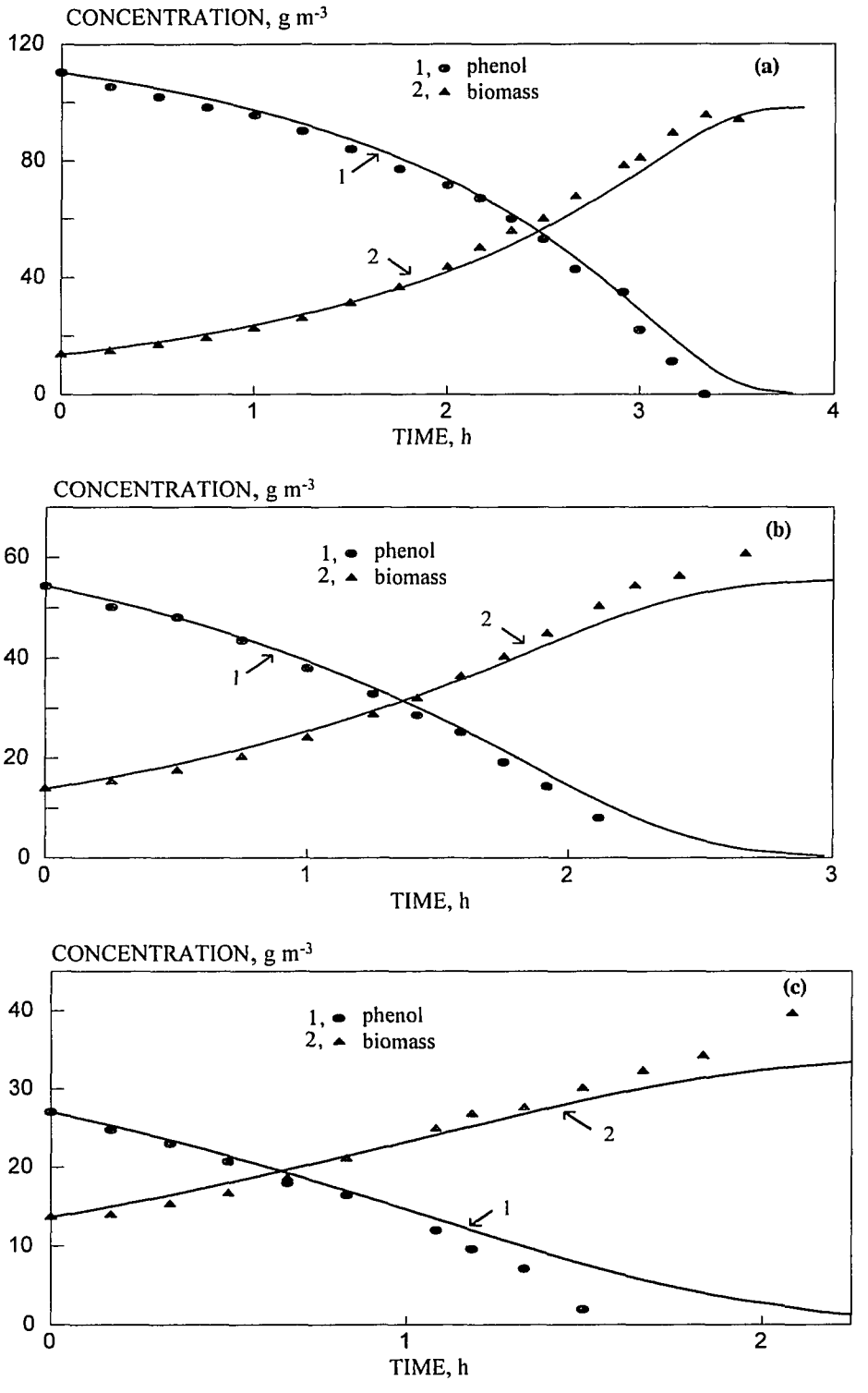

Figure C2-1 Comparison between experimentally obtained and model-predicted concentration profiles for experiments PG-4 (a), PG-8 (b), and PG-12 (c). Information for these experiments is given in Table C2-1.

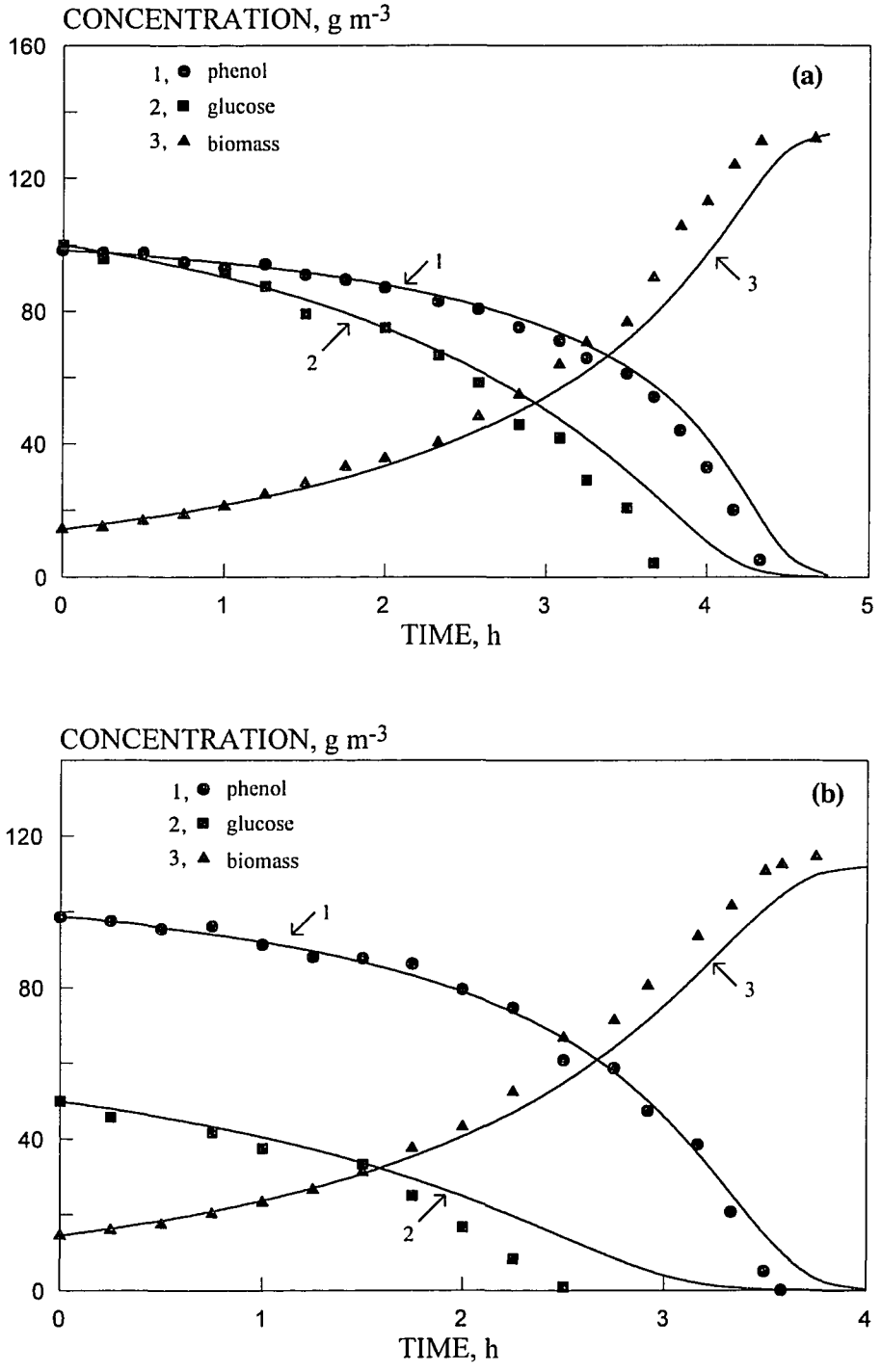

Figure C2-2 Experimentally obtained (symbols) and fitted (curves) concentration profiles for experiments PG-1 (a) and PG-2 (b). Information for these experiments is given in Table C2-1.

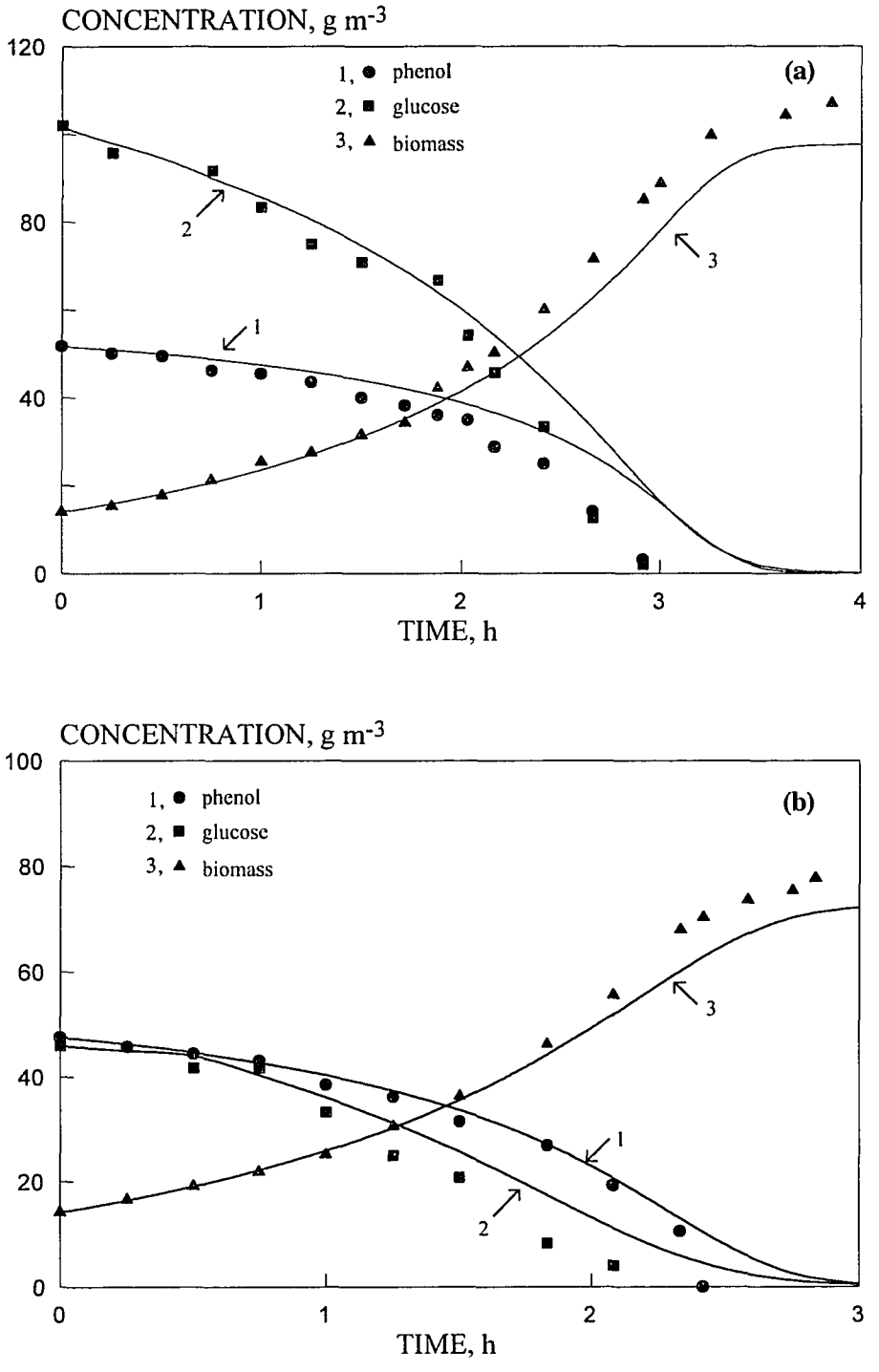

Figure C2-3 Experimentally obtained (symbols) and fitted (curves) concentration profiles for experiments PG-5 (a) and PG-6 (b). Information for these experiments is given in Table C2-1.

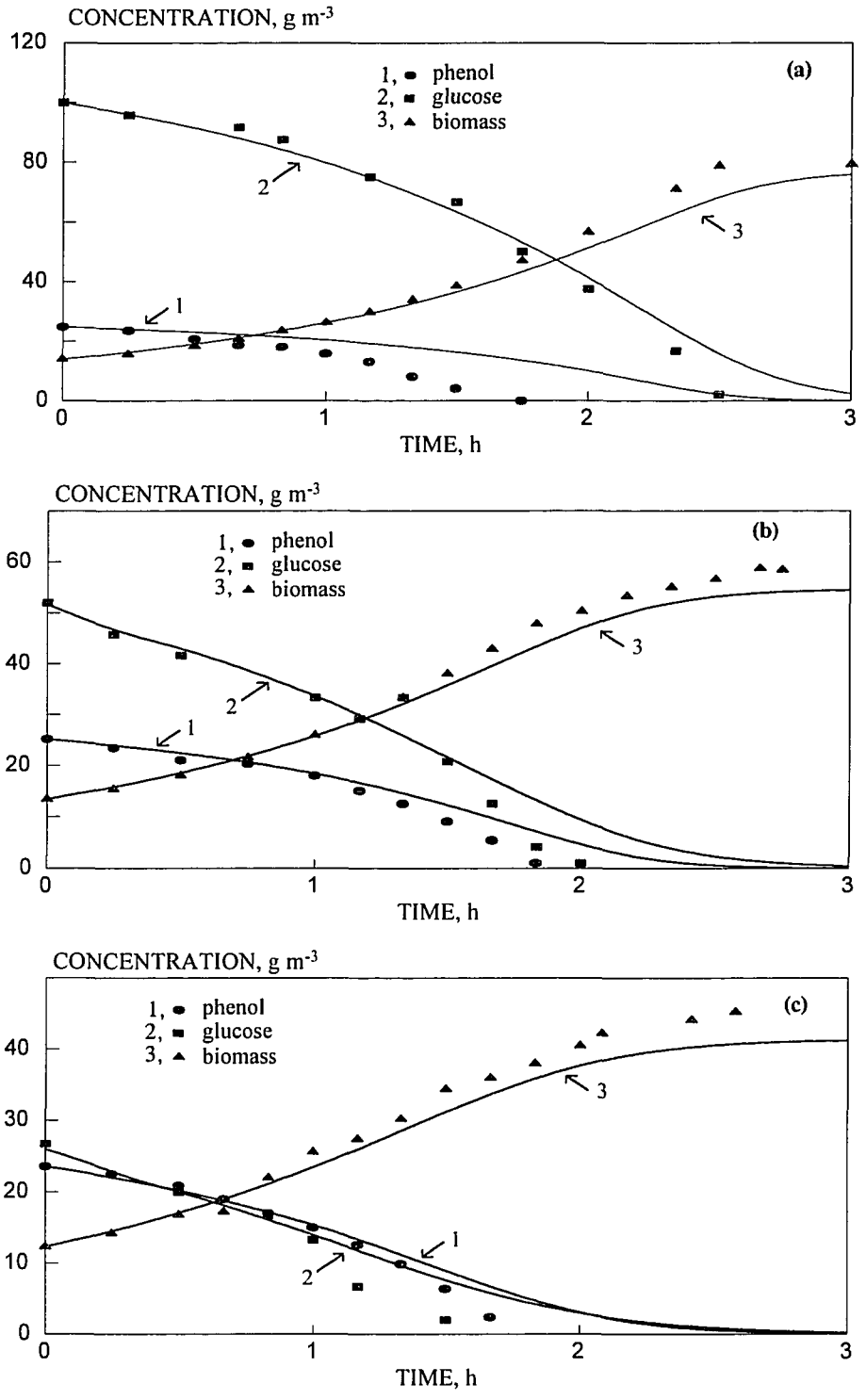

Figure C2-4 Experimentally obtained (symbols) and model-predicted (curves) concentration profiles for experiments PG-9 (a), PG-10 (b), and PG-11 (c). Information for these experiments is given in Table C2-1.

APPENDIX D

CONDITIONS, GRAPHS, AND RAW DATA FOR EXPERIMENTS C-1 THROUGH C-5

Table D-1 Operating and start-up conditions for experiments C-1 through C-5.

Parameter	Experiment C-1	Experiment C-2	Experiment C-3	Experiment C-4	Experiment C-5
t_1 (h)	0.7245	0.613	0.613	1	0.7245
t_2-t_1 (h)	0.5578	0.446	0.446	0.833	0.5578
t_3 (h)	1.449	1.226	1.226	2	1.449
Q_f^* (L h^{-1})	2.76	3.262	3.262	2	2.76
s_{1f} (g m^{-3})	98.3	102.3	100.2	50.2	51.7
s_{2f} (g m^{-3})	47	50	54	48	97
$s_{1f,0}$ (g m^{-3})	0	0	79.8	0	0
$s_{2f,0}$ (g m^{-3})	0	0	40	0	0
b_o (g m^{-3})	98.141	94.782	4.921	60.08	81.145
V_o (L)	2	2	2	2	2
V_m (L)	4	4	4	4	4
σ_1	0.5	0.5	0.5	0.5	0.5
δ	0.5	0.5	0.5	0.5	0.5
β	2.6	2.2	2.2	3.588	2.6
u_f	8.055	8.382	8.21	4.13	4.236
u_o	0	0	6.539	0	0
z_f	1.575	1.675	1.809	1.608	3.25
z_o	0	0	1.34	0	0
x_o	10.471	10.112	0.525	6.41	8.658
Region in Figure 7.4	III(b)	II(b)	II(b)	III(b)	III(c)
Region in Figure 7.5	III(c)	II(c)	II(c)	III(b)	III(b)

Table D-2 Data from experiment C-1. Operating conditions are given in Table D-1.

Cycle 1				Cycle 5			
Time (h)	Phenol ($g\ m^{-3}$)	Glucose ($g\ m^{-3}$)	Biomass ($g\ m^{-3}$)	Time (h)	Phenol ($g\ m^{-3}$)	Glucose ($g\ m^{-3}$)	Biomass ($g\ m^{-3}$)
0	0	0	98.144	5.8	0	0	97.598
0.167	13.1	7.69	84.475	5.967	13.5	6.67	86.936
0.333	22	9.62	78.734	6.133	19.6	8.33	79.828
0.5	24.5	11.54	74.633	6.3	22	10.00	76.547
0.617	24.5	9.62	73.813	6.417	23.4		75.727
0.725	27.3		72.720	6.525	24.6	10.00	75.727
0.833	20.3	3.85	77.367	6.633	21.2	3.33	79.828
1	11.6	3.85	85.022	6.8	13.5	0	87.756
1.167	1.9	0	92.677	6.967	3.4	0	94.317
1.283	0	0	97.598	7.083	0	0	98.418
1.45	0	0	98.144	7.25	0	0	97.871

Cycle 6				Cycle 10			
Time (h)	Phenol ($g\ m^{-3}$)	Glucose ($g\ m^{-3}$)	Biomass ($g\ m^{-3}$)	Time (h)	Phenol ($g\ m^{-3}$)	Glucose ($g\ m^{-3}$)	Biomass ($g\ m^{-3}$)
7.25	0	0	97.871	13.05	0	0	97.051
7.417	12.7	6.67	87.482	13.217	11.8	5.00	88.849
7.583	19.1	6.67	79.828	13.383	17.8	6.67	81.468
7.75	23.4	10.00	76.000	13.55	21.6		78.461
7.867	23.9	10.00	75.180	13.667	23.4	8.33	76.547
7.975	25.8	10.00	74.907	13.775	24.8	10.00	76.000
8.083	19.9	5.00	80.648	13.883	19.5	3.33	79.828
8.25	12.3	3.33	86.662	14.05	11.1	0	85.022
8.417	4.4	0	94.864	14.217	2.1	0	92.403
8.533	0	0	98.144	14.333	0	0	96.777
8.7	0	0	98.418	14.5	0	0	97.324

Table D-3 Data from experiment C-2. Operating conditions are given in Table D-1.

Cycle 1				Cycle 2			
Time (h)	Phenol (g m^{-3})	Glucose (g m^{-3})	Biomass (g m^{-3})	Time (h)	Phenol (g m^{-3})	Glucose (g m^{-3})	Biomass (g m^{-3})
0	0	0	94.864	1.226	2.28	0	96.504
0.167	18.5	10.42	79.281	1.393	19	8.33	81.195
0.333	27.3	12.50	74.633	1.559	26		74.633
0.5	32.1		71.080	1.726	30.5	12.50	70.533
0.613	34.5	12.50	70.259	1.839	33.3	12.50	69.166
0.75	28.1	8.33	76.547	1.976	28	8.33	74.633
0.917	22.2	4.17	82.288	2.143	19.9	4.17	84.475
1.059	13		91.036	2.285	9.5		90.216
1.226	2.28	0	96.504	2.452	1.1	0	95.957

Cycle 7				Cycle 8			
Time (h)	Phenol (g m^{-3})	Glucose (g m^{-3})	Biomass (g m^{-3})	Time (h)	Phenol (g m^{-3})	Glucose (g m^{-3})	Biomass (g m^{-3})
7.356	0.7	0	94.317	8.582	1.1	0	94.864
7.523	16	7.14	82.015	8.749	15.5	7.14	81.468
7.689	24.6	7.14	74.087	8.915	23.6		74.633
7.856	29.9		69.439	9.082	27.3	10.71	70.259
7.969	32.1	10.71	67.252	9.195	33.3	12.50	69.713
8.106	24.6	7.14	74.087	9.332	25.7	7.14	75.727
8.273	15.2		82.288	9.499	16	3.57	81.741
8.415	8.8	3.57	91.036	9.641	8.8		91.036
8.582	1.1	0	94.864	9.808	0.9	0	94.864

Table D-4 Data from experiment C-3. Operating conditions are given in Table D-1.

Cycle 1				Cycle 2			
Time (h)	Phenol ($g\ m^{-3}$)	Glucose ($g\ m^{-3}$)	Biomass ($g\ m^{-3}$)	Time (h)	Phenol ($g\ m^{-3}$)	Glucose ($g\ m^{-3}$)	Biomass ($g\ m^{-3}$)
0	80.3	40.00	4.921	1.226	89	43.33	4.374
0.167	84		3.827	1.393	91.5	43.75	4.101
0.333	87	41.67	3.554	1.559	92.4	45.83	3.554
0.5	89.3	43.33	3.007	1.726	93.1		3.554
0.613	90.8	45.00	3.007	1.839	94.7	45.83	3.281
0.75	90		3.281	1.976	94	45.83	3.281
0.917	89.7	43.33	3.554	2.143	93.2		3.554
1.059	88.8		4.101	2.285	93	43.75	3.827
1.226	89	43.33	4.374	2.452	91.8	43.75	4.374

Cycle 8				Cycle 9			
Time (h)	Phenol ($g\ m^{-3}$)	Glucose ($g\ m^{-3}$)	Biomass ($g\ m^{-3}$)	Time (h)	Phenol ($g\ m^{-3}$)	Glucose ($g\ m^{-3}$)	Biomass ($g\ m^{-3}$)
8.582	97	46.88	2.734	9.808	98	47.81	2.460
8.749	97.9	47.81	2.460	9.975	98.6	48.44	2.187
8.915	98.3	48.44	2.187	10.141	98.9		2.187
9.082	98		2.187	10.308	99	48.44	1.914
9.195	98.6	48.44	2.050	10.421	99.3		1.640
9.332	98		2.187	10.558	99	48.44	1.777
9.499				10.725	98.7		1.914
9.641	98.3	48.44	2.460	10.867	99	48.44	2.187
9.808	98	47.81	2.460	11.034	98.8		2.187

Table D-5 Data from experiment C-4. Operating conditions are given in Table D-1.

Cycle 1			
Time (h)	Phenol (g m^{-3})	Glucose (g m^{-3})	Biomass (g m^{-3})
0	0	0	59.597
0.167	4.9	6.6	54.130
0.333	8.2		50.029
0.5	10.2	10	47.842
0.667	10.4		46.475
0.833	11.2	11.6	47.569
1	9.7	10	49.209
1.167	6.6	6.6	51.669
1.333	2.3	1.5	54.950
1.5	0	0	59.051
1.667	0	0	60.144
1.833	0	0	60.418
2	0	0	60.418

Cycle 2			
Time (h)	Phenol (g m^{-3})	Glucose (g m^{-3})	Biomass (g m^{-3})
2	0	0	60.418
2.167	5.1	6.6	54.130
2.333	7.9	8.3	51.123
2.5	9.7	10	48.662
2.667	9.7	10	47.842
2.833	10.9	11.6	47.842
3	9.6	10	48.936
3.167	6.7	6.6	52.763
3.333	1.5	3.3	56.043
3.5	0	0	58.777
3.667	0	0	59.871
3.833	0	0	60.691
4	0	0	60.418

Cycle 3			
Time (h)	Phenol (g m^{-3})	Glucose (g m^{-3})	Biomass (g m^{-3})
4	0	0	60.418
4.167	4.9	6.6	54.130
4.333	7.9		50.849
4.5	9.4	10	49.209
4.667	9.7		48.389
4.833	10.5	10	47.842
5	9.2		48.662
5.167	6.3	6.6	52.489
5.333	1.9	3.3	55.497
5.5	0	0	58.504
5.667	0	0	60.144
5.833	0	0	60.418
6	0	0	60.691

Table D-6 Data from experiment C-5. Operating conditions are given in Table D-1.

Cycle 1				Cycle 5			
Time (h)	Phenol ($g\ m^{-3}$)	Glucose ($g\ m^{-3}$)	Biomass ($g\ m^{-3}$)	Time (h)	Phenol ($g\ m^{-3}$)	Glucose ($g\ m^{-3}$)	Biomass ($g\ m^{-3}$)
0	0	0	80.921	5.8	0	0	81.195
0.167	7.5	12.50	71.353	5.967	6.1	12.50	71.353
0.333	10.1	20.83	67.252	6.133	8.9	20.83	66.432
0.5	11.7	25.00	63.972	6.3	11.1	20.83	62.331
0.617	13		62.331	6.417	12.3	25.00	61.784
0.725	12.8	25.00	61.238	6.525	12	27.08	61.784
0.833	8.2	18.75	65.612	6.633	8.9	20.83	67.252
1	4.5	8.33	72.720	6.8	4.6	10.42	72.446
1.167	0.4	0	78.461	6.967	0.7	4.17	79.828
1.283	0	0	81.741	7.083	0	0	81.468
1.45	0	0	82.015	7.25	0	0	81.195

Cycle 6				Cycle 10			
Time (h)	Phenol ($g\ m^{-3}$)	Glucose ($g\ m^{-3}$)	Biomass ($g\ m^{-3}$)	Time (h)	Phenol ($g\ m^{-3}$)	Glucose ($g\ m^{-3}$)	Biomass ($g\ m^{-3}$)
7.25	0	0	81.195	13.05	0	0	81.195
7.417	5.6	12.50	71.626	13.217	6.3	16.67	71.626
7.583	9.5	18.75	67.252	13.383	9.2	18.75	66.979
7.75	10	25.00	62.878	13.55	10.5	20.83	63.972
7.867	11.1	25.00	62.331	13.667	12.3	25.00	62.878
7.975	11.9	27.08	61.784	13.775	12.3	25.00	62.331
8.083	8.8	20.83	65.885	13.883	8.9	16.67	67.252
8.25	4.4	12.50	72.720	14.05	4.8	8.33	72.720
8.417	0	0	79.828	14.217	1.1	4.17	79.008
8.533	0	0	81.468	14.333	0	0	81.195
8.7	0	0	81.741	14.5	0	0	81.468

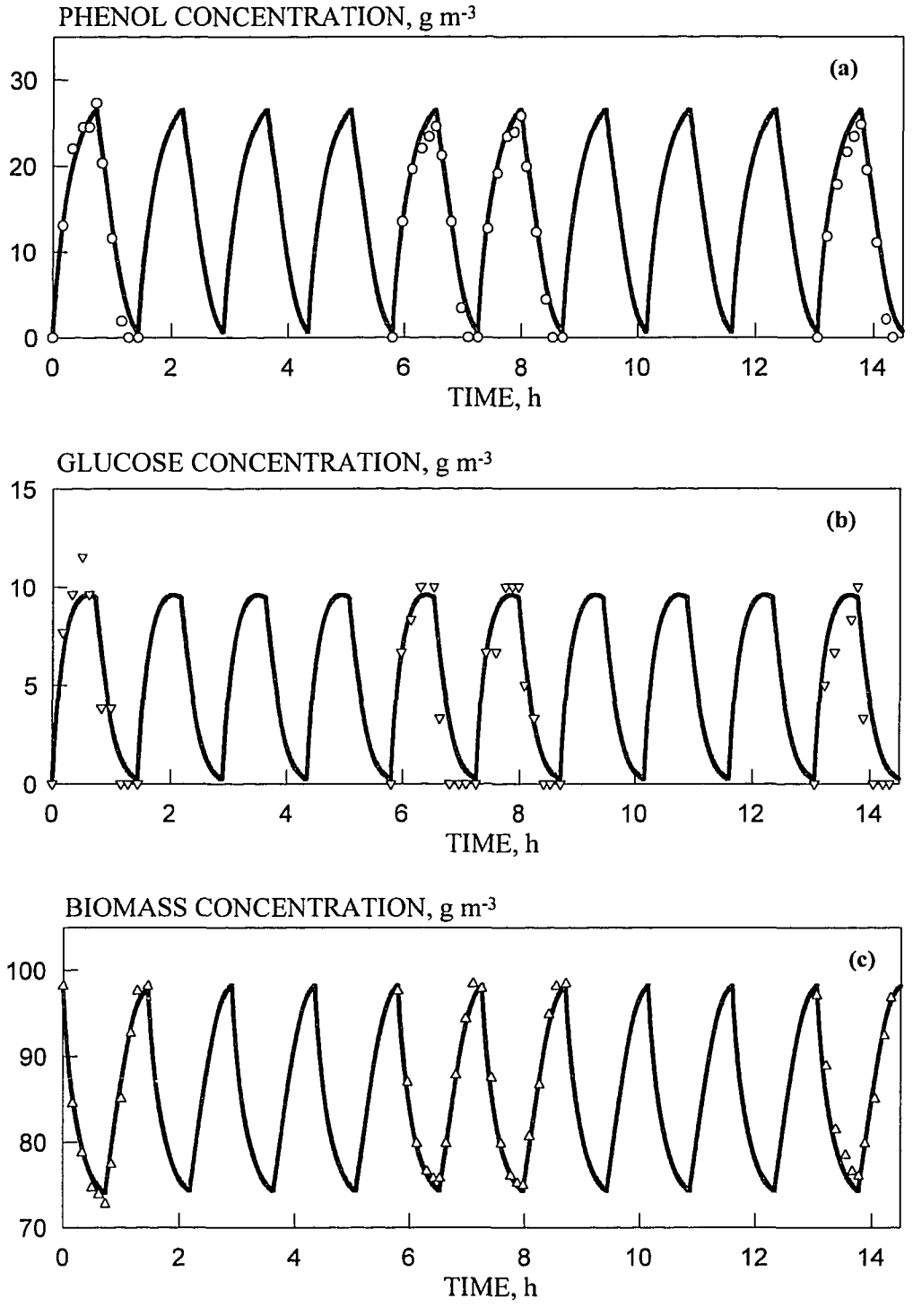

Figure D-1 Experimentally obtained and model-predicted concentration profiles for phenol (a), glucose (b), and biomass (c) for experiment C-1. Conditions for this experiment are given in Table D-1. The system reaches a survival periodic state.

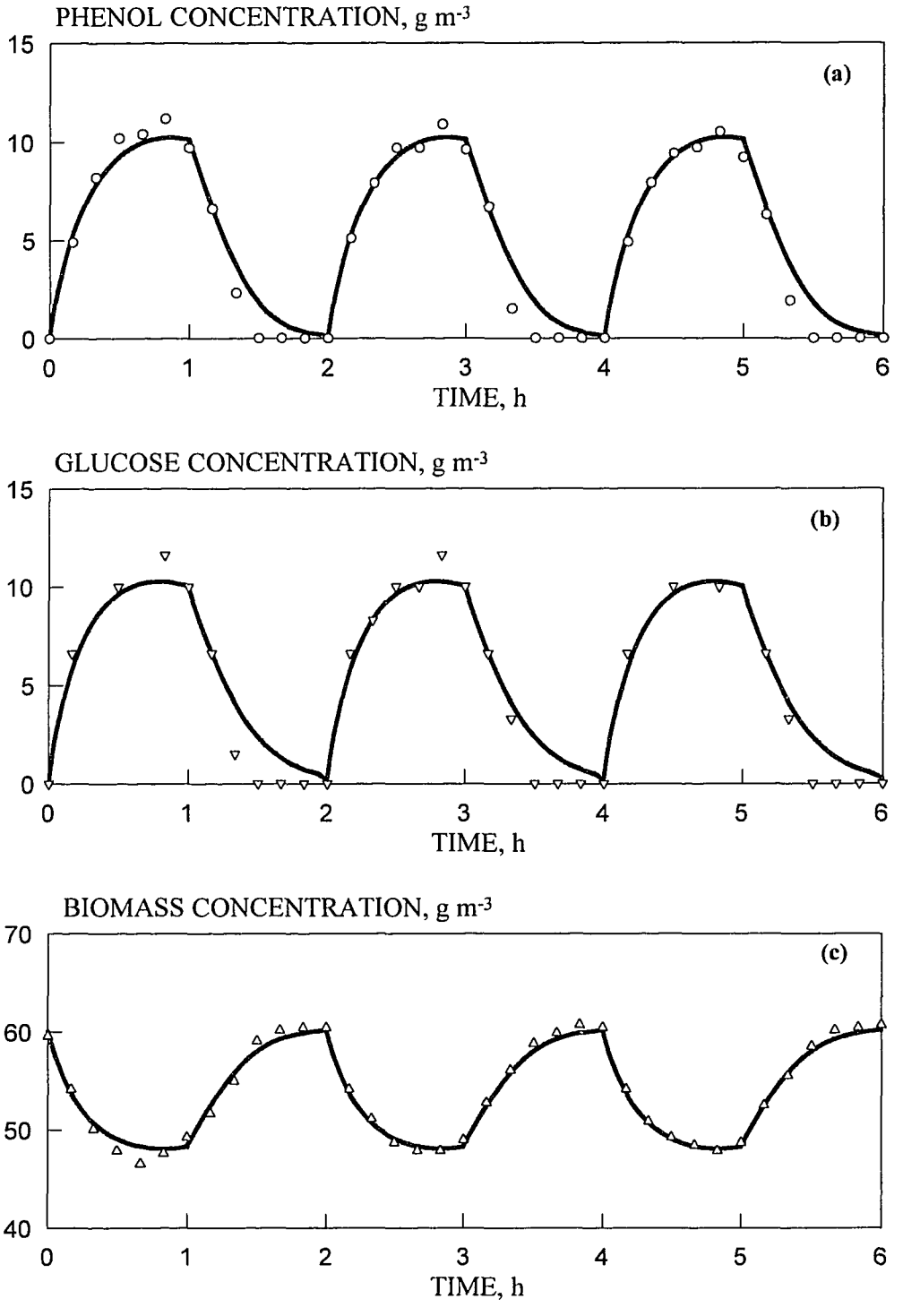

Figure D-2 Experimentally obtained and model-predicted concentration profiles for phenol (a), glucose (b), and biomass (c) for experiment C-4. Conditions for this experiment are given in Table D-1. The system reaches a survival periodic state.

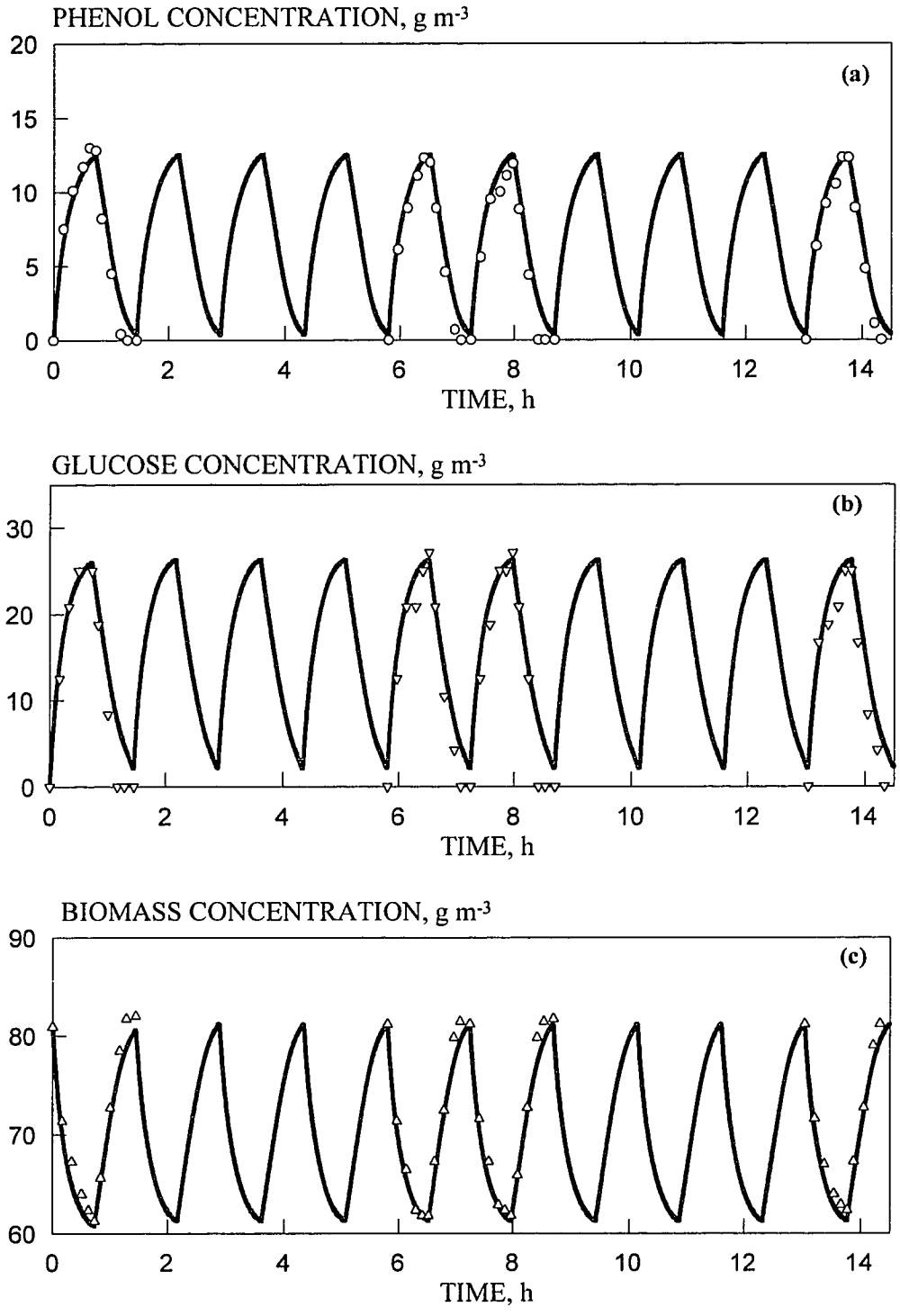

Figure D-3 Experimentally obtained and model-predicted concentration profiles for phenol (a), glucose (b), and biomass (c) for experiment C-5. Conditions for this experiment are given in Table D-1. The system reaches a survival periodic state.

APPENDIX E

COMPUTER CODES

E-1 Computer Code for Predicting Glucose and Biomass Concentration Profiles in Batch Reactors (Media without Phenol).

E-2 Computer Code for Predicting Glucose, Phenol, and Biomass Concentration Profiles in Batch Reactors.

E-3 Computer Code for Predicting Glucose, Phenol, and Biomass Concentration Profiles in Continuously Operated Cyclic Reactors.

APPENDIX E-1

Computer Code for Predicting Glucose and Biomass Concentration Profiles in Batch Reactors (Media without Phenol).

```
**********************************************************************
C       PROGRAM FOR PREDICTING GLUCOSE CONCENTRATION PROFILES
C       IN BATCH REACTORS (MEDIA WITHOUT PHENOl).
**********************************************************************

        REAL U,KS
        OPEN (5,FILE = 'PLOTMS.DAT',STATUS = 'OLD')
        OPEN (6,FILE = 'PLOTMS.OUT',STATUS = 'NEW')
        READ (5,*) U, KS, YE, S0, B0
        WRITE (*,*) U, KS
C       ***************************************************
C       YIELD COEFFICIENT VALUE TO BE GIVEN AS
C       YE
C       INITIAL BIOMASS AND SUBSTRATE CONC. IN PPM
C       TO BE GIVEN AS B0, S0
C       ***************************************************
        S = S0
        WRITE (6,181) B0, S0
181     FORMAT ('INITIAIL BIOMASS = ',F9.5, 'INITIAL SUBS. = ',F9.5)
10      A1 = (1/U)*ALOG((B0+YE*(S0-S))/B0)
        A3 = (YE*KS/U)*(1/(YE*S0+B0))*ALOG((S*B0)/(S0*(B0+YE*(S0-S))))
        TIME = A1 - A3
        WRITE (6,*) TIME, S
        S = S-0.25
        IF (S.GE.0.001) THEN
        GO TO 10
        ENDIF
        STOP
        END
```

```
**********************************************************************
C       PROGRAM FOR PREDICTING BIOMASS CONCENTRATION PROFILES
C       IN BATCH REACTORS (MEDIA WITH GLUCOSE ONLY).
**********************************************************************

        REAL U,KS
        OPEN (5,FILE = 'PLOTMB.DAT', STATUS = 'OLD')
        OPEN (6,FILE = 'PLOTMB.OUT', STATUS = 'NEW')
        READ (5,*) U, KS, B0, S0, YE
        WRITE (*,*) U, KS
        WRITE (6,181) B0, S0
181     FORMAT (2X,'INITIAL BIOMASS = ',F10.4, 'INITIAL SUBS = ',F10.4)
C       ****************************************************
C       YIELD COEFFICIENT VALUE TO BE GIVEN AS
C       YE
C       INITIAL BIOMASS AND SUBSTRATE CONC. IN PPM
C       TO BE GIVEN AS B0, S0
C       ****************************************************
        B = B0
        BFINAL = B0 + (YE*S0)
        AZ1 = B0 + (YE*S0)
10      A1 = ((KS*YE)/(U*AZ1))*ALOG((B*(YE*S0))/(B0*(AZ1-B)))
        A2 = (1/U)*ALOG(B/B0)
        TIME = A1+A2
C       WRITE (*,*) A1, A2
        WRITE (6,*) TIME,B
        B = B+0.1
        IF (B.LE.BFINAL) THEN
        GO TO 10
        ENDIF
        STOP
        END
```

APPENDIX E-2

Computer Code for Predicting Glucose, Phenol, and Biomass Concentration Profiles in Batch Reactors.

```
**************************************************************
C       PROGRAM FOR FINDING THE INTERACTION PARAMETERS
C       K3 AND K4 AND PREDICTING THE GLUCOSE, PHENOL, AND
C       BIOMASS CONCENTRATION PROFILES IN BATCH REACTORS.
**************************************************************

        INTEGER     MXPARM, NEQ
        PARAMETER  (MXPARM = 50, NEQ = 3)
C
          INTEGER   IDO, ISTEP, NOUT
          REAL              FLOAT, PARAM(MXPARM), T, TEND, TOL, Y(NEQ)
          INTRINSIC  FLOAT
          EXTERNAL  FCN, IVPRK, SSET, UMACH
C
        COMMON/PR/A, B
        OPEN (6, FILE = 'AB.OUT', STATUS='NEW')
        WRITE (*,*) 'ENTER VALUE FOR A'
        READ (*,*) A
        WRITE (*,*) 'ENTER VALUE FOR B'
        READ (*,*) B
        WRITE (*,*) 'A,B IS'
        WRITE (*,*) A, B
C
C                   SET INITIAL CONDITIONS
C       Y(1) = GLU CONC.,    Y(2) = BIO CONC.,     Y(3) = PHENOL CONC. (IN PPM)
        T = 0.0
        Y(1) = 25.399
        Y(2) = 47.391
        Y(3) = 52.388

C                   SET ERROR TOLERANCE
                          TOL = 0.0005

C                   SET PARAM TO DEFAULT
                  CALL SSET (MXPARM, 0.0, PARAM, 1)

C                   SELECT ABSOLUTE ERROR CONTROL
                          PARAM(10) = 1.0
```

```
C                    PRINT HEADER
      WRITE (6,99999)
99999 FORMAT (4X, 'ISTEP', 5X, 'TIME', 9X, 'Y1G', 11X, 'Y2B', 11X,'Y3P')
        IDO = 1
        DO 10 ISTEP = 1, 201
        TEND = FLOAT (ISTEP-1)/100
      CALL IVPRK (IDO, NEQ, FCN, T, TEND, TOL, PARAM, Y)
      WRITE (6,'(I6, 4F12.3)') ISTEP, T, Y
10      CONTINUE
C                    FINAL CALL TO RELEASE WORKSPACE
      IDO = 3
      CALL IVPRK (IDO, NEQ, FCN, T, TEND, TOL, PARAM, Y)
      END
      SUBROUTINE FCN (NEQ, T, Y, YPRIME)
      INTEGER      NEQ
      REAL         T, Y(NEQ), YPRIME(NEQ)
      COMMON/PR/A,B

      SPG1 = 0.84*Y(1)/(29.84+Y(1)+A*Y(1)*Y(3))
      SPG2 = 0.897*Y(3)/(12.204+Y(3)+Y(3)**2/203.678+B*Y(1)*Y(3))
        YPRIME(1) = -1/0.44*SPG*Y(2)
        YPRIME(2) = (SPG+SPG2)*Y(2)
        YPRIME(3) = -SPG2*Y(2)/0.768
      RETURN
      END
```

APPENDIX E-3

Computer Code for Predicting Glucose, Phenol, and Biomass Concentration Profiles in Continuously Operated Cyclic Reactors.

```
**************************************************************************
C       THIS PROGRAM FOR PREDICTING THE CONCENTRATION PROFILES
C       OF PHENOL GLUCOSE AND BIOMASS IN CONTINUOUS OPERATED
C       CYCLIC REACTORS WITH RESPECT TO TIME.
C       THE RUNGE KUTTA NUMERICAL METHOD IS USED TO SOLVE
C       A SET OF NONLINEAR ORDINARY DIFFERENTIAL EQUATIONS.
**************************************************************************

        IMPLICIT DOUBLE PRECISION (A-H, O-Z)
        CHARACTER*10 FNAME
695     FORMAT (A10)
        WRITE (*, 691)
691     FORMAT ('$ ENTER THE OUTPUT FILE NAME CYCLE 1:')
        READ (*, 695) FNAME
        OPEN (1,FILE = FNAME,STATUS = 'UNKNOWN')
        WRITE (*, 692)
692     FORMAT ('$ ENTER OUTPUT FILE NAME ALL CYCLES:')
        READ (*, 695) FNAME
        OPEN (6,FILE = FNAME,STATUS = 'UNKNOWN')
        WRITE (*, 693)
693     FORMAT ('$ ENTER OUTPUT FILE NAME CYCLE 25:')
        READ (*, 695) FNAME
        OPEN (4,FILE = FNAME,STATUS = 'UNKNOWN')
        WRITE (*, 694)
694     FORMAT ('$ ENTER OUTPUT FILE NAME CYCLE 5:')
        READ (*, 695) FNAME
        OPEN (10, FILE = FNAME, STATUS = 'UNKNOWN')
        OPEN (11, FILE = 'SBR.DAT', STATUS = 'OLD')
C       ***********************************************
C       KINETIC PARAMETERS OF ANDREWS MODEL FOR PHENOL TO BE GIVEN AS
C       AMU, AKS, AKI
C       KINETIC PARAMETERS OF MONOD MODEL FOR GLUCOSE TO BE GIVEN AS
C       AMM, AKM
C       KINETIC PARAMETERS FOR INTERACTION OF CROSS INHIBITION
C       AK1, AK2
C       ***********************************************
        READ (11,*) AMU, AKS, AKI, AMM, AKM, AK1, AK2
        WRITE (*,*) AMU, AKS, AKI, AMM, AKM, AK1, AK2
C       ***********************************************
```

```
      GA = AKS/AKI
      RHO = (AKS/AKM)*(0.768/0.44)
      ALAM1 = AKM*AK1
      ALAM2 = AKS*AK2
      ETA = AMM/AMU
      BETA = AMU*2.4526
C     ************************************************
      X0 = 94.99/(AKS*0.768)
      UF = 100.0/AKS
      VF = 50.0/AKM
C     ************************************************
      DATA DEL, S1, S3/0.5, 0.5, 0.136/
      DATA H, U0, V0, N/0.001, 0.0, 0.0, 100/
C     ************************************************
      U = U0
      V = V0
      X = X0
      WRITE (6,185)
185   FORMAT (7X,'TIME',8X,'BIO. CONC.',5X,'PHENOL CONC.','GLUCOSE')
      ICOUNT = 1
      B1 = AKS*0.768*X
      SPH = AKS*U
      SGLU = AKM*V
      TIME = 0.0
      INDEX = (ICOUNT/4)*4-ICOUNT
      IF (INDEX.EQ.0) THEN
      WRITE (6,181) TIME, B1, SPH, SGLU
      ENDIF
      DO 130 I = 1, 999
      AL = 1.0
      T = 0.001
C
C     FILL PHASE
C
      ICOUNT = 0
      WRITE (6,184) I
184   FORMAT (5X,'FILL PHASE',2X,'CYCLE NO.=',I4)
50    ICOUNT = ICOUNT+1
      CALL RUNGE (H, T, U, V, X, S1, DEL, BETA, UF, VF, AL, GA, RHO, ALAM1,
     & ALAM2, ETA)
      B1 = AKS*0.768*X
      SPH = AKS*U
      SGLU = AKM*V
      T1 = T-0.001
      T2 = 2.4526*T1
      INDEX = (ICOUNT/4)*4-ICOUNT
      IF ((I.EQ.999).AND.((ICOUNT.EQ.1).OR.(INDEX.EQ.0))) THEN
      WRITE (4,181) T2, B1, SPH, SGLU
      ENDIF
```

```
      IF ((I.EQ.1).AND.((ICOUNT.EQ.1).OR.(INDEX.EQ.0))) THEN
      WRITE (1,181) T2, B1, SPH, SGLU
      ENDIF
      IF ((I.EQ.5).AND.((ICOUNT.EQ.1).OR.(INDEX.EQ.0))) THEN
      WRITE (10,181) T2, B1, SPH, SGLU
      ENDIF
181   FORMAT (4(5X,F9.5))
      IF (T.LE.(1.0-DEL)*S1) THEN
      GO TO 50
      ENDIF
      WRITE (6,181) T2, B1, SPH, SGLU
C
C     REACT PHASE
C
      WRITE (6,186)I
186   FORMAT (5X,'REACT PHASE',2X,'CYCLE NO.=',I4)
      AL = 0
70    ICOUNT = ICOUNT+1
      CALL RUNGE (H, T, U, V, X, S1, DEL, BETA, UF, VF, AL, GA, RHO, ALAM1
     &  ALAM2, ETA)
      B1 = AKS*0.768*X
      SPH = AKS*U
      SGLU = AKM*V
      T1 = T-0.001
      T2 = 2.4526*T1
      INDEX = (ICOUNT/4)*4-ICOUNT
      IF ((I.EQ.999).AND.(INDEX.EQ.0)) THEN
      WRITE (4,182) T2, B1, SPH, SGLU
      ENDIF
      IF ((I.EQ.1).AND.((ICOUNT.EQ.1).OR.(INDEX.EQ.0))) THEN
      WRITE (1,181) T2, B1, SPH, SGLU
      ENDIF
      IF ((I.EQ.5).AND.((ICOUNT.EQ.1).OR.(INDEX.EQ.0))) THEN
      WRITE (10,181) T2, B1, SPH, SGLU
      ENDIF
182   FORMAT (4(5X,F9.5))
      IF (T.LE.(1.0-DEL)*(1.0-S3)) THEN
      GO TO 70
      ENDIF
      WRITE (6,181) T2, B1, SPH, SGLU
C
C     DRAW PHASE
C
      WRITE (6,187) I
187   FORMAT (5X,'DRAW PHASE',2X,'CYCLE NO.=',I4)
80    ICOUNT = ICOUNT+1
      CALL RUNGE (H, T, U, V, X, S1, DEL, BETA, UF, VF, AL, GA, RHO, ALAM1,
     &  ALAM2, ETA)
```

```
      B1 = AKS*0.768*X
      SPH = AKS*U
      S4CPH = AKM*V
      T1 = T-0.001
      T2 = 2.4526*T1
      INDEX = (ICOUNT/4)*4-ICOUNT
      IF ((I.EQ.999).AND.(INDEX.EQ.0)) THEN
      WRITE (4,183) T2, B1, SPH, SGLU
      ENDIF
      IF ((I.EQ.1).AND.((ICOUNT.EQ.1).OR.(INDEX.EQ.0))) THEN
      WRITE (1,181) T2, B1, SPH, SGLU
      ENDIF
      IF ((I.EQ.5).AND.((ICOUNT.EQ.1).OR.(INDEX.EQ.0))) THEN
      WRITE (10,181) T2, B1, SPH, SGLU
      ENDIF
183   FORMAT (4(5X,F9.5))
      IF (T.LE.(1.00001-DEL)) THEN
      GO TO 80
      ENDIF
      WRITE (6,183) T2, B1, SPH, SGLU
      WRITE (6,105) I
105   FORMAT (2X,'***************END OF CYCLE*******',I4)
130   CONTINUE
      STOP
      END
C*************************************************************************
C     INTEGRATION TO SOLVE THE MASS BALANCE ON SUBSTRATE & BIOMASS
C     FOURTH ORDER RUNGE-KUTTA METHOD
C*************************************************************************
      SUBROUTINE RUNGE (H, T, U, V, X, S1, DEL, BETA, UF, VF, AL, GA, RHO,
     &  ALAM1, ALAM2, ETA)
      IMPLICIT REAL*8 (A-H, O-Z)
      F1(T,U,V,X) = AL*(UF-U)/(S1*DEL+T)-
     &              (X*U*BETA) /(1.0+U+GA*U**2 +ALAM1*U*V)
      F2(T,U,V,X) = AL*(VF-V)/(S1*DEL+T)-
     &              (BETA*X*RHO*V*ETA)/(1+V+ALAM2*U*V)
      F3(T,U,V,X) = -(AL*X)/(S1*DEL+T)+
     &              (X*BETA)*((U/(1.0+U+GA*U**2+ALAM1*U*V))+
     &              (ETA*V/(1.0+V+ALAM2*U*V)))
      AK1 = H*F1(T,U,V,X)
      BK1 = H*F2(T,U,V,X)
      CK1 = H*F3(T,U,V,X)
      AK2 = H*F1(T+H/2,U+AK1/2,V+BK1/2,X+CK1/2)
      BK2 = H*F2(T+H/2,U+AK1/2,V+BK1/2,X+CK1/2)
      CK2 = H*F3(T+H/2,U+AK1/2,V+BK1/2,X+CK1/2)
      AK3 = H*F1(T+H/2,U+AK2/2,V+BK2/2,X+CK2/2)
      BK3 = H*F2(T+H/2,U+AK2/2,V+BK2/2,X+CK2/2)
      CK3 = H*F3(T+H/2,U+AK2/2,V+BK2/2,X+CK2/2)
```

```
AK4 = H*F1(T+H,U+AK3,V+BK3,X+CK3)
BK4 = H*F2(T+H,U+AK3,V+BK3,X+CK3)
CK4 =H*F3(T+H,U+AK3,V+BK3,X+CK3)
U= U+(AK1+2*AK2+2*AK3+AK4)/6
V =V+(BK1+2*BK2+2*BK3+BK4)/6
X =X+(CK1+2*CK2+2*CK3+CK4)/6
T = T+H
RETURN
END
```

REFERENCES

Abufayed, A. A. and E. D. Schroeder. 1986a. "Performance of SBR/Denitrification with a Primary Sludge Carbon Source." *J. Water Pollut. Contr. Fed.*, **58**(5): 387-397.

Abufayed, A. A. and E. D. Schroeder. 1986b. "Kinetics and Stoichiometry of SBR/ Denitrification with a Primary Sludge Carbon Source." *J. Water Pollut. Contr. Fed.*, **58**(5): 398-405.

Alleman, J. E. and R. L. Irvine. 1980. "Storage-Induced Denitrification Using Sequencing Batch Reactor Operation." *Water Res.*, **14**: 1483-1488.

Andrews, J. F. 1968. "A Mathematical Model for the Continuous Culture of Microorganisms Utilizing Inhibitory Substrates." *Biotechnol. Bioeng.*, **10**: 707-723.

Arora, M. L., E. F. Barth, and M. B. Umphres. 1985. "Technology Evaluation of Sequencing Batch Reactors." *J. Water Pollut. Contr. Fed.*, **57**(8): 867-875.

Baltzis, B. C., G. A. Lewandowski, S. -H. Chang, and Y. -F. Ko. 1989. "Fill-and-Draw Reactor Dynamics in Biological Treatment of Hazardous Wastes." pp. 111-128. In: G. A. Lewandowski, P. M. Armenante, B. C. Baltzis (eds.), *Biotechnology Applications in Hazardous Waste Treatment.* Engineering Foundation, New York.

Baltzis, B. C., G. A. Lewandowski, and S. Sanyal. 1991. "Sequencing Batch Reactor Design in a Denitrifying Application." pp. 282-300. In: D. W. Tedder and F. G. Pohland (eds.), *Emerging Technologies in Hazardous Waste Management II.* ACS Symposium Series, **468**. American Chemical Society, Washington, DC.

Baltzis B. C. and M. Wu. 1994. "Steady-State Coexistence of Three Pure and Simple Competitors in a Four-Membered Reactor Network." *Math. Biosic.*, **123**: 147-165.

Bayly, R. C. and M. G. Barbour. 1984. "The Degradation of Aromatic Compounds by the *meta* and Gentisate Pathways." pp. 253-294. In: D. T. Gibson (ed.), *Microbial Degradation of Organic Compounds.* Marcel Dekker, New York and Basel.

Bayly, R. C. and G. J. Wigmore. 1973. "Metabolism of Phenol and Cresols by Mutants of *Pseudomonas putida.*" *J. of Bacteriol.*, **113**(3): 1112-1120.

Brenner, A., R. Chozick, and R. L. Irvine. 1992. "Treatment of a High-Strength Mixed Phenolic Waste in an SBR." *Water Environment Research*, **64**(2): 128-133

Buswell, J. A. 1975. "Metabolism of Phenol and Cresols by *Bacillus Stearothermophilus.*" *J. of Bacteriol.*, **124**(3): 1077-1083.

Chang, S. -H. 1987. *A Dynamic Model of a Fill-and-Draw Reactor and Its Implications for Hazardous Waste Treatment.* M.S. Thesis, New Jersey Institute of Technology, Newark, NJ.

Chang, M. -K., T. C., Voice, and C. S. Criddle. 1993. "Kinetics of Competitive Inhibition and Cometabolism in the Biodegradation of Benzene, Toluene, and *p*-Xylene by Two *Pseudomonas* Isolates." *Biotechnol. Bioeng.*, **41**:1057-1065.

Chaudhry G. R. and S. Chapalamadugu. 1991. "Biodegradation of Halogenated Organic Compounds." *Microbiological Reviews*, **55**(1): 59-79.

Chiesa, S. C. and R. L. Irvine. 1985. "Growth and Control of Filamentous Microbes in Activated Sludge: An Integrated Hypothesis." *Water Research*, **19**: 471-479.

Chozick, R. and R. L. Irvine. 1991. "Preliminary Studies on the Granular Activated Carbon-Sequencing Batch Biofilm Reactor." *Environmental Progress,* **10**(4): 282-289.

Dagley, S. and D. T. Gibson. 1965. "The Bacterial Degradation of Catechol." *Biochem. J.*, **95**: 466-474.

Dapaah S. Y. and G. A. Hill. 1992. "Biodegradation of Chlorophenol Mixtures by *Pseudomonas putida.*" *Biotechnol. Bioeng.*, **40**: 1353-1358.

Dennis, R. W. and R. L. Irvine. 1979. "Effect of Fill:React Ratio on Sequencing Batch Biological Reactors." *J. Water Pollut. Contr. Fed.*, **51**(2): 255-263.

Dikshitulu, S. 1993. *Competition Between Two Microbial Populations in a Sequencing Fed-Batch Reactor and its Implication for Waste Treatment Applications.* Ph.D. Thesis, New Jersey Institute of Technology, Newark, N.J.

Dikshitulu, S., B. C. Baltzis, G. A. Lewandowski, and S. Pavlou. 1993. "Competition Between Two Microbial Populations in a Sequencing Fed-Batch Reactor: Theory, Experimental Verification, and Implications for Waste Treatment Applications." *Biotechnol. Bioeng.*, **42**: 643-656.

Doedel, E. J. 1986. *Auto 86 User Manual: Software for Continuation and Bifurcation Problems in Ordinary Differential Equations.* Second Printing, VAX/VMS, CIT Press, Pasadena, CA.

Finn, R. K. 1983. "Use of Specialized Microbial Strains in the Treatment of Industrial Waste and in Soil Decontamination." *Experientia*, **39:** 1231-1236.

Gibson, D. T., J. M. Wood, P. J. Chapman, and S. Dagley. 1967. "Bacterial Degradation of Aromatic Compounds." *Biotechnol. Bioeng*, **9**: 33-44.

Haggblom, M. M., D. Janke, and M. S. Salkinoja-Salonen. 1989. "Transformation of Chlorinated Phenolic Compounds in the Genus *Rhodococcus.*" *Microbial Ecology,* **18**: 147-159.

Hess, T. F., S. K. Schmidt, J. Silverstein, and B. Howe. 1990. "Supplemental Substrate Enhancement of 2,4-Dinitrophenol Mineralization by a Bacterial Consortium." *Appl. Environ. Microbiol.*, **56:** 1551-1558.

Hess, T. F., J. Silverstein, and S. K. Schmidt. 1993. "Effect of Glucose on 2,4-Dinitrophenol Degradation Kinetics in Sequencing Batch Reactors." *Water Environ. Res.*, **65**: 73-81.

Hoepker, E. C. and E. D. Schroeder. 1979. "The effect of Loading Rate on Batch-Activated Sludge Effluent Quality." *J. WPCF*, **51**(2): 264-273.

Hsu, E. -H. 1986. "Treatment of a Petrochemical Wastewater in Sequencing Batch Reactors." *Environ. Progress,* **5**(2): 71-81.

Hutchinson, D. H. and C. W. Robinson. 1988. "Kinetics of the Simultaneous Batch Degradation of *p*-cresol and Phenol by *Pseudomonas putida.*" *Appl. Microbiol. Biotechnol.*, **29**: 599-604.

Irvine, R. L. and A. W. Busch. 1979. "Sequencing Batch Biological Reactors -- An Overview." *J. Water Pollut. Contr. Fed.*, **51**(2): 235-243.

Irvine, R. L., J. P. Earley, G. J. Kehrberger, and B. T. Delaney. 1993a. "Bioremediation of Soils Contaminated with Bis-(2-EthylHexyl) Phthalate (BEHP) in a Soil Slurry-Sequencing Batch Reactor." *Environmental Progress,* **12**(1): 39-44.

Irvine, R. L., L. H. Ketchum, R. Breyfogle, and E. F. Barth. 1983. "Municipal Application of Sequencing Batch Treatment." *J. Water Pollut. Contr. Fed.*, **55**(5)**:** 484-488.

Irvine, R. L. and R. O. Richter. 1978. "Comparative Evaluation of Sequencing Batch Reactors." *J. Environ. Eng. Div. ASCE.*, **104**: 503-514.

Irvine, R. L., P. S. Yocum, J. P. Early, and R. Chozick. 1993b. "Periodic Processes for In Situ and On-Site Bioremediation of Leachates and Soils." *Wat. Sci. Tech.*, **27**: 97-104.

Jones, W. L., E. D. Schroeder, and P. A. Wilderer. 1990a. "Denitrification in a Batch Wastewater Treatment System Using Sequestered Organic Substances." *J. Water Pollut. Contr. Fed.*, **62**(3): 259-267.

Jones, W. L., P. A. Wilderer, and E. D. Schroeder. 1990b. "Operation of a Three-Stage SBR System for Nitrogen Removal from Wastewater." *J. Water Pollut. Contr. Fed.*, **62**(3): 268-274.

Ketchum, Jr. L. H., R. L. Irvine, P. -C. Liao. 1979. "First Cost Analysis of Sequencing Batch Biological reactors." *J. Water Pollut. Contr. Fed.*, **51**(2): 288-297.

Ketchum, Jr. L. H. and P. -C. Liao. 1979. "Tertiary Chemical Treatment for Phosphorus Reduction Using Sequencing Batch Reactors." *J. WPCF*, **51**(2): 298-304.

Kim, C. J. and W. J. Maier. 1986. "Acclimation and Biodegradation of Chlorinated Organic Compounds in the Presence of Alternate Substrates." *Journal WPCF,* **58**(2): 157-164.

Knackmuss H. -J. 1981. "Degradation of Halogenated and Sulfonated Hydrocarbons," pp. 189-211. In: T. Leisinger, R. Hutter, A. M. Cook and J. Niiesch (eds.), *Microbial Degradation of Xenobiotics and Recalcitrant Compounds.* FEMS Symp. No. 12, Academic Press, London.

Knackmuss, H. -J. and M. Hellwig. 1978. "Utilization and Cooxidation of Chlorinated Phenols by *Pseudomonas* sp. B13." *Arch. Microbiol.*, **117**: 1-7.

Ko, Y. -F. 1988. *A Dynamic Model of Fill-and-Draw Reactor Utilizing an Inhibitory Substrate*. M.S. Thesis, New Jersey Institute of Technology, Newark, NJ.

Kolenc, R. J., W. E. Inniss, B. R. Glick, C. W. Robinson, and C. I. Mayfield. 1988. "Transfer and Expression of Mesophilic Plasmid-Mediated Degradative Capacity in a Psychrotrophic Bacterium." *Appl. Environ. Microbiol.*, **54**: 638-641.

Lackmann R. K., W. J. Maier, and N. A. Shamat. 1980. "Removal of Chlorinated Organics by Conventional Biological Waste Treatment." *Proc. 34th Ind. Waste Conf. Purdue Univ.*, 502-515.

Lenas, P., B. C. Baltzis, G. A. Lewandowski, and Y. -F. Ko. 1994. "Biodegradation of Wastes in a Cyclically Operated Reactor: Theory, Experimental Verification and Optimization Studies." *Chem. Eng. Sci.*, **49**: 4547-4561.

Lewandowski, G. A. and B. C. Baltzis. 1992. "Analysis of Sequencing Batch Bioreactors in Large-Scale Denitrifying Applications." *Chem. Eng. Sci.*, **47:** 2389-2394.

Molin, G. and I. Nilsson. 1985. "Degradation of Phenol by *Pseudomonas putida* ATCC 11172 in Continuous Culture at Different Ratios of Biofilm Surface to Culture Volume." *Appl. Environ. Microbiol.*, **50**: 946-950.

Monod, J. 1942. *Recherches sur la croissance des cultures bactériennes.* Hermann et Cie., Paris.

Nishizuka, Y., A. Ichiyama, S. Nakamura, and O. Hayaishi. 1962. "A New Metabolic Pathway of Catechol." *J. of Biol. Chem.*, **237**: 268-270.

Oh, Y. S., Z. Shareefdeen, B. C. Baltzis, and R. Bartha. 1994. "Interactions Between Benzene, Toluene and *p*-Xylene (BTX) During Their Biodegradation." *Biotechnol. Bioeng.*, **44**: 533-538.

Orhon D., I. Talinli., and O. Tunay. 1989. "The Fate of 2,4-D in Microbial Cultures." *Wat. Res.*, **23**(11): 1423-1430.

Palis, J. C. and R. L. Irvine. 1985. "Nitrogen Removal in a Low-Loaded Single Tank Sequencing Batch Reactor." *J. Water Pollut. Contr. Fed.*, **57**(1): 82-85.

Papanastasiou, A. C. and W. J. Maier. 1982. "Kinetics of Biodegradation of 2,4-Dichloro-Phenoxyacetate in the Presence of Glucose." *Biotechnol. Bioeng.*, **24**: 2001-2011.

Pavlou, S., I. G. Kevrekidis, and G. Lyberatos. 1990. "On the Coexistence of Competing Microbial Species in a Chemostat under Cycling." *Biotechnol. Bioeng.*, **35:** 224-232.

Pavlou, S. and I. G. Kevrekidis. 1992. "Microbial Predation in a Periodically Operated Chemostat: A Global Study of the Interaction Between Natural and Externally Imposed Frequencies." *Math. Biosci.*, **108:** 1-55.

Rochkind, M. L., J. W. Blackburn, and G. S. Sayler. 1986. "Microbial Decomposition of Chlorinated Aromatic Compounds." EPA/600/2-86/090, Hazardous Waste Engineering Research Laboratory. Cincinnati, Ohio.

Rozich A. F. and R. J. Colvin 1986. "Effects of Glucose on Phenol Biodegradation by Heterogeneous Populations." *Biotechnol. Bioeng.*, **28**: 965-971.

Sala-Trepat, J. M., K. Murray, and P. A. Williams. 1972. "The Metabolic Divergence in the *meta* Cleavage of Catechols by *Pseudomonas putida* NCIB 10015." *Eur. J. Biochem.*, **28**: 347-356.

Sanyal, S. 1990. *Mathematical Modeling and Computer Simulations of Biodenitrification in Batch and Sequencing Batch Reactor.* M.S. Thesis, New Jersey Institute of Technology, Newark, NJ.

Schmidt, S. K., K. M. Scow, and M. Alexander. 1987. "Kinetics of *p*-Nitrophenol Mineralization by a *Pseudomonas* sp.: Effects of Second Substrates." *Appl. Environ. Microbiol.*, **53**(11): 2617-2623.

Shuler, L. M. and F. Kargi. 1992. *Bioprocess Engineering.* Prentice Hall, Englewoods Cliffs, New Jersey.

Silverstein, J. A. and E. D. Schroeder. 1983. "Performance of SBR Activated Sludge Processes with Nitrification/Denitrification." *J. Water Pollut. Contr. Fed.*, **55**(4): 377-384.

Wang, J. -H. 1994. *Biological Denitrification: Fundamental Kinetic Studies, and Process Analysis for Sequencing Batch Reactor Operation.* Ph.D. Thesis, New Jersey Institute of Technology, Newark, NJ.

Wang, J. -H., B. C. Baltzis, and G. A. Lewandowski. 1995a. "Reduction of Nitrate and Nitrite in a Cyclically Operated Continuous Biological Reactor." *Biotechnol. Bioeng.*, **46**: 159-171.

Wang, J. -H., B. C. Baltzis, and G. A. Lewandowski. 1995b. "Fundamental Denitrification Kinetic Studies with *P. denitrificans.*" *Biotechnol. Bioeng.* (in press).

Wang, K. -W. 1991. *Biodegradation of Phenol and 4-Chlorophenol Using a Single Species in a Sequencing Batch Reactor.* M.S. Thesis, New Jersey Institute of Technology, Newark, NJ.

Wilderer, P. A., W. L. Jones, and U. Dau. 1987. "Competition in Denitrification Systems Affecting Reduction Rate and Accumulation of Nitrite." *Water Res.*, **21:** 239-245.

Yang, R. D. and A. E. Humphery. 1975. "Dynamic and Steady State Studies of Phenol Biodegradation in Pure and Mixed Cultures." *Biotechnol. Bioeng.*, **17**: 1211-1235.

Yoon, H., G. Klinzing, and H. W. Blanch. 1977. "Competition for Mixed Substrates by Microbial Populations." *Biotechnol. Bioeng.*, **19**: 1193-1210.